

DESIGN AND ANALYSIS OF A STRUCTURAL COMPONENT OF A
HEAVY TRANSPORT AIRCRAFT

A THESIS SUBMITTED TO
THE GRADUATE SCHOOL OF NATURAL AND APPLIED SCIENCES
OF
MIDDLE EAST TECHNICAL UNIVERSITY

BY

DAVUT ÇIKRIKCI

IN PARTIAL FULFILLMENT OF THE REQUIREMENTS
FOR
THE DEGREE OF MASTER OF SCIENCE
IN
AEROSPACE ENGINEERING

FEBRUARY 2010

Approval of the thesis:

**DESIGN AND ANALYSIS OF A STRUCTURAL COMPONENT OF
A HEAVY TRANSPORT AIRCRAFT**

submitted by **DAVUT ÇIKRIKCI** in partial fulfillment of the requirements
for the degree of **Master of Science in Aerospace Engineering**
Department, Middle East Technical University by,

Prof. Dr. Canan Özgen
Dean, Graduate School of **Natural and Applied Sciences** _____

Prof. Dr. Ozan Tekinalp
Head of Department, **Aerospace Engineering** _____

Prof. Dr. Yavuz Yaman
Supervisor, **Aerospace Engineering Dept., METU** _____

Examining Committee Members:

Prof. Dr. Serkan Özgen
Aerospace Engineering Dept., METU _____

Prof. Dr. Yavuz Yaman
Aerospace Engineering Dept., METU _____

Assist. Prof. Dr. Melin Şahin
Aerospace Engineering Dept., METU _____

Assoc. Prof. Dr. Metin Uymaz Salamcı
Mechanical Engineering Dept., GAZI UNIVERSITY _____

Murat Sorguç, M.Sc.
Manager of Structural Design, TAI _____

Date: 5 February 2010

I hereby declare that all information in this document has been obtained and presented in accordance with academic rules and ethical conduct. I also declare that, as required by these rules and conduct, I have fully cited and referenced all material and results that are not original to this work.

Name, Last Name: DAVUT ÇIKRIKCI

Signature :

ABSTRACT

DESIGN AND ANALYSIS OF A STRUCTURAL COMPONENT OF A HEAVY TRANSPORT AIRCRAFT

Çıkrıkçı, Davut

M.Sc., Department of Aerospace Engineering

Supervisor: Prof. Dr. Yavuz Yaman

February 2010, 171 pages

This thesis aims to present the design and analysis of a structural component of a heavy transport aircraft. The designed component is the “coupling“ which is the interface member connecting two frames or two stringers in the fuselage assembly. The “frames”, which are the circumferential stiffeners, are joined together by the “frame couplings”. The “stringers”, which are the longitudinal stiffeners, are joined together by the “stringer couplings”.

At the preliminary design phase; the structural design principles of the frame and the stringer coupling parts are explained; which are based on the company experiences that were gained from previous aircraft projects. Afterwards, conceptual design phase is performed by structural analysis of the components. The structural analysis methods are defined and illustrated by analyzing typical examples of the frame and the stringer coupling parts.

Moreover, the critical load case selection process for the structural components is explained and brief information about the load cases that the structural components will be subjected to in their service life are also given in order to have a feeling

about flight regime of the aircraft. The applied loads used in structural analysis of the frame coupling and the stringer coupling components are obtained from the global finite element model of the aircraft. The verification process of the part of global finite element model where the developed components are located is also explained in the thesis.

Finally, the general conclusions of the thesis are specified and the recommendations for future work are proposed for similar design and analysis efforts.

Keywords: Aircraft Structures, Structural Design, Structural Analysis, Finite Element Method

ÖZ

AĞIR BİR NAKLİYE UÇAĞINA AİT BİR YAPISAL BİLEŞENİN TASARIMI VE ANALİZİ

Çıkrıkçı, Davut

Yüksek Lisans, Havacılık ve Uzay Mühendisliği Bölümü

Tez Yöneticisi: Prof. Dr. Yavuz Yaman

Şubat 2010, 171 sayfa

Bu tez ağır bir nakliye uçağına ait bir yapısal bileşenin tasarım ve analiz evrelerini sunmayı amaçlamaktadır. Tasarlanan bileşen olan “yapısal bağlantı elemanı”, uçağın gövde montajında iki kaburganın ya da iki takviye kirişinin birbirine bağlantısını sağlayan arayüz elemanıdır. Uçak gövdesindeki çevresel güçlendiriciler olan “kaburgalar” birbirlerine “kaburga bağlantı elemanları” ile; boylamsal güçlendiriciler olan “takviye kirişleri” ise “takviye kirişi bağlantı elemanları” ile birleştirilmektedir.

Tasarım evresinin başlangıcında, kaburga bağlantı elemanları ve takviye kirişi bağlantı elemanları için takip edilmesi gereken yapısal tasarım prensipleri anlatılmıştır. Bu tasarım prensipleri; tasarımın yapıldığı şirketin daha önceki uçak projeleri sırasında kazanmış olduğu deneyimlerden yararlanılarak listelenmiştir. Ön tasarım aşamasından sonra, ilgili yük koşulları altında bileşenlerin yapısal

analizlerinin yapıldığı kavramsal tasarım aşaması gerçekleştirilmiştir. Yapısal analiz yöntemleri tanımlanmış ve tipik bir kaburga bağlantı elemanı ve takviye kirişi bağlantı elemanı analizi yapılarak örneklenmiştir.

Tasarım prensipleri ve yapısal analiz metodlarına ek olarak, tasarımı yapılan bileşenlere ait kritik yük koşulu belirleme işlemi anlatılmıştır. Bununla birlikte; uçağın uçuş rejimleri hakkında fikir sahibi olunmuş, tasarlanan parçaların hizmet süreleri boyunca karşılaşacakları yük koşulları hakkında bilgiler edinilmiştir. Kaburga ve takviye kirişi bağlantı elemanlarının yapısal analizleri sırasında uygulanan yükler, uçağın global sonlu elemanlar modelinden elde edilmiştir. Bu bağlamda; tasarımı yapılan bileşenlerin içinde bulunduğu gövde parçasının global sonlu elemanlar modeline ait verifikasyon işlemleri de bu tez içinde anlatılmıştır.

Son olarak, seçilen bileşenlerin tasarım ve analizi ile ilgili genel sonuçlar dile getirilmiş, gelecekte olası yapılabilecek benzer çalışmalar için öneriler sunulmuştur.

Anahtar kelimeler: Uçak Yapıları, Yapısal Tasarım, Yapısal Analiz, Sonlu Elemanlar Yöntemi

*To My Dear Wife; Demet ıkırcı,
My Dear Mom; Canan ıkırcı and
My Dear Dad; zcan ıkırcı
Thanks for their presence in my life...*

ACKNOWLEDGMENTS

I would like to express my gratitude and sincere thanks to my supervisor Prof. Dr. Yavuz Yaman for his guidance, encouragement, and, surely, his patience during the thesis study. He will always be more than a supervisor and as he is now and he was in the past.

Also; I would like to thank to my committee members, Prof. Dr. Serkan Özgen, Assist. Prof. Dr. Melin Şahin, and Assoc. Prof. Dr. Metin Uymaz Salamcı for their helpful criticism.

I would like to thank to my committee member in the thesis study and my manager in the company, Mr. Murat Sorguç, Manager of Structural Design in TAI, for his support and positive criticism.

I specially thank to Dr. Varlık Özerçiyes, who have marked a new and permanent era in my mind, for his endless support.

Finally, my wife Demet Çıkrıkçı and my parents Özcan Çıkrıkçı and Canan Çıkrıkçı, thank you for your endless support, patience and eternal love.

TABLE OF CONTENTS

ABSTRACT	iv
ÖZ	vi
ACKNOWLEDGMENTS	ix
TABLE OF CONTENTS	x
LIST OF TABLES.....	xii
LIST OF FIGURES	xiii
ABBREVIATIONS	xvii
CHAPTERS	
1. INTRODUCTION	1
1.1 Motivation, Justification and Aim of the Study	1
1.2 Scope of the Thesis.....	9
1.3 Limitations of the Study	10
2. METHODOLOGY	11
2.1 Introduction to Design and Analysis.....	11
2.2 Methods and Principles for Analysis and Design.....	14
2.2.1 Design Principles used for Preliminary Design	17
2.2.2 Structural Analysis Methods.....	23
2.2.3 Finite Element Analysis Modeling Methods.....	56
2.2.3 Material Specifications	70
2.3 Loads and Loads Selection Criterion	72
2.3.1 Verification of Loads	72
2.3.2 Aircraft Load Types and The Effects on Frame and Stringer Couplings	74
3. TYPICAL FRAME COUPLING DESIGN.....	100
3.1 Geometrical and Material Properties.....	100
3.2 Reserve Factor Calculations.....	110
3.2.1 Shear & Bearing Failure of the Fasteners	110

3.2.2 Tension Check of the Middle Section of the Coupling.....	114
3.2.3 Local Crippling Check.....	114
3.2.4 Inter-rivet Buckling Check.....	117
3.3 Summary of the Reserve Factors.....	119
4. TYPICAL STRINGER COUPLING DESIGN.....	120
4.1 Geometrical and Material Properties.....	120
4.2 Calculation of the Load Sharing Factors, α_A and α_M	128
4.3 Justification of the Stringer Coupling.....	130
4.4 Justification of the Stringer Coupling Fasteners.....	131
4.5 Justification of the Butt-Joint.....	132
4.6 Justification of the Butt-Joint Fasteners.....	133
4.7 Summary of the Reserve Factors.....	134
5. CONCLUSION.....	135
5.1 General Conclusions.....	135
5.2 Recommendation for Future Work.....	137
REFERENCES.....	139
APPENDICES.....	141
A. PARAMETRIC CALCULATIONS OF THE GEOMETRIC PROPERTIES OF FRAME COUPLINGS.....	141
B. GEOMETRIC AND MATERIAL PROPERTIES OF STRINGER COUPLINGS.....	146
C. INFORMATION ABOUT THE MATERIAL SELECTION AND LOAD VERIFICATION STUDIES.....	152
C.1 Material Strength Properties and Material Design Values.....	152
C.2 Verification of Loads.....	154
D. DEVELOPED FRAME AND STRINGER COUPLING DESIGNS.....	157
E. DEVELOPED PROGRAM FOR ANALYTICAL CALCULATIONS.....	165

LIST OF TABLES

TABLES

Table 1: Crippling Corrective Factor Calculation [4].....	40
Table 2: Definition of the components in equation (36).....	45
Table 3: Geometric Properties of the Frame Coupling based on Appendix A	102
Table 4: Additional Calculations for determining of the CG and the Second Moment Area of the Frame Coupling.....	103
Table 5: Cross-sectional Properties of the Frame.....	104
Table 6: Applied Stress on each element.....	106
Table 7: Fastener Properties	107
Table 8: Distribution of the Applied Load and Moment on Each Fastener.....	109
Table 9: Reserve Factor Calculation for the Shear Failure of the Fasteners	111
Table 10: Reserve Factor Calculation for the Bearing Failure of the Plates	113
Table 11: Allowable Crippling Load of Each Sub-Element.....	115
Table 12: Reserve Factor for the Local Crippling	116
Table 13: Reserve Factor for the Inter-rivet Buckling.....	118
Table 14: Summary of the Reserve Factors.....	119
Table 15: Stringer Coupling Geometry	121
Table 16: Stringer Geometry	121
Table 17: Applied Loads to the Stringer Coupling System.....	124
Table 18: Allowable Crippling Force of the Stringer	126
Table 19: Skin Effective Area Iteration.....	127
Table 20: Allowable Crippling Load Calculation of Stringer Coupling.....	130
Table 21: Maximum Allowable Load of the Fasteners	131
Table 22: Reserve Factor Summary of the Stringer Coupling Analysis.....	134

LIST OF FIGURES

FIGURES

Figure 1.1 Typical Structural View of a Contemporary Aircraft [2].....	3
Figure 1.2 Typical Example of a Developed Semi-monocoque Structure.....	5
Figure 1.3 Rear Fuselage Upper Shell Portion Including Couplings to be Developed Within This Thesis [3].....	6
Figure 1.4 Typical Frame Coupling Design.....	7
Figure 1.5 Typical Stringer Coupling System.....	8
Figure 2.1 Critical Phases of the Design of the Component.....	11
Figure 2.2 Sufficient Space, Δ , for Repair [6].....	16
Figure 2.3 “J” Type of Frame and Frame Couplings to be used in the Design.....	18
Figure 2.4 “C” Type of Frame and Frame Couplings to be used in the Design.....	18
Figure 2.5 Typical Design Solution for Frame Coupling for “J” Type Frames [4].....	19
Figure 2.6 Load Path on Upper Shell During Landing and During Cruise Phases [1]	21
Figure 2.7 Fastener Pitch, Edge Margin, and Fastener Row Distance.....	22
Figure 2.8 Frame Coupling Designs within This Thesis for Frame Types 1 and 2.....	24
Figure 2.9 Stringer Coupling Geometry.....	25
Figure 2.10 Transformation of Frame Loads to the CG of Rivets [4].....	27
Figure 2.11 Distribution of Loads on the Frame Couplings; (a) Axial, (b) Shear, (c) Bending Moment [4].....	28
Figure 2.12 Shear Loads on a Single Fastener [4].....	30
Figure 2.13 Fastener Shear-Off Failure [9].....	33

Figure 2.14 Bearing Failure of the Plates [9].....	34
Figure 2.15 Representation of “e” and “d” of the Fasteners.....	35
Figure 2.16 The Middle Section of the Coupling Frame Type 1.....	37
Figure 2.17 Local Crippling Failure [9].....	39
Figure 2.18 Reference Profile for Constant Thickness [4].....	41
Figure 2.19 Critical Inter-rivet Buckling Regions [4].....	43
Figure 2.20 Inter-rivet Buckling Stress Based on Auxiliary Parameter “ ψ ” [4].....	44
Figure 2.21 Types of Fasteners [4].....	46
Figure 2.22 Load Ratio and the Corresponding Sections for Stringer Couplings.....	47
Figure 2.23 Representation of the Sectional Forces of Finite Element Analysis.....	50
Figure 2.24 Free Edge Check for Upper Shell.....	58
Figure 2.25 Coincident Elements Check for Upper Shell.....	59
Figure 2.26 Aspect Ratio for TRIA3 and QUAD4 Elements.....	60
Figure 2.27 Aspect Ratio Check for Upper Shell.....	61
Figure 2.28 Taper Ratio for QUAD4 Elements.....	61
Figure 2.29 Taper Ratio Check for Upper Shell.....	62
Figure 2.30 Warping Angle Calculation for QUAD4 Elements in MSC/PATRAN®.....	63
Figure 2.31 Warping Angle Check for Upper Shell.....	64
Figure 2.32 Skew Angle and Skew Factor for TRIA and QUAD Elements.....	65
Figure 2.33 Internal Angle Check for Upper Shell.....	65
Figure 2.34 The Results of the Static Check for Upper Shell.....	68
Figure 2.35 Dynamic Check for Upper Shell.....	69
Figure 2.36 Sign Convention for Loads [4].....	75
Figure 2.37 Load Distribution in Symmetric Landing Load Cases [3].....	77
Figure 2.38 Payload Effect on Frame Cross-section.....	78
Figure 2.39 Deformation Plot for Symmetric Landing Cases.....	79
Figure 2.40 One-wheel Landing [5].....	82
Figure 2.41 Braked roll Condition for Nose Wheel Type Aircraft [5].....	83

Figure 2.42 Ground Turning of the Aircraft with Nose Wheel [5].....	84
Figure 2.43 Static Equilibrium on Pivoting Situation [5].....	85
Figure 2.44 Load Distribution of Static Ground Cases [3].....	86
Figure 2.45 Load Deformation Plot for Static Ground Cases.....	87
Figure 2.46 Loading and Deformation Plot of Aircraft under Static Flight Loads [3].....	89
Figure 2.47 Loading and Deformation Plots for One Engine Out Loads [3].....	92
Figure 2.48 Fuselage Deformation Plots of Gust and Turbulence Loads.....	94
Figure 2.49 Fuselage Shear, Bending, and Torsion and Longitudinal Force [3].....	96
Figure 2.50 Schematic Representation of the Critical Load Case Selection Envelopes of Rear Fuselage Upper Shell [3].....	99
Figure 3.1 Illustrative Example Model of Frame Coupling.....	101
Figure 3.2 Transformation of the Applied Force and Moments to the Frame Coupling.....	105
Figure 4.1 Illustrative Model for a Typical Stringer Coupling Design.....	120
Figure A.1 Rectangular Sub-element.....	141
Figure B.1 Stringer Coupling System.....	146
Figure B.2 Area of the Fasteners.....	147
Figure B.3 Stress Distribution in Stiffened Plates under Compression.....	148
Figure B.4 Effective Skin Area for Mechanically Fastened Skin Stringer Assemblies [4].....	150
Figure D.1 Frame Coupling Design, General Overview.....	158
Figure D.2 Middle Section of the Frame Coupling of Type 1.....	159
Figure D.3 Middle Section of the Frame Coupling of Type 2.....	160
Figure D.4 Frame Coupling Components of Type 1.....	161
Figure D.5 Frame Coupling Components of Type 2.....	162
Figure D.6 Stringer Coupling Design, General Overview.....	163
Figure D.7 Stringer Coupling Design, Stringer Coupling and Butt-Joint.....	164
Figure E.1 Main Parts of the Developed Program.....	165
Figure E.2 View of Part 1.2 of the Developed Program.....	166
Figure E.3 View of Part 1.3 of the Developed Program.....	167

Figure E.4 View of Part 1.5 of the Developed Program.....	168
Figure E.5 View of Part 1.6 of the Developed Program.....	169
Figure E.6 View of Part 2.1 of the Developed Program.....	170
Figure E.7 View of Part 2.6 of the Developed Program.....	171

ABBREVIATIONS

A	Crosssectional Area
AMC	Acceptable Means of Compliance
APU	Auxiliary Power Unit
ASTM	American Society for Testing Material
BS	Butt-Strap
b_{BS_T}	Effective Width of the Butt-Strap in Tension
b_i	Width of the i th sub-element
b_{SKIN_T}	Effective width of Skin in Tension
C	Clamping Factor for Inter-rivet Buckling
CAD	Computer Aided Design
CAS	Calibrated Air Speed
CG	Centre of Gravity
CS	Certification Specifications
Cnn	Frame number (nn)
d	Fastener Diameter
e	Distance from the Centre of the Fastener to the end of the Plate
E	Modulus of Elasticity
EASA	European Aviation Safety Agency
EA_{tot}	Tensile Stiffness of the Frame Coupling
EFF	Effective
EN	European Aerospace Series Standards
E_{sk}	Stringer Secant Modulus at Strain
E_{st}	Stringer Secant Modulus at Stress
E_{tot}	Average Elastic Modulus
F_{bru}	Ultimate Allowable Bearing Stress of the Corresponding Plate
$F_{bru-MIN}$	Minimum Allowable Bearing Stress
F_{bry}	Limit Allowable Bearing Stress of the Corresponding Plate

$F_{\text{butt-joint},y}$	Applied Load on Butt-Joint in $-y$ direction
F_{CG}	The Axial Force Acting on the CG
F_{coupling}	Applied Axial Load on the Coupling
$F_{\text{cr},i}$	Allowable Compressive Force for Each Sub-element
FEA	Finite Element Analysis
FEM	Finite Element Model
$F_{\text{fastener all}}$	Allowable Load of the Fasteners in the Butt-strap to Stringer Joints
F_{i-F}	Axial Force Applied to the Frame
F_{i-M}	Bending Moment Applied to the Frame
F_{i-v}	Vertical Shear Force Applied to the Frame
F_{mid}	Axial Force in the Middle Section
$F_{\text{Riv,allow}}$	Summation of the Allowable Forces on the Fasteners
$F_{\text{riv,butt-joint:/skin}}$	Summation of the Allowable Forces on the Fasteners between butt-joint and the skin
F_{st}	Allowable Crippling Stress of the Stringer
F_{stringer}	Applied Load on the Stringer
F_{su}	Ultimate Shear Stress of the Fastener Material
F_{tu}	Material Ultimate Stress
F_{tu}	Ultimate Tension Allowable Stress
F_{ty}	Material Yield Stress
F_{ty}	Tension Yield Stress
$F_{x,\text{skin1}}$	Axial Force on Skin 1
$F_{x,\text{skin2}}$	Axial Force on Skin 2
$F_{x,\text{stringer}}$	Axial Force on Stringer
ft	Feet
G	Modulus of Rigidity
GA_{tot}	Shear Stiffness of the Frame Coupling
G_{tot}	Average Shear Modulus
I_{mid}	Second Moment of Area of the Middle Section
I_r	The Polar Second Moment of Area of the Fasteners
k	Fitting Factor
LC	Load Case

LHS	Left Hand Side
m	Meter
MLP	Multi Load Path
MLW	Maximum Landing Weight
MMPDS	Metallic Materials Properties Development and Standardization
MPC	Multi Point Constraint
MTOW	Maximum Take-Off Weight
M_{CG}	Bending Moment on the CG
mm	Milimeter
M_{mid}	Bending Moment in the Middle Section
MOS	Military Operating Standards
Mpa	Megapascal
P_{br}	Applied Shear Force on the Fastener Used In Bearing Analysis
P_{bru}	Allowable Bearing Force
P_s	Applied Shear Force on the Fastener
P_{su}	Allowable Shear Force of the Fastener
REF	Datum Point Representing the Outer Mold Line of the Skin/Frame Combination
RF	Reserve Factor
r_i	Distance From a Single Fastener to the Centre of Stiffness of the Fasteners
RHS	Right Hand Side
SLP	Single Load Path
S_n	Sub-element Length
t	Thickness
t_{BS_T}	Thickness of the Butt-Joint in Tension
$t_{buttstrapL}$	Thickness of the Butt-Joint L
$t_{buttstrapR}$	Thickness of the Butt-Joint R
T_n	Sub-element Thickness
t_{SKIN_T}	Thickness of the Skin in Tension
V_A	Design Maneuvering Speed
V_B	Design Speed of Maximum Gust Intensity

V_C	Design Cruising Speed
V_{CG}	The Shear Force acting on CG
V_D	Design Dive Speed
V_{DD}	Design Drag Device Speed
V_F	Design Wing-Flap Speed
V_{MC}	Minimum Control Speed with the Critical Engine Inoperative
V_{CG}	Shear Force on the CG
V_{mid}	Shear Force in the Middle Section
W_e	Effective Skin Width on One Side of the Attachment Line
wt	Fastener row distance
x_{CG}	x coordinate of CG
y_{CG}	y coordinate of CG
y_F	The Distance of Inner Flange Fasteners to the Centre of the Stiffness of the Fasteners
β	Load Share of the Fastener Row
ε	Element Strain
ν	Poisson's Ratio
ξ	Corrective Factor of Crippling Depending on the Alloy Constituents
$\sigma_{\text{compression allow}}$	Allowable Stress of the Stringer Coupling Section in terms of Local Crippling Failure
$\sigma_{cr,irb}$	Allowable Interrivet Buckling Stress
σ_{cy}	Compression Yield Stress
σ_{in}	The Inner Fibre Stress of the Frame Coupling
σ_{out}	The Outer Fibre Stress of the Frame Coupling
$\tau_{\text{butt-joint}}$	Shear Force on the Butt-Joint
τ_u	Ultimate Shear Stress
ψ_i	Parameter for Calculation of Crippling Corrective Factor

CHAPTER 1

INTRODUCTION

1.1 Motivation, Justification and Aim of the Study

Through the past two decades, a need for a heavy transport aircraft emerged among the European Countries; which has to meet new airlift requirements specified by European Union such as;

- Extended reach
- Outsize and heavy load capability
- Fast transit/high cruise altitude
- High cruise speed for a rapid response
- Autonomous ground handling and rapid role change capability
- Short, soft field performance
- Low speed characteristics for airdrop and tactical flight
- Reliability, maintainability, testability and dispatch availability
- and, above all, affordability

In order to meet these needs a multi-national consortium is constructed including Turkey.

From Turkey's point of view, considerable experience in terms of aerospace engineering, aircraft design and certification is gained by participating in this program as an industrial partner with the other European Nations; which are

England, Germany, Spain and France. In light of these experiences and lessons learnt from this program, great contribution is provided to other aircraft programs within Turkey defence industry and a great leap forward is made in the way of design and certification process of a national aircraft.

It is beneficial to introduce some necessary information about the large transport aircraft to be designed and manufactured. Main requirements of the aircraft are the appropriateness to airworthiness from both the civil and military authorities point of view. Both authorities are required since the aircraft is appropriate to be used for the future military operations as well as for the civil cargo transporting operations. Civil authority, EASA (European Aviation Safety Agency), introduces the specifications of certification for large aircraft in CS25 (Certification Specifications–25). A military consortium is constructed to provide recommendations to Military Airworthiness Authorities of the participating nations for certification and airworthiness. Design and analysis of the aircraft is performed based on the specifications defined both by civil and military authorities.

The heavy transport aircraft is expected to have the following design features;

- Large cargo hold that is optimized to effectively transport current and future loads,
- High payload capacity coupled with a long range for strategic deployment of troops and delivery of humanitarian assistance,
- High cruise speeds to meet the needs of rapid response missions,
- Good soft field performance in order to permit direct relief or supply to remote destinations,
- Good low speed/low level handling characteristics for airdrop missions and tactical flight,
- Capability to receive fuel in flight and act as an air-to-air tanker.

All these design features directly affects the design loads of the aircraft and have great impact on the analysis of the components and sub-components of the aircraft.

For example; good soft field performance results in higher ground taxi loads than a civil aircraft, or high cruise speeds to meet the needs of rapid response missions increase the design loads of the aircraft in terms of static flight conditions. Maneuver types, loads and load selection criteria for the designed and analyzed components within this thesis are expressed in detail in the following chapters.

Modern aircraft structures are designed using “semi-monocoque concept” that is a basic load carrying shell reinforced by frames and longerons in the bodies, and a skin-stringer construction supported by spars and ribs in the surfaces as shown in Figure 1.1.

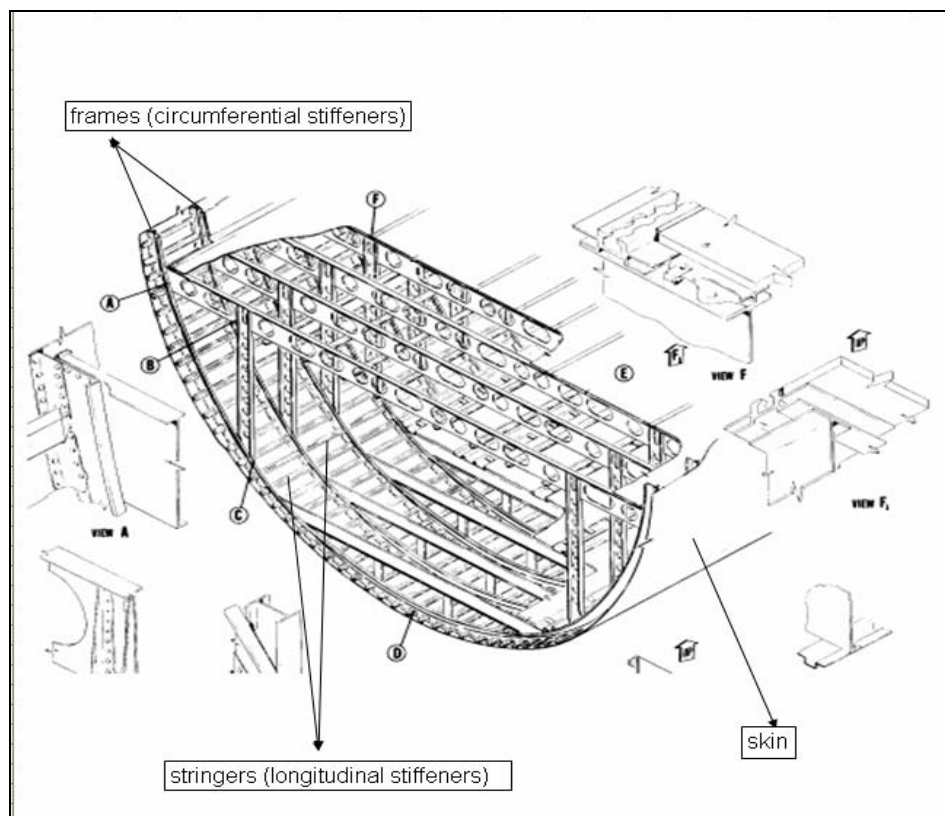


Figure 1.1: Typical Structural View of a Contemporary Aircraft [2]

Semi-monocoque manufacturing concept is a preferred method of constructing an all-aluminum fuselage. First, series of “frames” in the shape of the fuselage cross-sections are held in position on a rigid fixture, or jig. Then, frames are joined together with light-weight longitudinal elements called “stringers”. These are in turn covered with a skin of aluminum sheet, attached by riveting of fasteners or bonding with special adhesives. The jig is then disassembled and removed from the completed fuselage shell, which is equipped with wiring, controls and interior equipment such as system brackets, cargo palettes, etc. This technique is used in most of the aircraft designs. As the accuracy of the final product is determined by the costly fixture, this form is suitable for series production, where a large number of identical aircraft are planned to be manufactured.

Semi-monocoque structures are defined as “stressed-skin” structures as all or a portion of the external load (i.e. from wings and empennage, and from discrete masses such as the engine) is taken by the surface covering as shown in Figure 1.2. In addition, all loads coming from internal pressurization is carried by the external skin as skin tension. Semi-monocoque concept was also used in the design of the developed transport aircraft.



Figure 1.2: Typical Example of a Developed Semi-monocoque Structure

In order to meet the requirements of the developed transport aircraft; the design had been started by preliminary design parameters. First parameter is the material selection for the design. Detailed information for material selections and material properties are given in Section 2.2.4 of the thesis.

Furthermore, from the fuselage design and manufacturing point of view, the joining systems for frame-to-frame, skin-to-skin and stringer-to stringer connections need to be developed in order to assemble the main fuselage components together.

This thesis is aimed to give details of the design and analyses of such interface joining members consisting of frame coupling and stringer coupling parts of rear fuselage upper shell of the developed transport aircraft; which is shown in Figure 1.3.

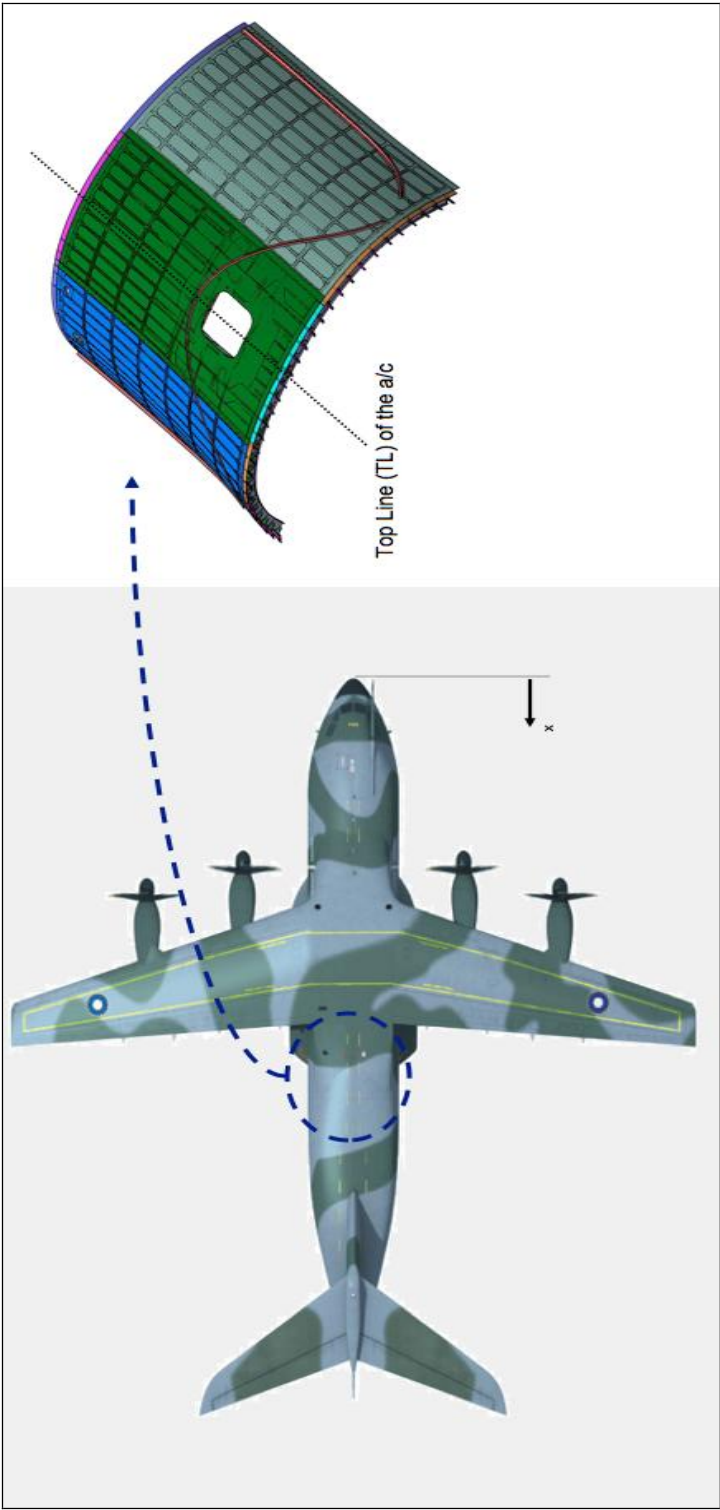


Figure 1.3: Rear Fuselage Upper Shell Portion Including Couplings to be Developed Within This Thesis [3]

The coupling parts on rear fuselage upper shell are divided into two main parts according to their usage. First part is the “frame couplings”. As it was informed before, in the fuselage structures, the loads in circumferential direction of the surrounding skin; are carried by skin-frame combinations. Connections between skin-frame combinations are provided mainly by “frame couplings”; which are shown in Figure 1.4. Frame couplings transfer the bending moment, axial force and shear force acting on the frame cross-section from one to the other. As a basic general assumption; for frame coupling loads, only the frame loads are transferred via frame couplings and skin loads remain the same, which means; in skin-frame combination in the circumferential direction of the fuselage; some portion of the force distributed on the frame cross-section is transferred to the other frame by frame coupling components, and remaining force which belongs to the skin is not carried by frame couplings. Actually; this force is directly transferred to the adjacent skin segment.

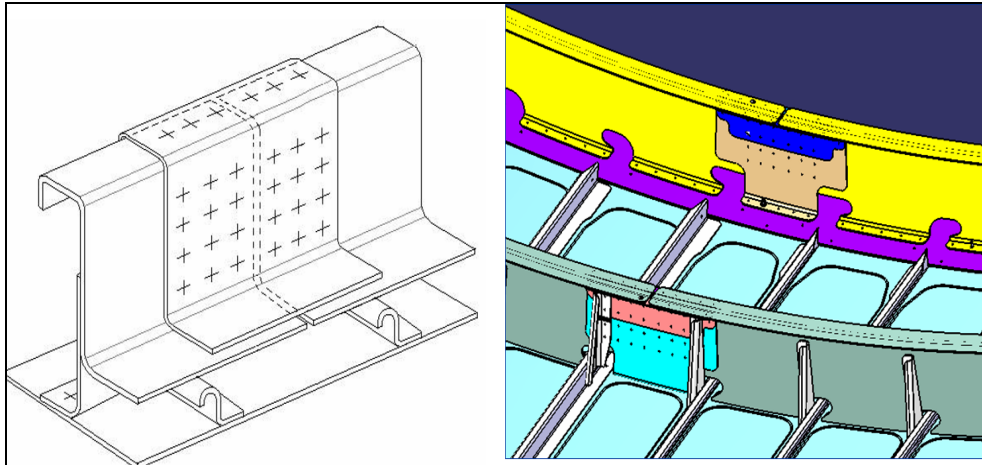


Figure 1.4: Typical Frame Coupling Design

Detailed information about the preliminary design methodology, load selection criterion, main failure modes to be analyzed within this thesis for frame couplings are explained in Chapter 2.

Second aircraft component type whose design and analysis are given within this thesis is the stringer coupling. The stringer couplings are the connection parts between skin and the longitudinal stiffeners “stringers”, and the adjacent skin – stringer elements. In the stringer coupling systems; coupling part is joined between two neighboring stringers and strap is employed to connect skin parts together. This is illustrated in Figure 1.5.

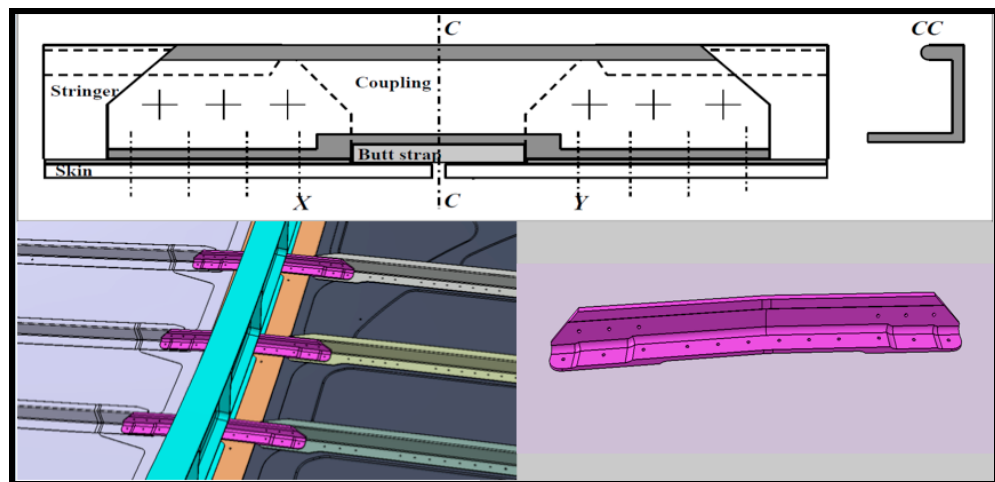


Figure 1.5: Typical Stringer Coupling System

Detailed information about the preliminary design principles, driving load case selection criterion and failure modes to be analyzed is explained in Chapter 2 of the thesis.

The aim of this thesis was to design and analysis of the frame couplings and stringer couplings of the developed transport aircraft. In order to verify the structural design and analysis results; several tests were performed including component tests and full-scale tests. After the experiments the flight test of the aircraft was also performed. That is the main success of the methodologies followed in the thesis.

1.2 Scope of the Thesis

A brief introduction, including the general statements and design features of the aircraft, its components and sub-components; which are planned to be designed and analyzed, are presented in Chapter 1. Since in aerospace industry, the companies usually keep their development of indigenous designs to themselves, a formal type of literature survey was very difficult to obtain and hence was not included. Limitations of the study are also described in Chapter 1.

Chapter 2 mainly consists of the phases of design and analysis of the components reinforced with flowcharts, design and analysis methods, design and company principles, necessary information and load selection criterion for the couplings, and the load cases that the aircraft will encounter during its operational life. Also some information about the analysis tools used in sizing procedures are given in Chapter 2 of the thesis.

In Chapter 3 and 4 typical frame coupling and typical stringer coupling designs are given respectively.

Chapter 5 outlines the general conclusions and recommendations for further studies.

1.3 Limitations of the Study

In this thesis, preliminary design phase is explained based on the relevant design principles agreed for the developed aircraft. Hence; this preliminary design restricts material selection and necessary thickness ratios such as the frame coupling to frame ratio or stringer coupling to stringer and skin ratios. Additionally the structural analyses of the components given in this thesis are limited to static strength analysis and fatigue and damage tolerance analysis. The dynamic analyses of the designed components are beyond the scope and intention of the thesis.

CHAPTER 2

METHODOLOGY

2.1 Introduction to Design and Analysis

Schematic representations of the milestones of the design methodology followed for the developed aircraft component is given in Figure 2.1.

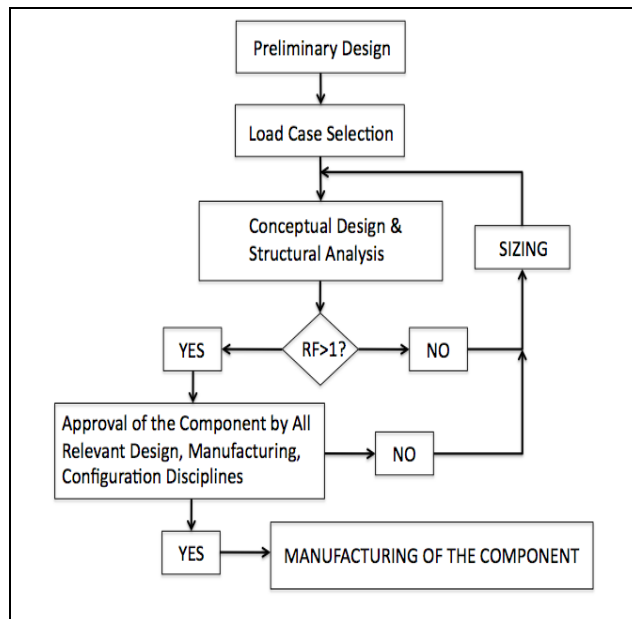


Figure 2.1: Critical Phases of the Design of the Component

Critical steps of the design methodology; which are demonstrated in Figure 2.1 of are explained below;

First of all; the design phase of the components according to the current design principles and design experience of the previous aircrafts is called the preliminary design phase. Structural analysis of the component under critical load conditions usually is not performed in this phase. The aim of this phase is to design the components so that they meet the intended requirements of the aircraft as much as possible.

Secondly; the preliminary design is followed by the selection of critical load cases in which the determination of the most critical load cases for the structure is performed according to decision of whether the component is safe from analysis methods, airworthiness and certification requirements points of view or not. The load case selection process is one of the main contributions of this thesis to the design of these components. For this; deformation and load path created on the fuselage for all kinds of loading conditions applicable during flight and ground maneuvers of the aircraft are investigated. The most critical loading conditions for the stringer couplings and the frame couplings are determined.

Considering the selected critical loading conditions, structural analysis is performed in order to check the design, from the airworthiness and the safety aspects of the flight.

The first part of the structural analysis used within this thesis is the static strength analysis. Static strength analysis of the coupling parts consists of the structural analysis for specific failure modes based on analysis methods of the company, under static and dynamic loading conditions. The analysis methods are verified by the tests performed during the design phase. The types of these tests vary from the coupon tests to the full-scale static test of the aircraft. Based on the results of the ground tests and flight tests, some updates may be required in the analysis methods and the Finite Element Model.

The second part of the structural analysis is the fatigue and damage tolerance analysis of the components; which is mainly the calculation of fatigue life of the structural parts, according to the calculation procedures and methodology of the company. For frame and stringer couplings within this thesis, fatigue and damage tolerance analysis were investigated based on the design principles and fatigue and damage tolerance analysis of the adjacent frame and stringer segments. This means that; from fatigue and damage tolerance point of view, main requirement of the frame and stringer couplings was appropriateness of the components to the company design principles. The fatigue life calculation and the damage tolerance inspection periods for the frame and stringer couplings are out of scope of the thesis, since they are defined based on the previous aircraft statistics and the corresponding spectrum calculations of different loads for different flight missions of the aircraft.

For the structural strength analysis, main parameters to be checked were the reserve factors of the structural components. “Reserve Factor” is the ratio of the allowable deformation/stress/force to the applied deformation/stress/force, which defines the margin of safety of the component.

For example; assuming that allowable stress of a structural component for crippling is 200MPa, if the applied compressive stress on that structural component is 100MPa, then reserve factor of crippling is determined to be equal to $200/100=2.00$ which means; the applied stress is doubled without failure of the structural component from crippling failure condition. The details of the crippling analysis are explained in Chapter 2.2. Reserve factor (RF) variations and their meanings are explained below;

RF<1: Failure of the component.

RF=1: Component is critical, but safe. Applied Load is equal to the allowable of the component.

RF>1: Component is safe and can carry higher loads than the applied load.

A reserve factor less than 1.00 means that the design of the structural component is insufficient from airworthiness and certification points of view. At that time, a new sizing loop will be required to raise the reserve factor above 1.00. Here; “sizing” means to reinforce the structural component, which is failing (RF<1.00) based on any of the structural analysis methods, by changing its design features such as geometrical or material properties. This update in geometry or material properties of the structural component directly depends upon the failure mode of the corresponding reserve factor.

“Failure Mode” is the criterion according to which the structural component is evaluated for being sufficient or not. Typical examples of the failure modes are crippling, inter-rivet buckling, material tension failure. etc.

2.2 Methods and Principles for Analysis and Design

In this section, the main design principles and the structural analysis methods used in the analysis and design of frame and stringer couplings of the developed transport are presented. The definitions of the common expressions used in the following chapters are explained below;

“Applied Load/Stress/Moment” is the load, resultant stress or moment, which are effectively applicable on the structural component in various aircraft maneuver conditions. Safety and qualification of the structural component are checked against this load, stress or moment in structural analysis methods.

“Allowable Load/Stress/Moment” is the load, stress or moment; which is calculated based on analysis methods for each of the failure modes.

“Limit Load” is the maximum load anticipated on the aircraft during its service life. According to the certification specifications [5], which are mandatory to be satisfied for airworthiness of the aircraft, the structure shall be capable of supporting the limit loads without suffering detrimental permanent deformation. For all loads up to “limit”, the deformation of the structure shall be such that it does not to interfere with the safe operation of the aircraft. An aircraft can easily be designed for loads greater than the limit loads, but such extra strength which is not necessary for safety would only increase the weight of the structure and decrease military payload or in general be detrimental to the design.

“Ultimate Load” is the design load and equal to the limit load multiplied by a factor of safety which is “1.5” according to the certification specifications [5] needed to be met for aircraft. Although aircraft is not supposed to undergo greater loads than the specified “limit” loads, a certain amount of reserve strength against complete structural failure of a component is necessary in the design of any part of the structure. This precaution is mainly due to;

- i) Approximations involved in the aerodynamic theory and also structural stress analysis theory.
- ii) Possible variations in the physical properties of materials
- iii) Possible variations in the fabrication and inspection standards
- iv) Possible exceedance of maximum velocity to be flown or acceleration to be subjected in flight or landing, especially during emergency conditions.

“Sizing Design Criterion” defines the type of maneuver, speed, useful load and gross weight, which is to be considered for structural design analysis.

“Sizing Analysis Criterion” defines the failure mode which gives the minimum reserve factor under specific loading of the structural component.

“Sizing Load” is the most critical loading/maneuver type of the aircraft for a specific failure mode of the structural component. In other words, sizing load is the load that gives minimum reserve factor for a specific failure mode.

“Repairability” means the structure can be repaired while the aircraft is in service; therefore, during the design stage the final size of the structural dimensions should allow sufficient space for future repair using fasteners. Sufficient space for repairs, which is designated by Δ , is shown in Figure 2.2.

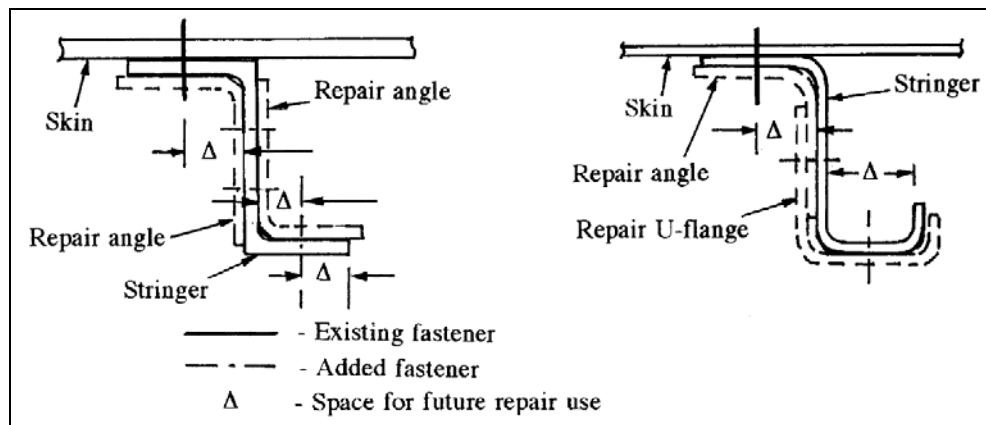


Figure 2.2: Sufficient Space, Δ , for Repair [6]

2.2.1 Design Principles used for Preliminary Design

Design principles are mainly the basic principles to be followed when initiating the detailed design of the structural components according to the experience of the design teams from the previous aircraft programs. Hence, these principles aim to assist and orient engineers for the achievement of a proof design, in compliance with applicable regulations, manufacturing processes and economical/environmental constraints.

It should be considered that; design principles are the rules which are needed to be followed for the preliminary design only. These rules could be omitted in the future design if the detailed structural analysis guarantees that there is no problem from the certification and airworthiness points of view.

2.2.1.1 Design Principles for Frame Couplings

In this part the design principles will be given for the frame couplings. The common fuselage frames are located at regular intervals. Because of the limited frame length (due to the manufacturing capabilities), the frames are produced part by part and then connected to each other by using frame couplings.

The geometry of a frame coupling strictly depends on the frame geometry. For the frame coupling design to be developed in this thesis, there exist two types of frames, namely “J” and “C” types which can be seen in Figures 2.3 and 2.4.

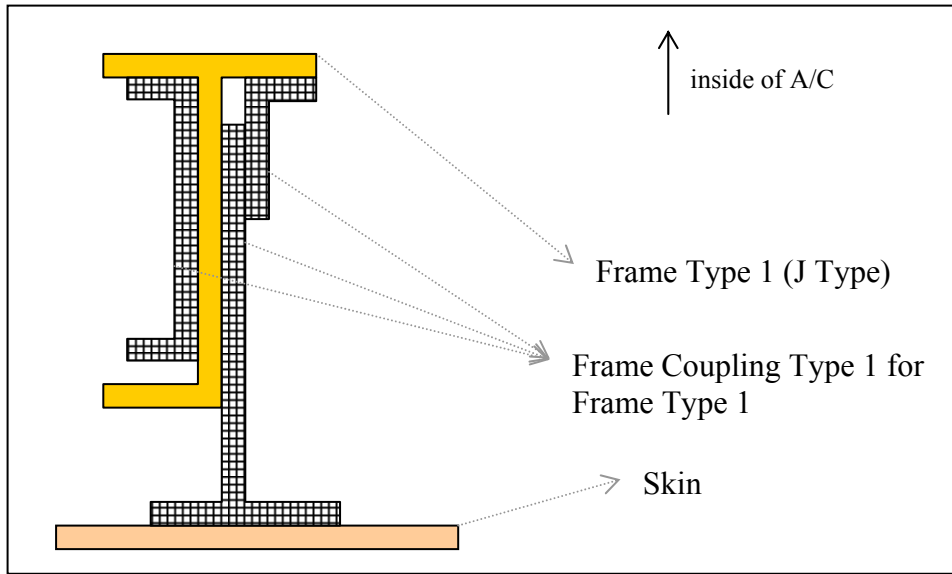


Figure 2.3: “J” Type of Frame and Frame Couplings to be used in the Design

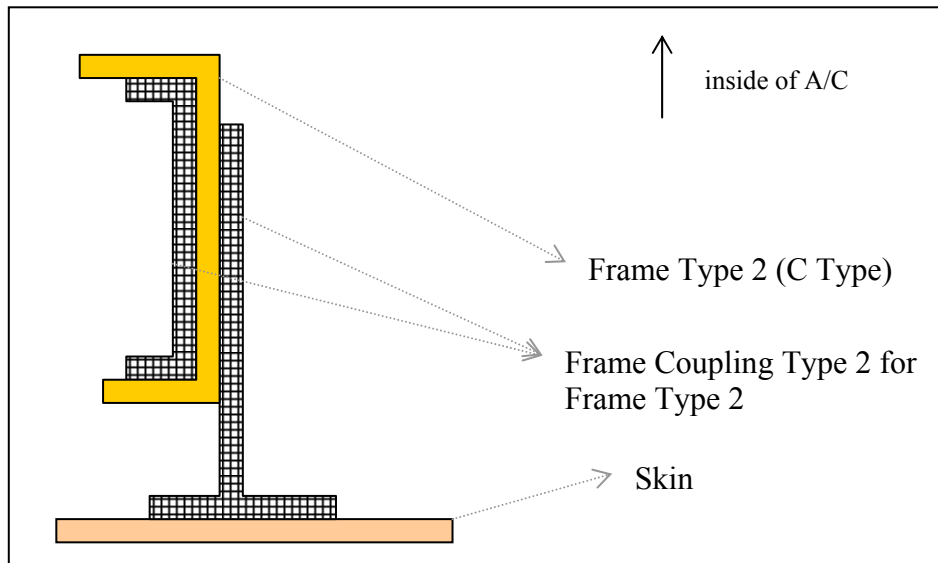


Figure 2.4: “C” Type of Frame and Frame Couplings to be used in the Design

For the “J” type frames; there are 3 sub-components representing the frame coupling.

On the other hand, for the “C” type frames; there are 2 sub-components representing the frame coupling.

The design principles require that the fastener pitch (distance between any two fasteners) should be within a common range defined in Figure 2.5.

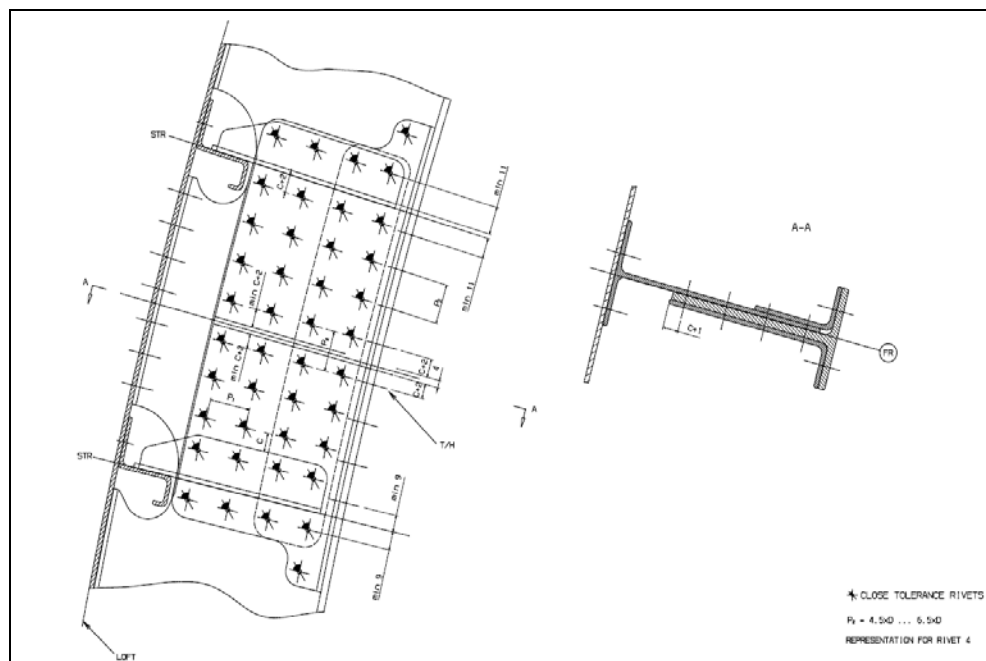


Figure 2.5: Typical Design Solution for Frame Coupling for “J” Type Frames. [4]

Figure 2.5 shows that the design principle for frame coupling parts is;

$$4.5d < wt < 6.5d \quad (1)$$

where “d” is the fastener diameter, and “wt” is the fastener row distance which means the distance between two fastener rows of the frame coupling design should be larger than the diameter of the fastener multiplied by 4.5 and should be smaller than the diameter of the fastener multiplied by 6.5.

2.2.1.2 Design Principles for the Stringer Coupling

The stringer couplings are the circumferential joints consisting of a stringer coupling and a butt joint which are submitted to loads in the direction of the flight resulting from fuselage shear, bending loads or/and internal pressure.

As a main critical condition, from “fatigue” point of view, the most critical locations of the stringer couplings are the regions of the fuselage that are loaded under tension.

For the most common critical loading conditions, which occur during landing and cruise phase of the flight, stringer coupling design is critical in terms of fatigue. Figure 2.6 represents the deformation and the load path on rear fuselage upper shell part of the aircraft under the loads during cruise and landing phases of the flight, for a better understanding.

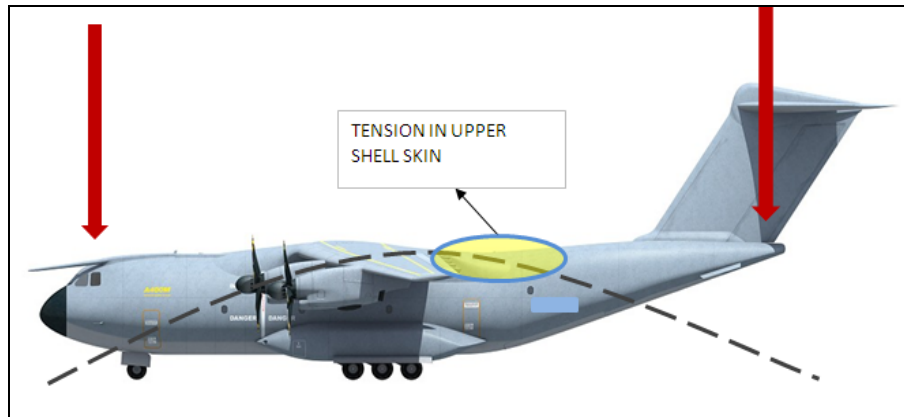


Figure 2.6: Load Path on Upper Shell During Landing and During Cruise Phases

[1]

In order to design the components in a cost effective manner; design must be sufficient both from the manufacturing and fatigue points of view.

First of all, in order to reduce the stress concentration at the beginning and the end section of the stringer coupling, thickness should be decreased by ~65% by three steps till the end of the coupling section.

In addition; the sufficiency in design is decided by considering the number of fasteners, fittings, stepping and surface treatment. Hence, design principles are needed to be followed to perform the optimum design. According to TAI Design Principles [4]; below conditions will be followed for stringer coupling parts within this thesis. The correct fastener pitch should be in the range as shown in equation (2) where “d” indicates the diameter of the fastener.

$$4d \leq \text{Fastener Pitch} \leq 5d$$

(2)

Similarly; the edge margin of the fastener, which is the distance from the center of the fastener hole to the edge of the plate is designed to be higher than “2d”.

Edge Margin > 2d

(3)

Furthermore, inner fastener row distance is designed to be larger than 25 times the summation of the skin thickness.

Inner Fastener Row Distance > 25 * (skin thickness)

(4)

In Figure 2.7, definitions for fastener row distance, edge margin and inner fastener row distance are shown.

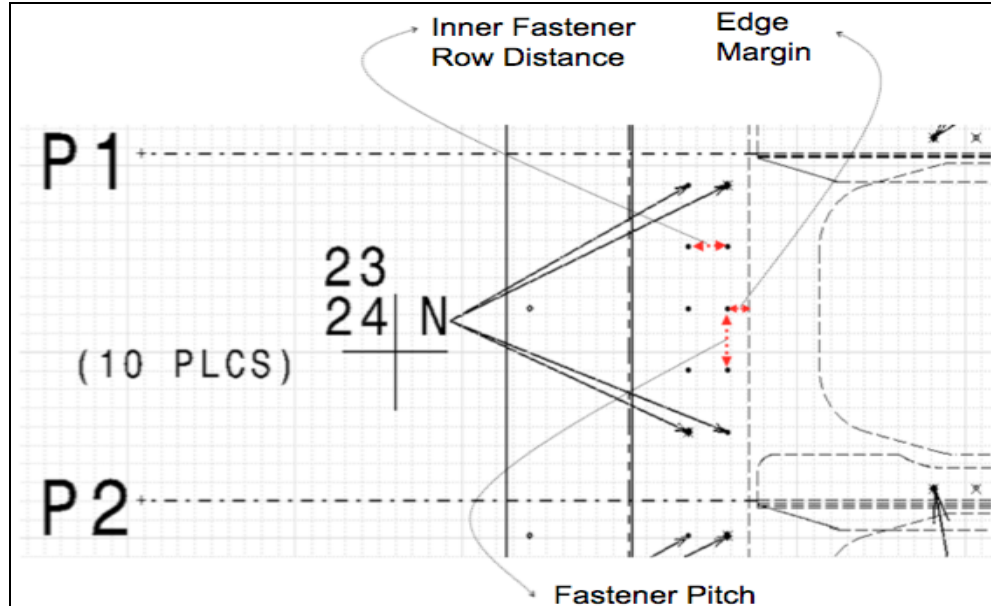


Figure 2.7: Fastener Pitch, Edge Margin, and Fastener Row Distance.

In addition to the design principles defined above, below expressions are taken as key items for the appropriate stringer coupling design;

- i) The fastener number and orientation must be same and symmetrical for both side of the butt joint and stringer coupling. This allows easy repair.
- ii) Installation of the oversized fastener must be taken into account by edge margins, which means the design principles for edge margins defined above is applicable also for the fasteners having one larger diameter than used in the design. Common diameter types available are given in millimeters below;
... $d = 4.0 \rightarrow d = 4.8 \rightarrow d = 5.6 \rightarrow d = 6.4 \rightarrow d = 7.9 \rightarrow d = 9.5$...

To illustrate ii); if the fasteners having diameters of 4.8mm are used in the design, the design principles about the edge margin should also be satisfied for 5.6mm fasteners.

2.2.2 Structural Analysis Methods

This section explains the structural analysis methods; which are used to determine the strength of the structural components and to verify the safety of the developed aircraft in terms of airworthiness and certification.

Also in this section those structural analysis methods for each failure mode of typical frame and stringer couplings are given in detail.

2.2.2.1 The Geometric and Material Properties of Frame Couplings

The frame couplings designed within the thesis are given in Figure 2.8. The parametric calculations of the geometry and the properties; which were used in structural analysis methods are given in Appendix A.

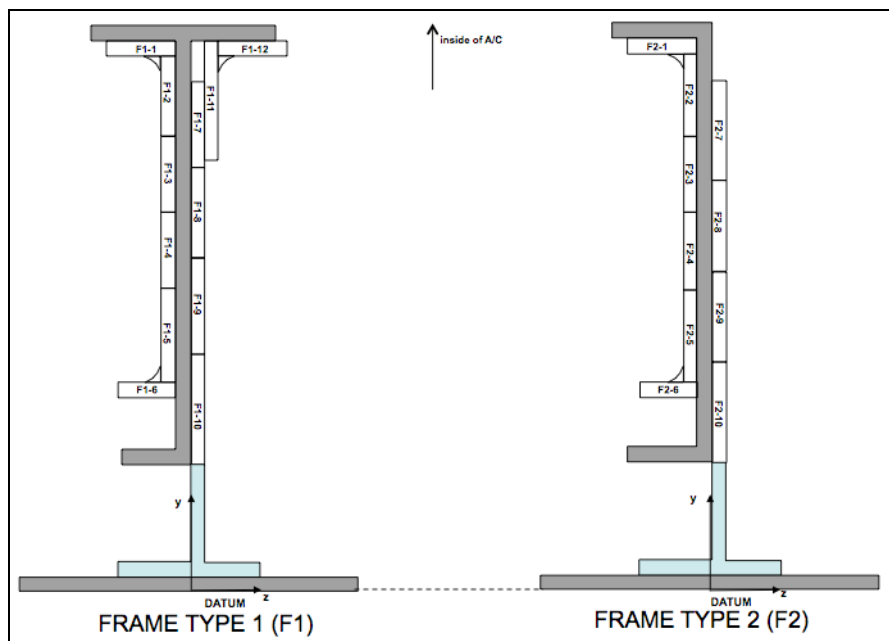


Figure 2.8: Frame Coupling Designs within This Thesis for Frame Types 1 and 2

2.2.2.2 The Geometric and Material Properties of Stringer Couplings

Similar to the frame couplings, basic geometrical properties of the stringer couplings were obtained by dividing the total geometry into sub-elements as shown in Figure 2.9.

Main difference of the stringer and the stringer coupling design from the frame and the frame coupling design in typical aircrafts is that, the height of the stringer and the stringer coupling are very small with respect to the frames and the frame couplings. The small height of the stringer and the stringer coupling design prevents the occurrence of the stress variation, resulting from bending moment, between inner flange and outer flange of the stringer and the stringer coupling.

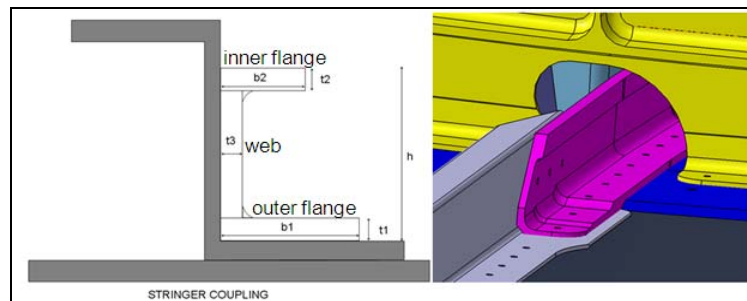


Figure 2.9: Stringer Coupling Geometry

In addition, axial load carrying capacity of the stringer coupling depends on the load sharing between the stringer coupling and the butt-joint according to their cross-sectional areas.

The area of the stringer coupling is calculated by the summation of the areas of the inner flange, the outer flange and the web, similar to the frame coupling area calculation. But, the area of the butt joint depends on the type of the load applied to the system whether it is under tension or compression. In tension, all the butt-joint area are assumed to carry the load effectively, but in compression, effective area of the butt joint is calculated based on the loading and the material properties.

The geometric and material properties are calculated and listed in Appendix B.

2.2.2.3 Load Distribution on the Frame Couplings

In this section the load distribution on the frame couplings are presented based on TAI Design and Structural Analysis Manual [4]. The flight and ground loads acting on the aircraft transversal planes, are carried both by the frame and the skin segments.

The basic assumption for the frame coupling analysis is that, the loads transferred by the coupling segments are the portion of the air-loads that are carried by the frame parts only. In this thesis the loads on the frame couplings are obtained from the Finite Element Analysis. The concept of frame load transfer to the coupling fasteners is shown in Figure 2.10.

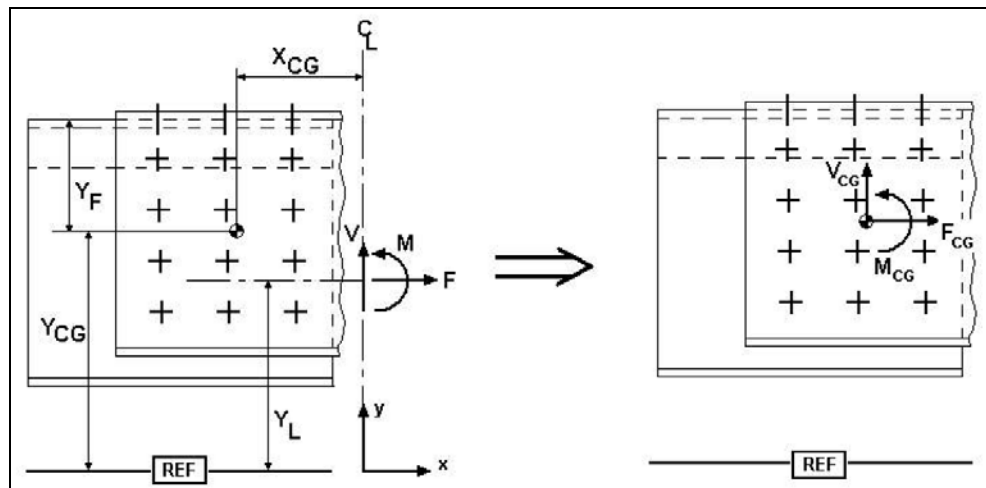


Figure 2.10: Transformation of Frame Loads to the CG of Rivets [4]

In Figure 2.10; the following notation is used based on [4];

CG: Center of Gravity,

Y_{CG} : -y coordinate of the center of gravity of the frame coupling fasteners,

X_{CG} : -x coordinate of the center of gravity of frame coupling fasteners,

Y_L : -y coordinate of the center of gravity of frame cross-section,

Y_F : Distance between frame inner flange and Y_{CG} of frame coupling fasteners,

F , M , V : Axial Force, Bending Moment and Shear Force, respectively, applied on frame section, which is obtained from Finite Element Analysis,

F_{CG} , M_{CG} , V_{CG} : Axial Force, Bending Moment and Shear Force, respectively, which is transformed to the center of stiffness of the frame coupling fasteners,

REF: Datum point representing the outer mold line of the skin/frame combination.

The axial force (F_{CG}) is carried by all fasteners (inner flange and web fasteners), whereas the shear force (V_{CG}) cannot be carried by the flange fasteners but only by the fasteners on web connection. In addition, the moment load is carried by all the

fasteners, but flange fasteners contribute to support only in the shear direction. The schematic representations of the load distributions are viewed in Figure 2.11.

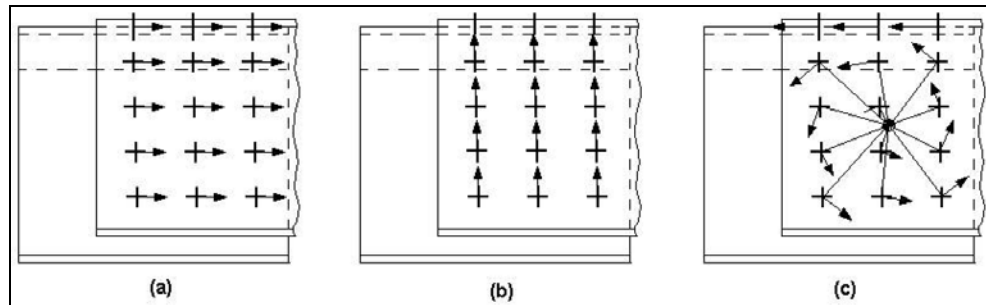


Figure 2.11: Distribution of Loads on the Frame Couplings. (a) Axial, (b) Shear, (c) Bending Moment. [4]

Under the effect of the bending moment loads, the fasteners in the flange act like a single fastener (with an area equal to the total area of the flange fasteners) with a vertical distance Y_F , which is shown in Figure 2.9, to the center of stiffness of the fasteners. Therefore; the horizontal distance of center of stiffness (X_{CG}) is calculated without considering the horizontal distances of the fasteners in the flange section. The vertical distance of the center of stiffness of the fasteners (Y_{CG}) is the weighted average of the vertical distances of all the fasteners available.

Hence based on TAI Design and Structural Analysis Manual [4];

$$x_{CG} = \frac{\sum_{i(web)} A_i \cdot x_i}{\sum_{i(web)} A_i} \quad (5)$$

$$y_{CG} = \frac{\sum_{i(all)} A_i \cdot y_i}{\sum_{i(all)} A_i}$$

(6)

The distances of the fasteners to the center of stiffness are calculated such that;

for the fasteners on the web connection;

$$r_i = \sqrt{(x_{CG} - x_i)^2 + (y_{CG} - y_i)^2}$$

(7)

for the fasteners on the flange connection;

$$r_i = y_F$$

(8)

The polar second moment of area of the fasteners are determined to be;

$$I_r = \sum_i A_i \cdot r_i^2$$

(9)

The applied loads and moments on the frame, which are obtained from the Finite Element Analysis, are transferred to the center of stiffness of the fasteners such as;

$$F_{CG} = F \tag{10}$$

$$V_{CG} = V \tag{11}$$

$$M_{CG} = M + F \cdot |y_{CG} - y_L| + V \cdot |x_{CG}| \tag{12}$$

The shear loads on the fasteners resulted from the axial force F_{CG} ; which are represented as (a) in Figure 2.11;

$$F_{i-F} = \frac{F_{CG} \cdot A_i}{\sum_{i(All)} A_i} \quad (13)$$

The shear loads on the fasteners resulted from the shear force V_{CG} ; which are represented as (b) in Figure 2.11;

$$F_{i-V} = \frac{V_{CG} \cdot A_i}{\sum_{i(Web)} A_i} \quad (14)$$

The shear loads on the fasteners resulted from the moment; which is represented as (c) in Figure 2.11 based on [4];

$$F_{i-M} = \frac{M_{CG} \cdot A_i \cdot r_i}{I_r} \quad (15)$$

The shear loads on a single fastener is represented in Figure 2.12;

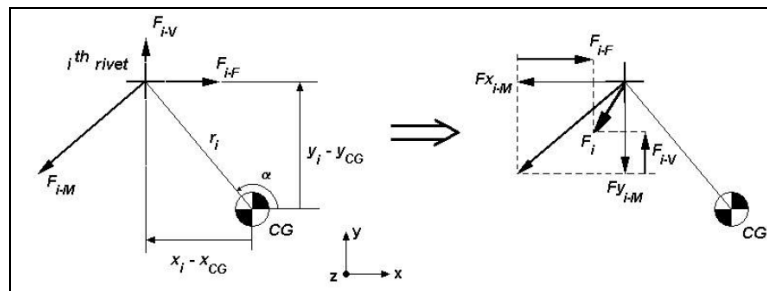


Figure 2.12: Shear Loads on a Single Fastener [4]

As shown in Figure 2.11 the total horizontal shear force acting on the i^{th} single fastener (F_{x_i}) depend on the axial force applied to the frame (F_{i-F}) and the horizontal component of the fastener shear force resulted from the bending moment applied to the frame (F_{i-M}).

In addition; the total vertical shear force acting on the i^{th} single fastener (F_{y_i}) depend on the vertical shear force applied to the frame (F_{i-V}) and the vertical component of the fastener shear force resulted from the bending moment applied to the frame (F_{i-M}).

The horizontal and vertical shear forces acting on the i^{th} fastener are formulated respectively from [4] as;

$$F_{x_i} = -F_{i-M} \sin \alpha + F_{i-F} \quad (16)$$

$$F_{y_i} = F_{i-M} \cos \alpha + F_{i-V} \quad (17)$$

where;

$$\sin \alpha = \frac{y_i - y_{CG}}{r_i} \quad (18)$$

and

$$\cos \alpha = \frac{x_i - x_{CG}}{r_i} \quad (19)$$

Hence, the resultant force on the i^{th} single fastener is;

$$F_i = \sqrt{F_{x_i}^2 + F_{y_i}^2} \quad (20)$$

The resultant force calculated in equation (20) is used to check the reserve factor for the two failure modes of the coupling fasteners, which are;

- i) Shear Failure of the Fasteners
- ii) Bearing Failure of the Fastened Plates

The methodology of the reserve factor calculation for the two failure modes above are explained in Chapters 2.2.2.4 and 2.2.2.5 respectively.

In addition to the load distribution of the frame coupling fasteners, the method of applied load transfer from the center of gravity of the frame to the center of gravity of the coupling fasteners used in equations (10), (11) and (12) are also used in order to transfer the applied load of the frame to the center of gravity of the middle section of the coupling. Hence; the transferred force and moment F_{mid} and M_{mid} are obtained additionally.

The force and moments transferred to the center of gravity of the frame coupling (F_{mid} and M_{mid}) are used in order to calculate the reserve factor of the tension and compression failure modes of the middle section of the frame couplings. The methods used these failure modes are explained in Chapters 2.2.2.6 (Tension and Compression Check of the Middle Section), 2.2.2.7 (Local Crippling) and 2.2.2.8 (Inter-rivet Buckling).

2.2.2.4 Shear Failure of the Fasteners

According to TAI Design and Structural Analysis Manual [4]; shear failure of a fastener is the cut-off of the fastener that is loaded in the shear direction based on the characteristics of the material. It is represented in Figure 2.13.

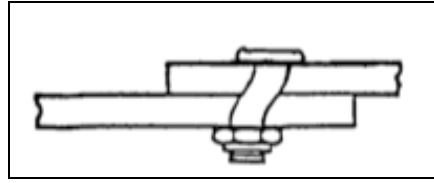


Figure 2.13: Fastener Shear-Off Failure [9]

The allowable force on the coupling fasteners are calculated as;

$$P_{su} = F_{su} \times A_{shr} \quad (21)$$

where F_{su} is the ultimate shear stress of the fastener material and A_{shr} is the area of the fastener cross-section. The ultimate shear stress is obtained from the material specifications referred in Chapter 2.2.4 of this thesis.

$$A_{shr} = \frac{\pi d^2}{4} \quad (22)$$

where d is the diameter of the fastener.

The allowable force P_{su} represents the maximum shear force that could be carried by the fastener in terms of shear failure. This force is compared with the maximum applied shear force P_s that is calculated in equation (20). Hence the reserve factor is calculated as;

$$RF_{shear_failure} = \frac{P_{su}}{P_s \times k} \quad (23)$$

where; “ k ” is the fitting factor to be used based on the Certification Specifications [5] and the company principles; which is explained in Chapter 2.2.4 in the thesis. Additionally; the reserve factor in Equation (23) is applicable for single shear

connection. For double shear connections; the distributed loads on the shear are half of themselves and hence the reserve factor is doubled [4].

The required reinforcements in case of a shear failure of fasteners are;

- i) Reduction of shear load by eliminating any abrupt increase on the stiffness of the joining elements,
- ii) Tighter fastener pitch,
- iii) Using stiffer fasteners.

2.2.2.5 Bearing Failure of the Fastened Plates

According to TAI Design and Structural Analysis Manual [4]; bearing failure is the structural failure of one of the plates of the mechanically fastened joint, which is represented in Figure 2.14.

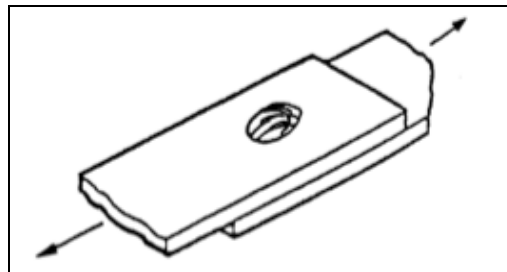


Figure 2.14: Bearing Failure of the Plates [9]

The reserve factor of the bearing failure is calculated as;

$$RF_{bearing} = \frac{P_{bru}}{P_{br} \times k} \quad (24)$$

where, P_{br} is the applied shear force on the fastener calculated in equation (20) and P_{bru} is the allowable bearing force that is calculated as;

$$P_{bru} = \min \left\{ (F_{bru-MIN} \times t \times D)_{plate1}, (F_{bru-MIN} \times t \times D)_{plate2}, \dots \right\} \quad (25)$$

where $F_{bru-MIN}$ is the minimum allowable bearing stress calculated as;

$$F_{bru-MIN} = \min \{ F_{bru}, 1.5 \times F_{bry} \} \quad (26)$$

where F_{bru} is the ultimate allowable bearing stress of the corresponding plate and F_{bry} is the limit allowable bearing stress of the corresponding plate. Both of the allowable bearing stress values are obtained from the material specifications referred in Chapter 2.2.4 of this thesis. Two different bearing stress values of the plate materials are available in the material specifications referred in Chapter 2.2.4 in terms of the “e/d” ratio of the joint. “e/d” is the ratio of the distance from the center of the fastener hole to the edge of the plate, over the diameter of the fastener. It is shown in Figure 2.15.

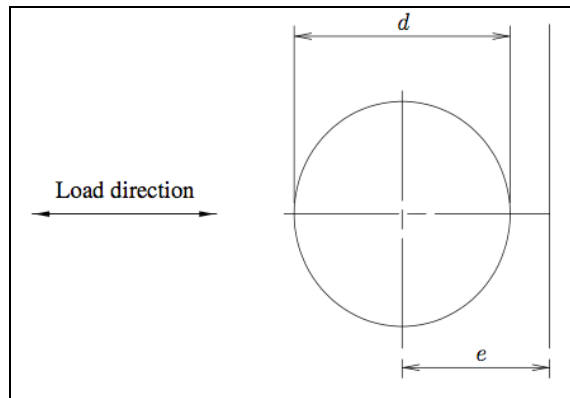


Figure 2.15: Representation of “e” and “d” of the Fasteners

The required reinforcements in case of a bearing failure of a plate are;

- i) Reduction of shear load by eliminating any abrupt increase on the stiffness of the joining elements,
- ii) Tighter fastener pitch,
- iii) Using thicker plates,
- iv) Using high strength plate materials

2.2.2.6 Tension and Compression Check of the Middle Section of the Frame Couplings

The tension and compression check of the middle section of the coupling means the check of the maximum stress concentration of the inner and the outer part of the middle section and comparison of these stress values with the material limit allowable stress (yield stress, F_{ty}) and the ultimate allowable stress (rupture, F_{tu}). In order to calculate the stress concentration in the inner and the outer part of the middle section, applied force and moments on the frame section is transferred to the center of gravity of the middle section of the coupling (F_{mid} and M_{mid}) based on equations (10), (11) and (12).

The methodology of the applied load transfer from the frame section to the middle section of the frame coupling is explained in chapter 2.2.2.3. The transferred loads on the middle section are shown in Figure 2.16.

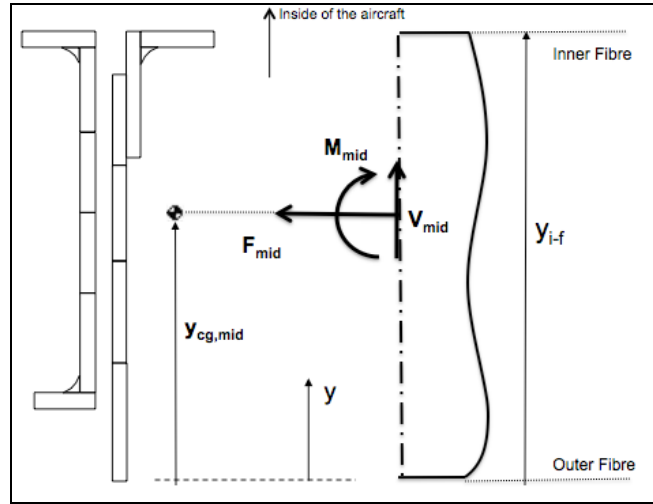


Figure 2.16: The Middle Section of the Coupling Frame Type 1

According to TAI Design and Structural Analysis Manual [4];

The inner fibre stress is calculated as;

$$\sigma_{in} = \frac{F_{mid}}{A_{mid}} - \frac{M_{mid} \times (y_{i-f} - y_{cg,mid})}{I_{mid}} \quad (27)$$

Similarly; the outer fibre stress is calculated as;

$$\sigma_{out} = \frac{F_{mid}}{A_{mid}} - \frac{M_{mid} \times (y_{o-f} - y_{cg,mid})}{I_{mid}} \quad (28)$$

where; A_{mid} , $y_{cg,mid}$ and I_{mid} are the cross-sectional properties of the middle section of the frame coupling that are calculated based on the equations A.6, A.7 and A.9 in this thesis, respectively.

Based on the applied stress in the inner and the outer fibre, the reserve factor of the tension check of the middle section is calculated as;

$$RF_{tens} = \min \left\{ \frac{(F_{tu})_{coupling}}{\sigma_{tens}}, \frac{1.5 \times (F_{ty})_{coupling}}{\sigma_{tens}} \right\} \quad (29)$$

where σ_{tens} is the maximum applied tension stress (ultimate) of σ_{in} and σ_{out} , whichever is the tension.

Finally, for the compression check of the middle part of the frame coupling, two failure modes, crippling and inter-rivet buckling, are checked according to the methodology explained in Chapters 2.2.2.7 and 2.2.2.8, respectively.

The required reinforcements in case of a tension failure of a section are;

- i) Using thicker material
- ii) Using high strength material.

2.2.2.7 Local Crippling

According to the TAI Design Manual [4]; local crippling failure is defined as;

Compression crippling is the inelastic distortion of the cross-section of a structural element in its own plane resulting in permanent deformation of the section. This failure mode is one of the most common failure types of structures under compression loading. Hence, crippling strength calculations form the basis for strength predictions for most common structures.

Actually, compression crippling involves elastic or inelastic buckling of less stable elements of a structural cross-section, and always involves inelastic axial compression of the more stable portions of the section. In contrast with the onset of buckling, crippling induced deformations do not disappear when the structure is unloaded. Although it is not directly related to the crippling analysis, crippling failure may cause lateral translation of

the cross-section or may cause triggering other failure modes at lower maximum loads.

It is significant that a structural section, which is made up elements that all have the same local buckling length, will fail at a lower load than a similar section with elements differing local buckling length.

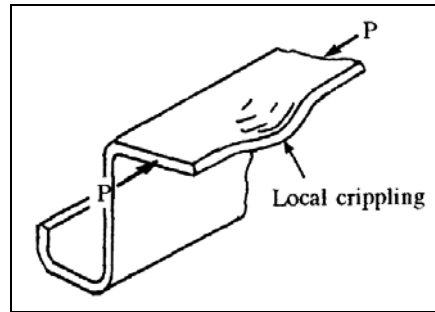


Figure 2.17: Local Crippling Failure [9]

A typical local crippling failure is given in Figure 2.17.

Crippling calculation for the frame couplings and the stringer couplings within this thesis is performed based on determining the allowable compressive forces $F_{cr,i}$ of all rectangular sub-elements separately and adding them in order to find the crippling strength of the corresponding cross-section.

$$\sigma_{st} = \frac{1}{A_{tot}} \cdot \sum_i F_{cr,i} \quad (30)$$

$F_{cr,i}$ is the allowable compressive force for each sub-element and it is calculated based on [4];

$$F_{cr,i} = l_i \times t_i \times \sigma_{yi} \times \xi_i \quad (31)$$

where;

l : Sub-element length

t : Sub-element thickness

σ_y : Yield Stress of the material

ξ : Corrective factor depending on the alloy constituents (Copper or Zinc) and on the degree of the support (RK) of the sub-element.

Prior to the determination of ξ , a new parameter ψ is calculated as;

$$\Psi_i = \frac{l_i}{t_i} \cdot \sqrt{\frac{\sigma_{yi}}{E_i \cdot RK_i}} \quad (32)$$

Where; RK is the factor of the support which can be one of the following two values;

RK = 0.41 for sub-element with one sided support

RK = 3.60 for sub-element with double-sided support

Subsequently; depending on ψ_i and alloy constituents, the corrective factor ξ_i is determined for each sub-element as follows;

Table 1: Crippling Corrective Factor Calculation [4]

Material	With Copper			With Zinc	
	>1.633	>1.095	<=1.095	>1.033	<=1.033
ξ_i	$\frac{0.69}{\Psi_i^{0.75}}$	$\frac{0.78}{\Psi_i}$	$1.4 - 0.628 \times \Psi_i$	$\frac{0.726}{\Psi_i^{0.8}}$	$1.3 - 0.574 \times \Psi_i$

The method for local crippling is valid if the following prerequisites are met;

- i) Only local buckling, no other forms of instability
- ii) Slenderness ratio ≤ 20
- iii) For components with constant thickness; $a_1 - t_1 > 0.2 \cdot a_2$ as shown in

Figure 2.18.

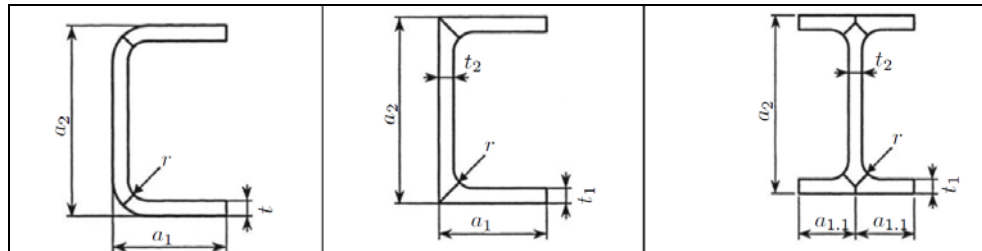


Figure 2.18: Reference Profile for Constant Thickness [4]

- iv) For components with variable thickness;

According to Windenburg approach [7], the necessary ratio for the appropriate dimensions of flange elements in order to provide at least a simple support condition to web elements is estimated in equation (33).

$$2.73 \frac{I_f}{l_w t_w^3} - \frac{A_f}{l_w t_w} \geq 5 \quad (33)$$

where I_f and A_f are the second moment of area and the area of the flange respectively.

$$A_f = l_f \cdot t_f \quad (34)$$

$$I_f = \frac{t_f \cdot l_f^3}{3} \quad (35)$$

The required reinforcements in case of a local crippling failure are;

- i) Installation of an additional rim,
- ii) Using thicker material,
- iii) Using higher strength material.

2.2.2.8 Inter-rivet Buckling

Inter-rivet buckling phenomena is simply the stability problem that occurs on the skin location between two fasteners. Stiffened panels are normally designed with fastener spacing that would prevent buckling of the skin between fasteners at stresses below the ultimate compressive strength of the attached stiffeners. This philosophy is also used to calculate skin effective width.

When a panel is loaded above the inter-rivet buckling capacity of the corresponding skin section, the skin continues to carry more loads at the onset of buckling. But, no additional load is carried since the behavior of the skin is that of wide column where failure and buckling are actually at the same load.

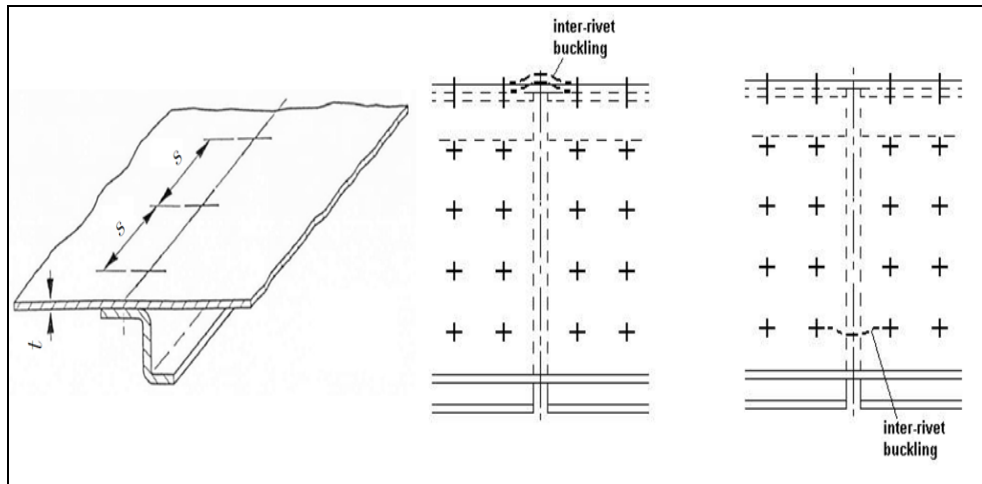


Figure 2.19: Critical Inter-rivet Buckling Regions [4]

In this part; method for sheet buckling analysis between two rivets (inter-rivet buckling) is investigated. The most critical inter-rivet buckling region for the frame coupling design is shown in Figure 2.19.

The determination of the critical inter-rivet buckling stress depends on the thickness “t” of the sheet, between the fasteners with a pitch in loading direction “s” due to compressive loading.

This method can be applied to all metallic materials. The required material data is the Elastic Modulus under compression E_c and compressive yield stress σ_{cy} .

Assuming an auxiliary parameter “ ψ ” which is determined as;

$$\psi = 1.1027 \cdot \frac{s}{t} \cdot \sqrt{\frac{\sigma_{cy}}{C \cdot E_c}} \quad (36)$$

With this auxiliary parameter “ ψ ”, the critical inter-rivet buckling stress $\sigma_{cr,irb}$ is calculated as;

For inelastic regime;

$$\psi \leq 1.5275: \rightarrow \sigma_{cr,irb} = (1 - 0.3027 \cdot \psi^{1.5}) \cdot \sigma_{cy} \quad (37)$$

For elastic regime, Euler Hyperbola;

$$\psi > 1.5275: \rightarrow \sigma_{cr,irb} = \frac{\sigma_{cy}}{\psi^2} \quad (38)$$

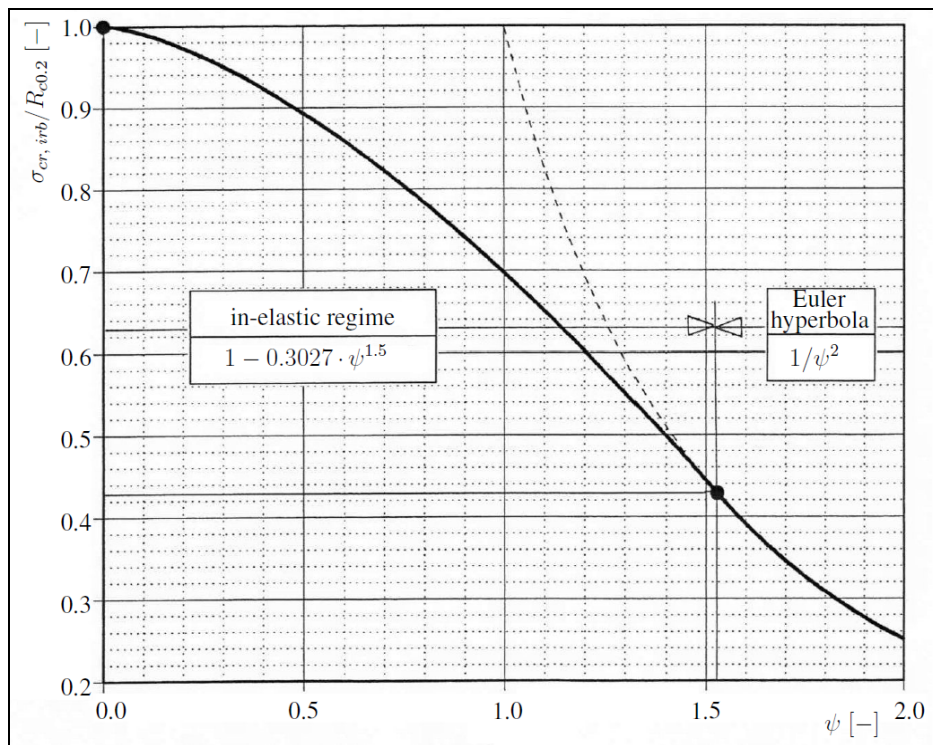


Figure 2.20: Inter-rivet Buckling Stress Based on Auxiliary Parameter “ ψ ” [4]

Table 2: Definition of the components in equation (36)

Symbol	Unit	Description
s	mm	Fastener pitch in loading direction
t	mm	Sheet thickness
C	-	Clamping factor C=1.5:solid rivet;flush head or countersunk head C=3.0:solid rivet;normal head C=2.0:lockbolt (rivet,close tolerance),flush head C=4.0:lockbolt (rivet,close tolerance), protruding head C=1.0:blind rivet, flush head or countersunk head C=2.0:blind rivet,normal head
E_c	MPa	Young's Modulus (Compression)
σ_{cy}	MPa	Compressive Yield Stress
ψ	-	Parameter (depending on geometry and material data)

The inter-rivet buckling stress calculation is plotted for both elastic and inelastic regime in Figure 2.20.

The clamping factor is mainly depending on the fastener type. Various fastener types are shown in Figure 2.21.

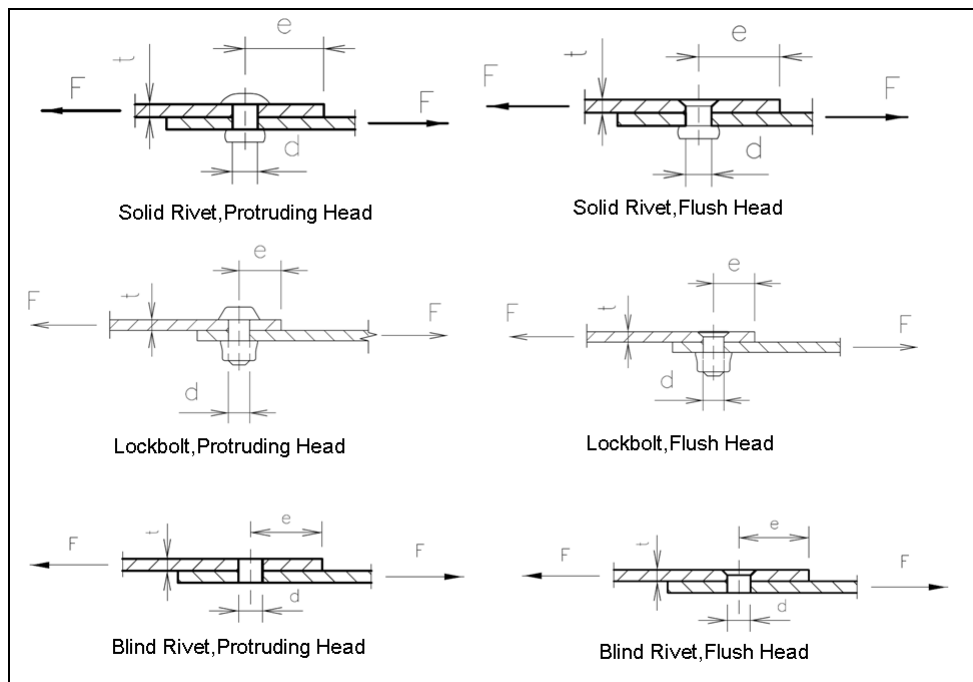


Figure 2.21: Types of Fasteners [4]

The required reinforcements in case of an inter-rivet buckling failure of the plate are;

- i) Using thicker material,
- ii) Tighter fastener pitch,
- iii) Using stiffer fasteners.

2.2.2.9 Load Distribution on the Stringer Couplings

This section details the load distribution on the stringer coupling system based on TAI Design and Structural Analysis Manual [4].

Stringer Couplings transfer the loads from one stringer/skin combination to the other. The coupling model analyzed in this thesis consists of the stringer and the skin elements at the beginning section and the stringer coupling and the butt joint at the middle section that are represented in Figure 2.22.

At the beginning section; the applied load is assumed to be shared by the skin and the stringer according to their ratio of the area and the elastic modulus. Similarly, the applied loads are shared according to the ratio of the area and the elastic modulus of the coupling and butt-joint in the middle section.

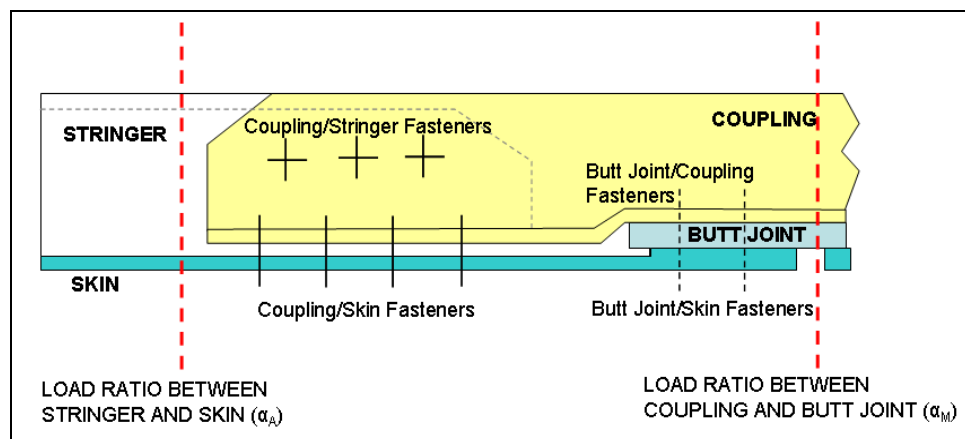


Figure 2.22: Load Ratio and the Corresponding Sections for Stringer Couplings

This means that, the first assumption of the structural analysis of the stringer couplings is the strain compatibility of the butt-joint/stringer coupling combination and the skin/stringer combination. Based on [4]

$$\mathcal{E}_{stringer} = \mathcal{E}_{skin} \quad (39)$$

$$\mathcal{E}_{Butt-Joint} = \mathcal{E}_{coupling} \quad (40)$$

The second assumption about the load distribution of the stringer coupling fasteners is that the loads on all fasteners are equally distributed because of the plasticity effects, which is applicable for all fasteners between butt-joint to skin and coupling to skin/stringer. This means; if a single fastener starts to be overloaded, that is beginning of the plasticity region, the excessive load will be carried by the fasteners in the neighborhood.

In Figure 2.22; two load distribution factors are represented for the applied load sharing between the stringer and the skin, and the stringer coupling and the butt-strap in the middle region of the joint.

α_A is the load-sharing factor of the stringer calculated based on the geometry and cross-sectional properties of the stringer and the skin segments as follows;

$$\alpha_A = \frac{A_{str}}{A_{str} + A_{skin} \cdot \left[\frac{E_{skin}}{E_{str}} \right]} \quad (41)$$

In addition; α_M , which is the factor representing the load sharing of the stringer coupling in the stringer coupling/butt-joint combination, is the load distribution factor calculated based on the geometry and cross-sectional properties of coupling and butt-joint similar to equation (41);

$$\alpha_M = \frac{A_{coupling}}{A_{coupling} + A_{ButtJoint}} \cdot \left[\frac{E_{ButtJoint}}{E_{coupling}} \right] \quad (42)$$

In order to calculate the total load on the “coupling/stringer fasteners” and the “coupling/skin fasteners” shown in Figure 2.22, the total applied load on the stringer is calculated. Because the applied load in the stringer is totally transferred by these fasteners to the coupling and the skin.

In order to calculate the total fastener load on the “butt-joint/skin fasteners”; the difference of the applied load (ΔF) between the stringer and the transferred load on the coupling is calculated. Additionally, based on the second assumption; recalculation would be needed in case ΔF is larger than the allowable load of the fasteners before plasticity occurred.

$$\Delta F = (\alpha_M - \alpha_A) \cdot F_x \quad (43)$$

Where; F_x is the axially applied load to the skin/stringer combination, which is the result of the Finite Element Analysis.

In order to prevent “butt-joint/skin fasteners” from overloading the following equation is employed if;

$$\Delta F > F_{fastener_{all}} \quad (44)$$

where, $F_{fastener_{all}}$ is the allowable load of the fasteners in the butt-strap to stringer joints.

$$F_{fastener_{all}} = \sum F_{fastener_{butt-joint/coupling}} \quad (45)$$

A re-distribution of loads is performed by modification of the load distribution factor $\alpha_{A,new}$ based on equations (43) and (44);

$$\alpha_{A,new} = \alpha_M - \left(\frac{F_{fastener,all}}{F_x} \right) \quad (46)$$

Here; the applied axial load, F_x (compression or tension), is obtained from Finite Element Analysis loads of the stringer and the skin, which are demonstrated in Figure 2.23;

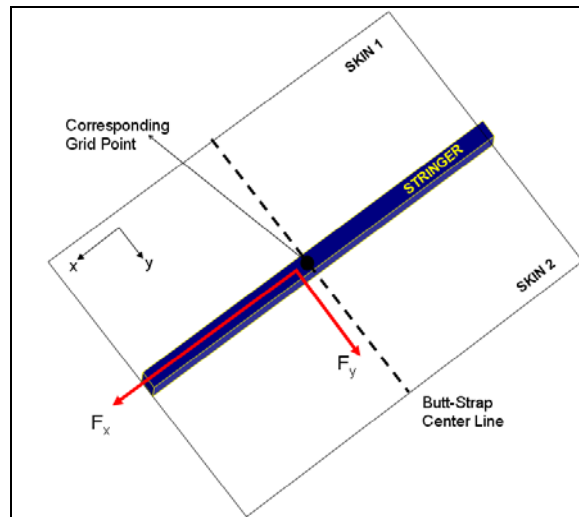


Figure 2.23: Representation of the Sectional Forces of Finite Element Analysis

In Figure 2.23, the environment of the sectional forces on the corresponding grid point in the Finite Element Model is described. F_x and F_y are the applied forces on the grid point in axial (x) and shear direction (y) of the stringer coupling system

respectively. These applied forces are resulted from “Skin 1”, “Skin 2” and “Stringer” in Figure 2.23.

In Figure 2.23;

Total shear load which is actually carried only by the butt-joint only is;

$$F_{butt-joint,y} = F_y \quad (47)$$

In addition to the shear load applied to the butt-joint, the axial load which can be tension or compression load applied to the butt-joint is;

$$F_{butt-joint,x} = (1 - \alpha_m) \cdot F_x \quad (48)$$

Hence; the resultant force on the butt-strap in equation (49) is the force, which will be carried by all the fasteners between the skin and the butt-strap is calculated as;

$$F_{butt-joint} = \sqrt{(1 - \alpha_m)^2 \cdot F_x^2 + F_y^2} \quad (49)$$

The applied force on the stringer section is;

$$F_{Stringer} = \alpha_A \cdot F_x \quad (50)$$

Similarly the applied force on the stringer coupling is calculated as;

$$F_{Coupling} = \alpha_M \cdot F_x \quad (51)$$

2.2.2.10 Justification of the Stringer Coupling

Based on [4]; justification of the stringer coupling is performed by comparison of the maximum applied stress on the middle section of the stringer coupling (F_{coupling} in equation (51)) with the maximum allowable stress of the coupling.

For the reserve factor for the loads acting on the coupling compressively;

$$RF_{\text{compression}} = \frac{\sigma_{\text{Compression Allow}} \times A_{\text{Coupling}}}{F_{\text{coupling}}} \quad (52)$$

where; $\sigma_{\text{compression,allow}}$ is the allowable stress of the stringer coupling section in terms of local crippling failure which is explained in Chapter 2.2.2.7 in this thesis.

The reserve factor for the loads acting on the coupling in tension;

$$RF_{\text{Tension}} = \frac{\sigma_{\text{Tension allow}} \times A_{\text{coupling}}}{F_{\text{Coupling}}} \quad (53)$$

where; $\sigma_{\text{tension,allow}}$ is minimum of the material ultimate stress (F_{tu}) and the material yield stress multiplied by safety factor 1.5 ($1.5 \times F_{\text{ty}}$).

2.2.2.11 Justification of the Fasteners on Stringer Couplings

As explained in Chapter 2.2.2.9; the applied load on the stringer is totally transferred to the coupling and the skin segments by the fasteners on the stringer coupling. These fasteners are divided into two groups in Figure 2.23 as; “coupling/skin fasteners” and “coupling/stringer fasteners”.

Based on [4]; the justification of these fasteners is mainly comparison of the applied load on the fasteners ($F_{stringer}$ in eqn.50) with the summation of the allowable forces of each fastener based on shear and bearing failure checks performed in Chapters 2.2.2.4 and 2.2.2.5.

Hence; the reserve factor of the stringer coupling fasteners is calculated as;

$$RF = \frac{F_{Riv_{allow}}}{F_{stringer}} \quad (54)$$

where $F_{Riv,allow}$ is the summation of the allowable forces of the fasteners based on equations (21) and (25) in Chapters 2.2.2.4 and 2.2.2.5.

$$F_{Riv_{allow}} = \sum (F_{Riv_{Coup/Str}}) + \sum (F_{Riv_{Coup/Skin}}) \quad (55)$$

where; $F_{Riv,Coup/Str}$ is the allowable force of each fastener between the coupling and the stringer, and $F_{Riv,Coup/Skin}$ is the allowable force of each fastener between the coupling and the skin.

2.2.2.12 Justification of the Butt-Joint

The applied loads on the butt-joint section of the stringer coupling system are calculated in equations (47) and (48). Hence, based on [4]; the applied stress values for different loading types (compression, tension and shear) are calculated as;

$$\sigma_{Butt-joint_{comp}} = \frac{(F_{butt-joint,x})_{compression}}{A_{EFF_BS}} \quad (56)$$

$$\sigma_{Butt-joint_{tension}} = \frac{(F_{butt-joint,x})_{tension}}{A_{BS_NET}} \quad (57)$$

$$\tau_{Butt-joint} = \frac{F_{butt-joint,y}}{A_{BS_NET}} \quad (58)$$

where A_{EFF_BS} is the effective area of the butt joint under compression, which based on equation (B.7) of Appendix B. Similarly A_{BS_NET} is the net area of the butt joint applicable under tension based on the equation (B.1) in Appendix B.

Reserve factor calculation for combined loads is performed by the structural analysis method based on [4], for combined tension/shear and compression/shear loads.

The Formula [4] for interaction of the combined loads is;

$$\left(\frac{\sigma_x}{\sigma_u}\right)^2 + \left(\frac{\sigma_y}{\sigma_u}\right)^2 - \frac{\sigma_x \times \sigma_y}{\sigma_u} + \left(\frac{\tau}{\tau_u}\right)^2 = 1 \quad (59)$$

Since in y direction in Figure 2.23; there is not axial load applicable for the butt-joints;

$$\sigma_y = 0 \quad (60)$$

$$\text{So; } \left(\frac{\sigma_x}{\sigma_u} \right)^2 + \left(\frac{\tau}{\tau_u} \right)^2 = 1 \quad (61)$$

$$\text{with } R_1 = \frac{\sigma_{butt-joint}}{\sigma_u}, R_2 = \frac{\tau_{butt-joint}}{\tau_u} \rightarrow R_1^2 + R_2^2 = 1 \quad (62)$$

The Reserve Factor is calculated as;

$$RF = \frac{1}{\sqrt{R_1^2 + R_2^2}} \quad (63)$$

2.2.2.13 Justification of the Fasteners on the Butt-Joint

The failure modes of the fasteners of the butt joint are same as the fasteners of the other parts investigated in this thesis. Based on [4]; total allowable force of each row of the butt-joint fasteners is calculated as the summation of the allowable forces of each single fastener of the corresponding fastener row calculated by equations (21) and (25);

$$F_{Riv_{allow,BS}} = \sum_{row} \left(F_{Riv_{Butt-joint/Skin}} \times n \right) \quad (64)$$

where “ $F_{Riv,Butt-joint/Skin}$ ” is the allowable force of a single fastener on the rivet row and “ n ” is the number of fasteners in the corresponding row.

The applied loads on each rivet row of the butt-joint/skin fasteners are calculated as;

$$F_{Riv_{appl}} = \beta \times F_{Butt-joint} \quad (65)$$

where “ β ” is the load share of the fastener row and $F_{Butt-joint}$ is the total load acting on the butt joint which is calculated in equation (49).

Finally the reserve factor of the butt-joint fasteners is calculated as;

$$RF = \frac{F_{Riv_{allow}}}{F_{Riv_{appl}}} \quad (66)$$

2.2.3 Finite Element Analysis Modeling Methods

2.2.3.1 Introduction

This thesis uses the package programs MSC/PATRAN[®] and MSC/NASTRAN[®] in the finite element modeling and analysis of the aircraft. MSC/PATRAN[®] version 2005r2 is used as the pre and post processor and MSC/NASTRAN[®] version 2005r2 is used as the processor. The applied loads used for the analysis and design of the stringer and frame couplings are obtained by using those programs under various loading conditions.

The basic properties of the upper shell finite element model, where the applied loads on the frame and stringer couplings are obtained, are;

- Skin segments are modeled by QUAD4 elements,
- Stringer segments are modeled by CROD elements,
- Frame segments are modeled by CBAR elements
- Nodes are located to the intersection points of frame and stringer elements.
- The finite element model is checked whether the requirements defined in Chapter 2.2.3.2 are satisfied or not.

2.2.3.2 Quality Assurance of the Finite Element Models

Each Finite Element Model is verified according to the following conditions below before used officially. Before each specific quality check, MSC/NASTRAN[®] Bulk Data are imported to the MSC/PATRAN[®] Deck so as to ensure that any errors in element connectivity, numbering and entity duplication.

2.2.3.2.1 Geometric Checks

These checks include the following basic model checks and can be done by the usage of MSC/PATRAN[®].

a) Coincident Nodes

This check is performed by using the command “Equivalence”; which is used to eliminate, the nodes located in the same coordinate with a user-defined tolerance and eliminating the undesired free edges.

b) Free Edges

The command “Verify/Element/Boundaries” is used to check the free edges of the surfaces and identify disconnections between two 2D elements. Free faces and free edges in the Finite Element Model are shown and proved that they are not connected to the other elements.

Finite Element Model check of the free edges of upper shell section of the developed transport, where the stringer and frame couplings within this thesis are located, are shown in Figure 2.24.

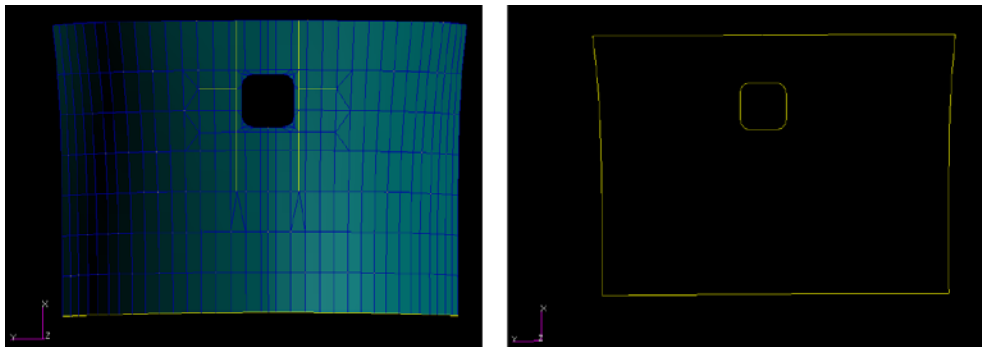


Figure 2.24: Free Edge Check for Upper Shell

It is seen from Figure 2.24 that, there is no free faces available in the Finite Element Model inside the upper shell, which means all the elements are well-connected.

c) Coincident Elements

The command “Verify/Element/Duplicates” is used to check for coincident elements, which shows and lists all the elements with the same nodal connectivity

and erases these duplications with the highest identification number. There can be planned duplications inside the Finite Element Model, but this check is aimed to be aware of the undesired duplications.

Finite Element Model check of Coincident Elements for the upper shell section of the developed transport, where the stringer and frame couplings within this thesis are located, are shown in Figure 2.25.

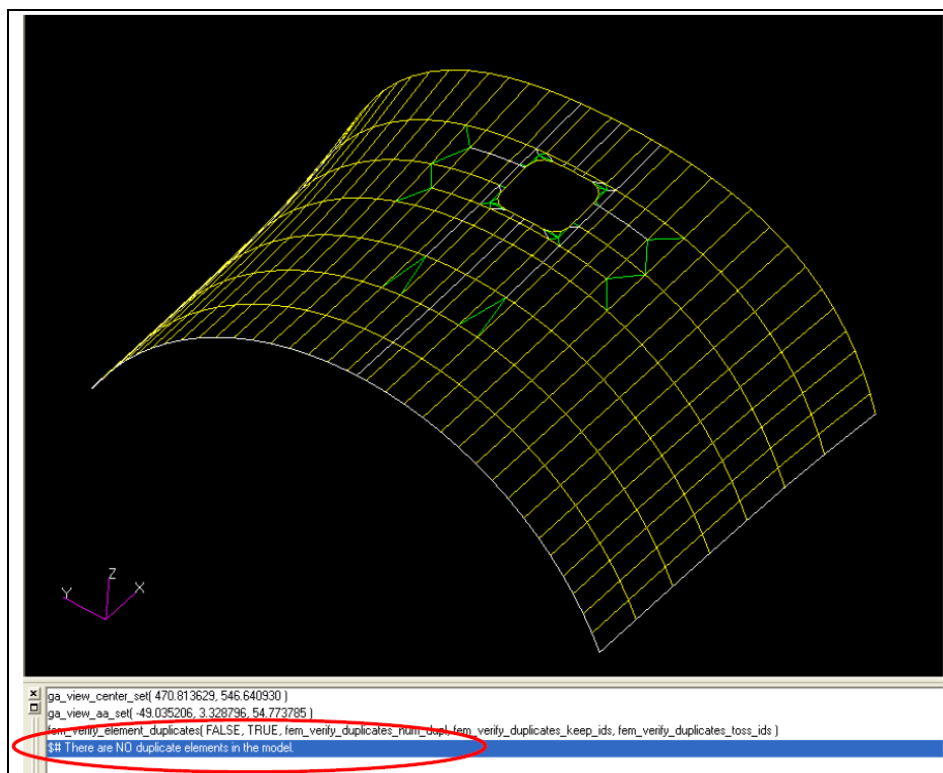


Figure 2.25: Coincident Elements Check for Upper Shell

There are not any specified duplicate elements in the finite element modeling of the upper shell hence; Figure 2.25 verifies that it is so.

d) Element Distortions

The command “Finite Element/Verify” is used to quality check for the element distortions. This process is mainly measurement of the divergence of the actual element from the ideal one. Based on the criteria proposed by MSC/PATRAN®, the worst element distortions must be kept away from the high stress concentration regions.

First parameter in terms of element distortions is the “aspect ratio” of the “QUAD4” and “TRIA3” elements. Elements with the aspect ratio smaller than 5 are recommended, and up to 10 is also acceptable. The aspect ratio calculation methods for the rectangular and triangular elements are shown in Figure 2.26.

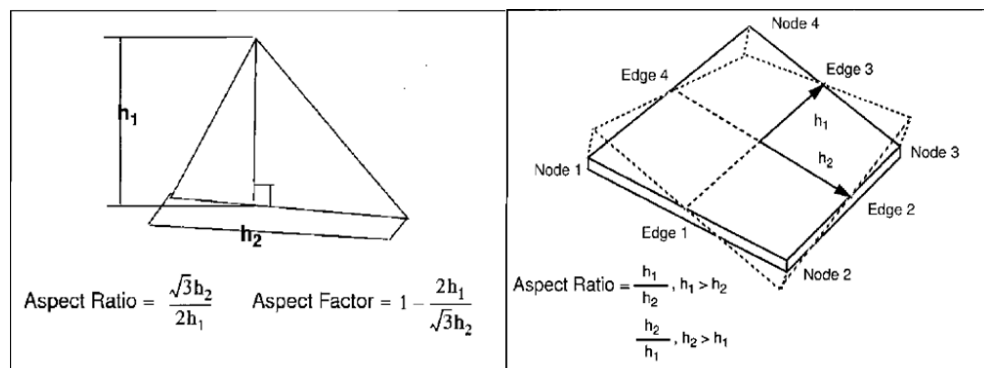


Figure 2.26: Aspect Ratio for TRIA3 and QUAD4 Elements

Finite Element Model check in terms of aspect ratio of the QUAD4 and TRIA3 elements used for upper shell section of the developed transport, where the stringer and frame couplings within this thesis are located, are shown in Figure 2.27.

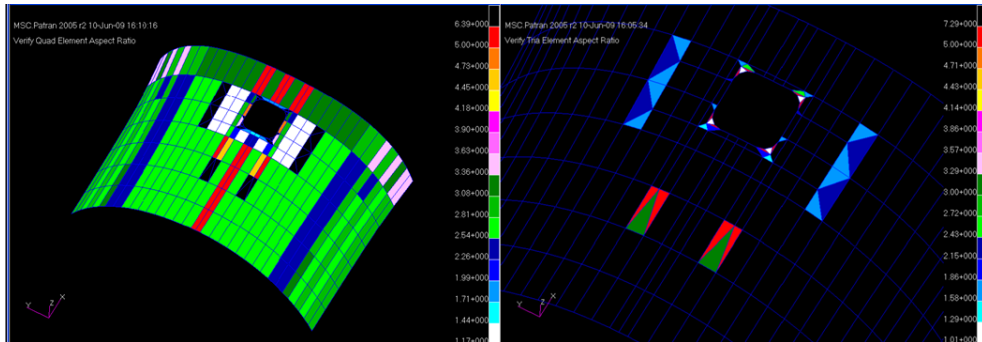


Figure 2.27: Aspect Ratio Check for Upper Shell

It is seen from Figure 2.27 that, maximum aspect ratio of the upper shell QUAD4 elements (on the left) is 6.39 and the maximum aspect ratio of the TRIA3 elements (on the right) is 7.29. Based on these results; the maximum aspect ratio for QUAD4 and TRIA3 elements are less than 10 hence; upper shell finite element model is sufficiently created from aspect ratio quality point of view.

Second parameter in terms of element distortions is the “Taper Ratio”. This ratio is calculated as shown in Figure 2.28.

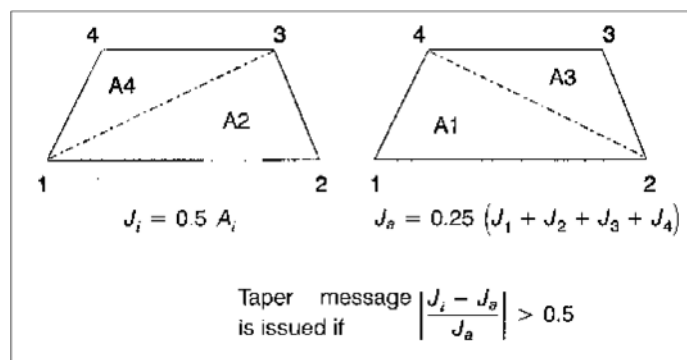


Figure 2.28: Taper Ratio for QUAD4 Elements

As a recommended value Taper Ratio should be less than 0.5. Taper Ratio check of Taper Ratio of the quad elements used within Finite Element Model of upper shell section of the developed transport, where the stringer and frame couplings within this thesis are located, are shown in Figure 2.29;

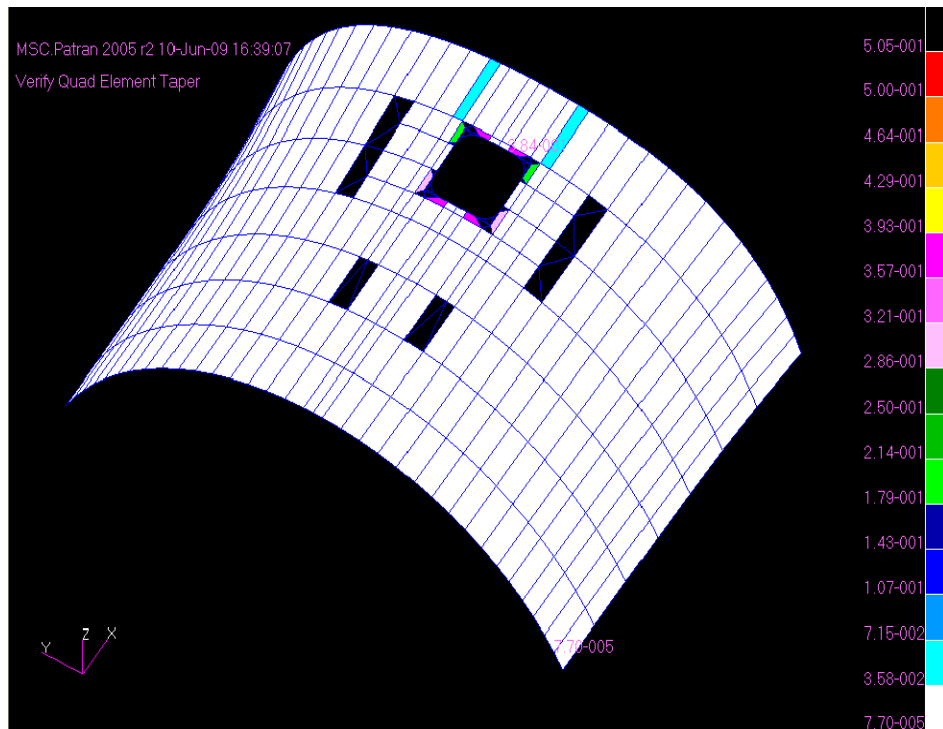


Figure 2.29: Taper Ratio Check for Upper Shell

In Figure 2.29, it is justified that maximum taper ratio for QUAD4 elements is 0.384 for upper shell FEM which is less than maximum allowable taper ratio (0.5).

e) Element Warping

The command “Finite Element/Verify/QUAD/Warp” is used to verify warping of rectangular elements. Angle of deviation with respect to the element plane is measured and warping angle is calculated as shown in Figure 2.30.

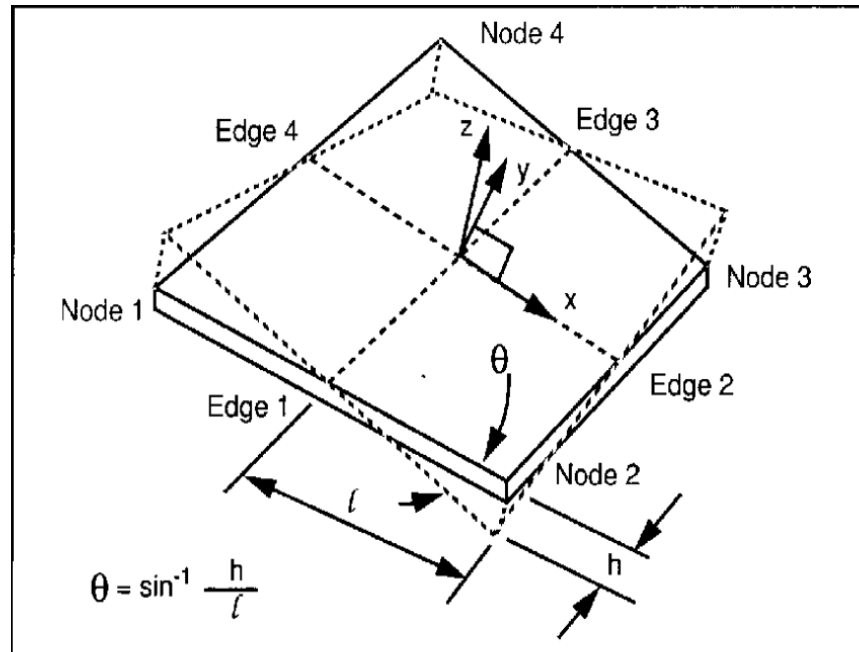


Figure 2.30: Warping Angle Calculation for QUAD4 Elements in MSC/PATRAN®

Recommended value to be checked for quad elements is “0.05” for warping angle. Check of warp angle of the quad elements used within finite element model of upper shell section of the developed transport, where the stringer and frame couplings within this thesis are located, are shown in Figure 2.31.

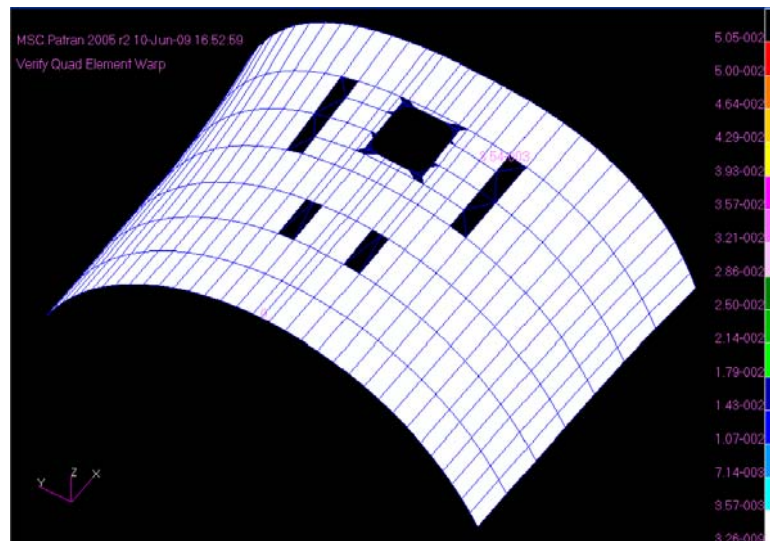


Figure 2.31: Warping Angle Check for Upper Shell

In Figure 2.31, it is justified that maximum warping angle for QUAD4 elements is 0.00354 in upper shell FEM; which is less than maximum allowable warping angle (0.05)

f) Internal Angle (Skew) and Skew Factor

The command “Verify/QUAD or TRIA/Skew” is used to verify internal angles of rectangular and triangular elements of the finite element model. Recommended value for this angle is to be greater than 30 degrees.

Skew factor is the ratio between the skew angle and 90 degrees. Recommended value for this factor is to be between 0 and 0.33. Elements having larger internal angles should be kept away from the high stress concentration regions in the finite element model. Skew angle and Skew factor calculation is represented in Figure 2.32.

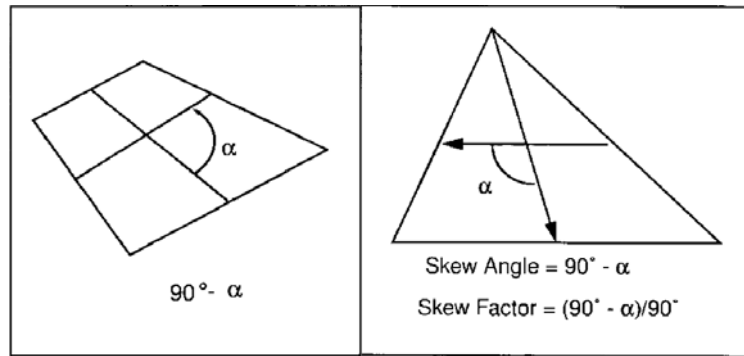


Figure 2.32: Skew Angle and Skew Factor for TRIA and QUAD Elements

Skew Angle and skew factor of the quad elements used within the Finite Element Model of upper shell section of the developed transport, where the stringer and frame couplings within this thesis are located, are shown in Figure 2.33.

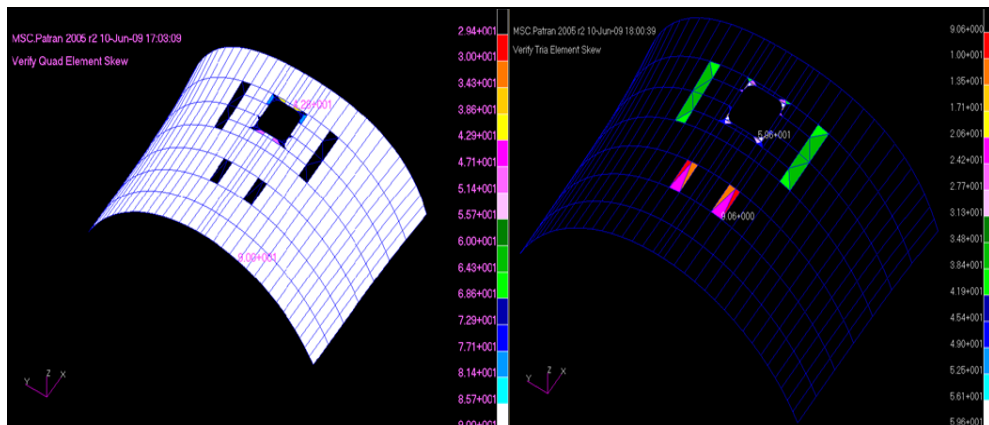


Figure 2.33: Internal Angle Check for Upper Shell

In Figure 2.33, it is shown that the minimum QUAD4 element skew angle (on the left) is 42.8 degrees; which is greater than minimum allowable skew angle (30 degrees).

Minimum skew angle of upper shell TRIA3 elements (on the right) is ~10 for two elements which are far away from the high stress concentration region, hence they are acceptable. Instead of those two, the minimum skew angle for the other TRIA3 elements is 31.4 degrees which is less than 30 and hence they are also acceptable.

g) Rigid Elements and MPCs

Multi Point Constraints (MPC) and rigid elements are mainly equations defining relationships between degrees of freedom of different nodes. These MPCs or rigid elements are verified that they do not produce changes to local load paths due to incorrect or undesired stiffness values. MSC/PATRAN® menu, “Finite Element/Show/MPC” or “Utilities/Display/Show/MPCs”, are used to verify this relationship.

h) Element Connectivity

By this verification, correct element force interpretations and correct pressure load application are ensured. The command “Utilities/FEM Elements/Modify 2D Connectivities” is used to check the connectivity. By this comment, connectivity for 2-dimensional elements are checked by displaying vectors between the first and the second node of each element.

i) Element Offsets

Element offsets are checked in BAR/BEAM and QUAD4/TRIA3 to verify the correct application in the Finite Element Model. MSC/PATRAN® command “Display/LBC/Element Properties/Beam Display 1D Line + Offset” are used for this process.

j) Element Co-ordinate Systems

For the correct interpretation of element stresses, forces and strains, the direction of the element co-ordinate systems are checked. MSC/PATRAN® option “Utilities/Display/Finite Element Coordinate Frames” are used to display the element co-ordinate systems.

2.2.3.2.2 The Static Checks

Some static analysis of the developed Finite Element Model of the upper shell section is performed to determine the load paths, deformations and local stresses. The model and boundary conditions are assessed by these checks which are shown in Figure 2.34.

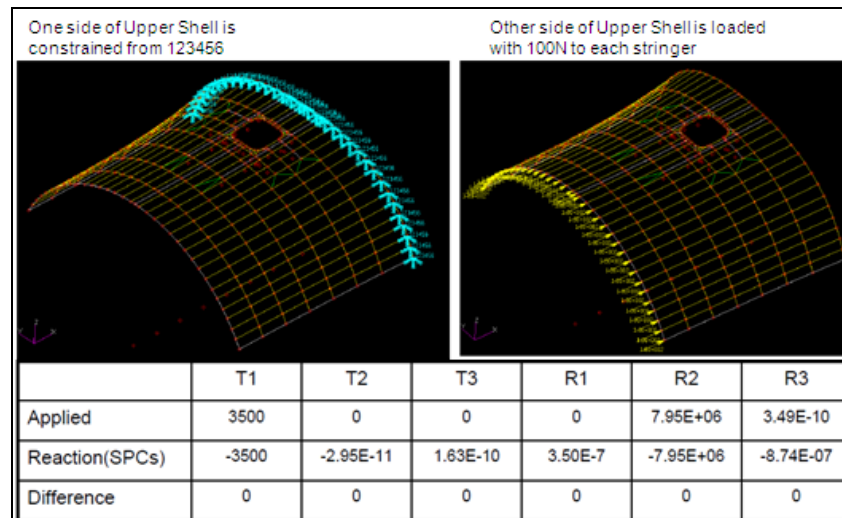


Figure 2.34: The Results of the Static Check for Upper Shell.

The results of the static checks do not reveal any significant problem in the model.

2.2.3.2.3 The Dynamic Checks

Similarly; some dynamic checks are also performed to confirm that all the nodes within the Finite Element Model are adequately connected to the structure. Those checks also reveal that there are not any mechanisms or low stiffness areas. These checks are performed by using the “SOL 103” solution module of MSC/NASTRAN® in which the Lanczos Method is used.

Lanczos Method is a way to find the Eigen-values of a large matrix.

These checks are performed via three steps, which are expressed as follows;

- (i) Calculation of rigid body modes within the range of -1 to +1 Hertz with the free Finite Element Model in the space and with moving surface or actuators are connected: There must be 6 modes (3 for translation and 3 for

rotation) that frequencies should be very small, nearly zero. Maximum frequency should be $f < 0.01$ Hertz.

(ii) Calculation of Rigid Body modes within the range of 0 to +1 Hertz for the Finite Element Models including movable surfaces and free in the space and the actuators are disconnected: There must be 6 rigid body modes and 1 rotation at 0 Hertz for each movable surfaces.

(iii) Calculation of first 15 flexible modes of the Finite Element Model free and the actuators are disconnected: Standard frequency range is 1 to 40 Hertz. Local and artificial modes, and flexible modes of structure modeled are detected by this calculation.

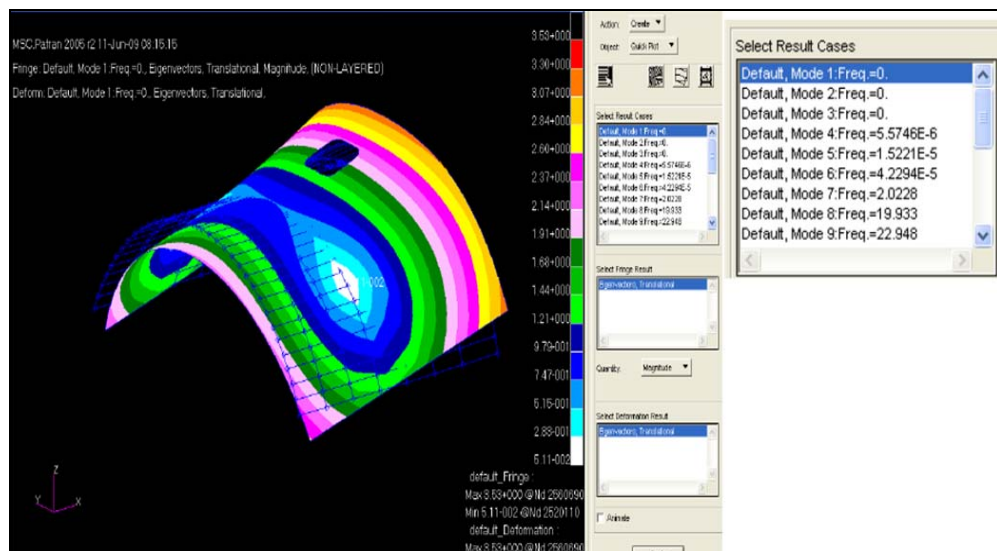


Figure 2.35: Dynamic Check for Upper Shell

The result of the upper shell Finite Element Model in Figure 2.35 shows that all nodes are adequately to the structure and there is not any low stiffness area since the first 6 modes are very near to zero.

2.2.3 Material Specifications

The specifications for the materials used in the design of the frame and stringer couplings are obtained from the known reference, which is American Military Handbook “Metallic Materials and Elements for Aerospace Vehicle Structures” [8].

The specifications of the materials in those references include;

- Form of the material such as Extrusion, Sheet Metal, Plate Metal.
- Temper of the material
- Cross-sectional area, thickness or diameter variations
- Mechanical Properties such as Tension or Compression Yield Stress, Tension or Shear Ultimate Stress, Bearing Ultimate and Yield Stress, Elastic and Shear Modulus, Poisson’s Ratio.
- Basis of the material such as A, B, S, T Basis.

Based on the certification specifications for large airplanes (CS-25) [5]; the material strength properties to be used in structural analysis, are based on enough tests of the material meeting approved specifications. The correct basis of the material design values should be chosen in order to minimize the structural failures due to the material variability.

The selection of the correct basis of the material design values depends on the configuration of the structural components on the aircraft. This variation in configuration is divided into two main parts according to the load path on the structural elements.

i) For redundant structures, the failure of the specific elements resulting in safely re-distribution of applied loads to the adjacent structural elements with 90% probability and 95% confidence based on test results. These structures are “Multi-Load Path” structures, for which B basis are used as the material specifications.

ii) When the applied loads are distributed through a single member, which could result in loss of structural integrity of the component with 99% probability and 95% confidence. These structures are “Single-Load Path” structures, for which A basis are chosen as the material specifications.

The important parts of CS-25 related to material specifications [5] were excerpted in Appendix C.1 for the completeness of the study.

In addition to the material properties and allowable, some special factors should be used for structural analysis. Based on CS-25 [5] while calculating reserve factors for some specific failure modes if;

- The structural strength of the aircraft component is uncertain, or
- The structural strength of the aircraft component is likely to deteriorate in service before replacement, or
- There is variability in terms of manufacturing processes or inspection methods.

There are three types of special factors to be applied;

- i) Casting Factors: Factors for casting materials defined based on inspections, tests, deformation requirements, etc.
- ii) Bearing Factors: Factors for joints having clearance (free fit) defined based on pounding and vibration.
- iii) Fitting Factors: Factors for joints to be applied to the fitting itself, means of attachment and bearing of the joined members.

The values of the special factors to be followed within this thesis are decided according to the company principles, which are appropriate to the certification specifications.

2.3 Loads and Loads Selection Criterion

For the structural design and the structural analysis of the aircraft, two definitions for loads are available. The first one is the “limit load” which is the maximum load to be expected in the service life of the aircraft and the second one is the “ultimate load” which is the limit load multiplied by specific factors of safety. This factor of safety is defined as “1.5” based on Certification Specifications (CS-25) for large civil/transport aircrafts [5].

As specified in military or civil certification specifications, $2\Delta P$ (1101.4 HPa) pressure, flight, ground, water (ditching) and tactical loads for to be developed transport aircraft must be placed in equilibrium with inertia forces by taking into account the mass distribution of the aircraft.

Accuracy of the calculated loads and the mass distribution applicable on the aircraft should be verified by flight or ground test measurements.

2.3.1 Verification of Loads

Verification of the generated loads applied to the aircraft structure was performed based on CS-25 [5]. The relevant and important parts of CS-25 related to load verification [5] were excerpted in Appendix C.2 for the completeness of the study.

The quoted passage from the certification specifications [5], in Appendix C.2, briefly explains the approach used in load verification process of a standard aircraft. This process is crucial from design and analysis point of view, since airworthiness and certification of the aircraft is accepted based on the structural

analysis results in which flight, ground, etc. loads are used as applied loads. Hence; correct loads have to be used in structural analysis calculations.

Another topic, besides the application of the correct loads, is the decision of correct load selection criterion for the corresponding structural part of the aircraft. Normally different parts of the aircraft give different response under same loading condition. For example, for a vertical down bending of fuselage, for which landing is a typical example, skin of upper shell of the aircraft is under tension, whereas skin segment of the lower shell is under compression loads. Actually; it is multi-disciplinary engineering with aerodynamics, flight physics, structural analysis and tests groups all involved and investigated the response of the aircraft structural components under each type of flight, ground loadings. Based on the observations on the structural response of the aircraft components, critical loadings for each part were discovered. Hence; structural analysis job finished by taken these loadings into consideration. Otherwise, structural analysis will be performed based on all the loads calculated according to the aircraft requirements. Thinking about the very high number of load cases (millions), it would be impossible to finish the aircraft project. With the help of the decision of the critical load selection criterion for each structural component, this number falls to acceptable amount of load cases; which are feasible to perform the structural analysis work in time.

Below, brief information about the different loading conditions were given and the effects that frame and stringer coupling regions of to be developed aircraft were investigated.

2.3.2 Aircraft Load Types and The Effects on Frame and Stringer Couplings

Load conditions for the developed transport are divided into below main parts as below;

A: Ground Loads

- Symmetric Landing Loads
- Book Cases
- Dynamic Taxiing Cases

B: Flight Loads (Ramp Open or Ramp Closed)

- Maneuver Cases (Lateral, Vertical)
- Gust and Turbulence Cases (Lateral, Vertical, etc.)

Each group have different characteristic effect on the fuselage of the developed transport, which means the response of the aircraft in terms of displacement, stress or force distribution through the fuselage is characteristically different for each loading type. In addition, based on the certification specifications CS-25 [5], all load types defined above are subjected to the structure with and without temperature and pressure additions.

As mentioned before, choosing the most critical loads among all the loading conditions in the load loop created by flight physics teams is one of the crucial missions of the structural analyst of the component. For the frame and stringer coupling components that are developed within this thesis, the relation between the internal loads and reserve factors is investigated in details so as to find out the correct load selection criterion.

The load selection criterion chosen for the corresponding frames and stringers have the major role in decision of the load case criteria selections.

For the explanations above, it is better to clarify the relation between the internal loads and reserve factors in more details;

Reserve Factor is the margin of safety of the structural component,

Internal Loads are the force and moments that an arbitrarily chosen cross-section of the fuselage has, under a specific loading condition. For a better feeling about the internal loads, sign conventions are available in Figure 2.36.

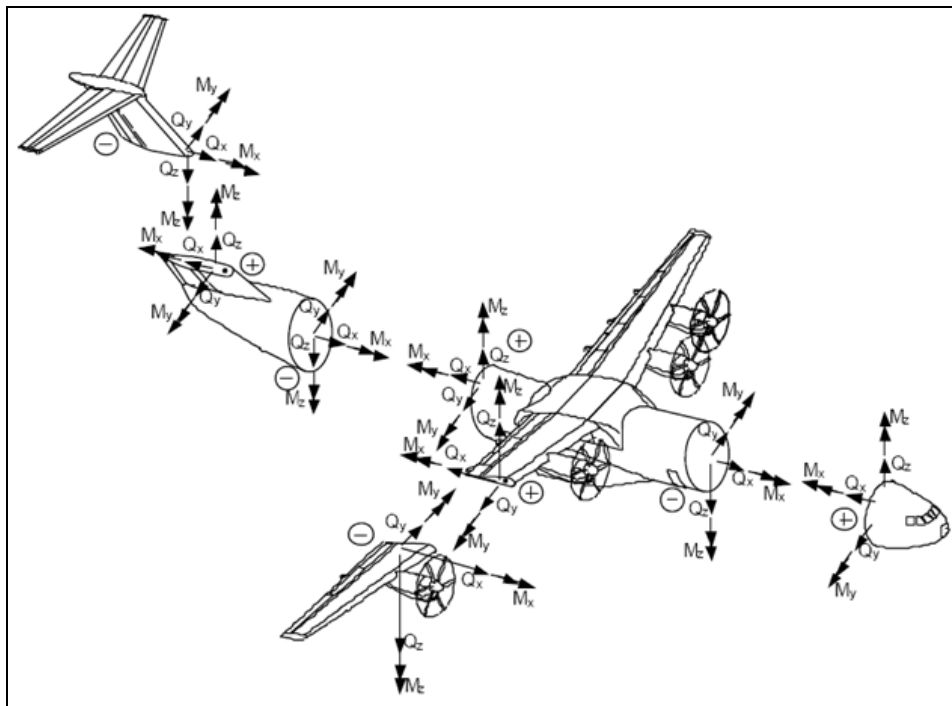


Figure 2.36: Sign Convention for Loads [4]

Based on Figure 2.36; for rear fuselage part;

$Q_x > 0$ Tensile Load

$Q_y > 0$ Shears the tail toward the right

$Q_z > 0$ Shears the tail upwards

$M_x > 0$ Right wing up

$M_y > 0$ Compression in the lower fuselage

$M_z > 0$ Compression in the right side

Right Hand Side and Left Hand Side of the aircraft are defined while looking from behind of the fuselage to the nose part.

Finding the relation between the reserve factors and the internal force and moments of the fuselage cross-sections and deciding the most critical load cases based on this relation was a quite new approach to be followed in the aircraft industry. With the helping of the internal force and moments, load envelopes were drawn for the chosen cross-sections. Based on the reserve factors for the structural components, maximum load envelope borders showing that the structure is safe inside of these borders were plotted.

These envelopes either were one-dimensional (e.g. max. M_y at frame position C51, min. F_z at frame position C42) or can be combination of two or more force or moment loads (e.g. M_y-F_z , F_x-M_z , F_x-F_y)

Below, brief information of the aircraft loading conditions were given so as to have a feeling about the characteristics of the aircraft loads, the response of the aircraft under these loadings and the critical load case selection criterion for the rear fuselage upper shell frame and stringer couplings to be developed within this thesis. Derivation and the application of the load conditions; which were explained below based on CS-25 [5] are out of scope of this thesis.

2.3.2.1 Symmetric Landing

Based on the Certification Specifications CS-25 [5] and the military requirements agreed for the developed transport; the aircraft is assumed to contact the ground with a limit descent velocity of 10fps (civil certification requirement) and 12fps (military certification requirement) at the design landing weight (maximum weight for landing conditions at maximum descent velocity). In addition it is also assumed to contact the ground with a limit descent velocity of 6fps at the design take-off weight (the maximum weight for landing conditions at a reduced descent velocity).

Based on Certification Specifications [5]; while calculating the landing loads;

- i) Landing gear dynamic characteristics,
- ii) Spin-up and spring back,
- iii) Rigid Body Response,
- iv) Structural dynamic response of the airframe,

were taken into consideration within the methods of analysis of the aircraft and the landing gear loads.

The response and the load path of the aircraft structure under symmetric landing condition are illustrated in Figure 2.37.

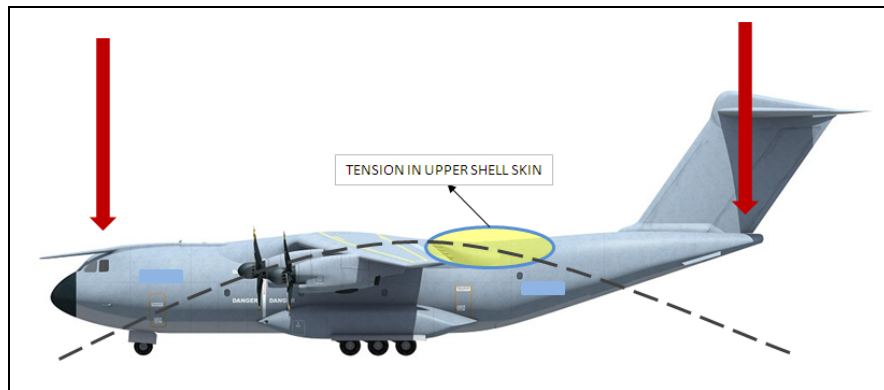


Figure 2.37 Load Distribution in Symmetric Landing Load Cases [3]

As it is understood from Figure 2.37; significant property of symmetric landing cases is the M_y and F_z distribution along the fuselage. This is called the “vertical down bending” of the aircraft and tension loads occurs in the rear fuselage upper shell region. This means that the skin and the stringer coupling segments are loaded in tension and hence the inner flange segments of the frame coupling of the upper shell are compressively loaded.

Actually; another characteristic of the symmetric landing cases is that the payload distribution that is taken into account over the fuselage sections that frame and stringer coupling are included. In Figure 2.38, additional moment created by payload and the effect of this moment is illustrated.

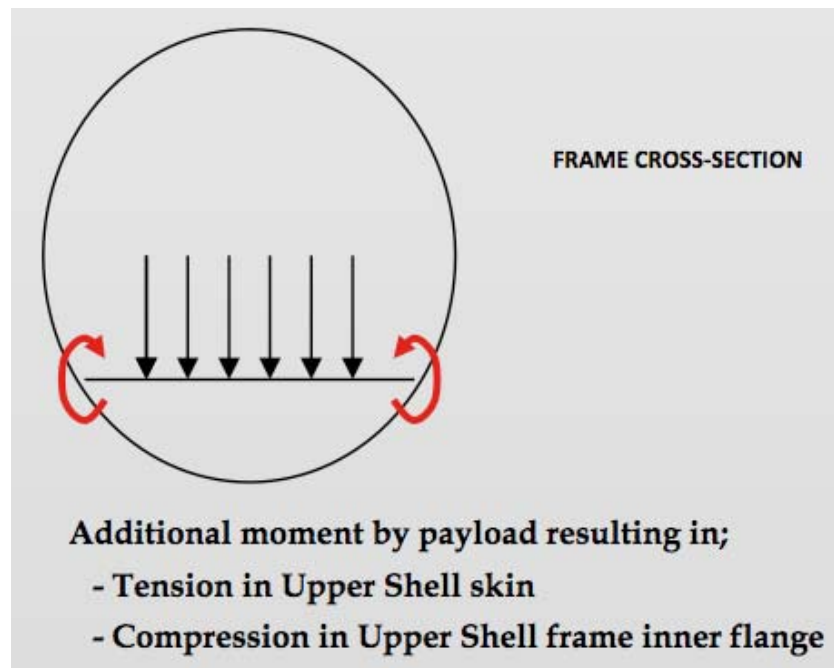


Figure 2.38: Payload Effect on Frame Cross-section

In addition, deformation plot of the aircraft under symmetric landing cases is given in Figure 2.39. This deformation plot is obtained from Finite Element Analysis and showing the undeformed shape of the aircraft in purple and the deformed part in blue.

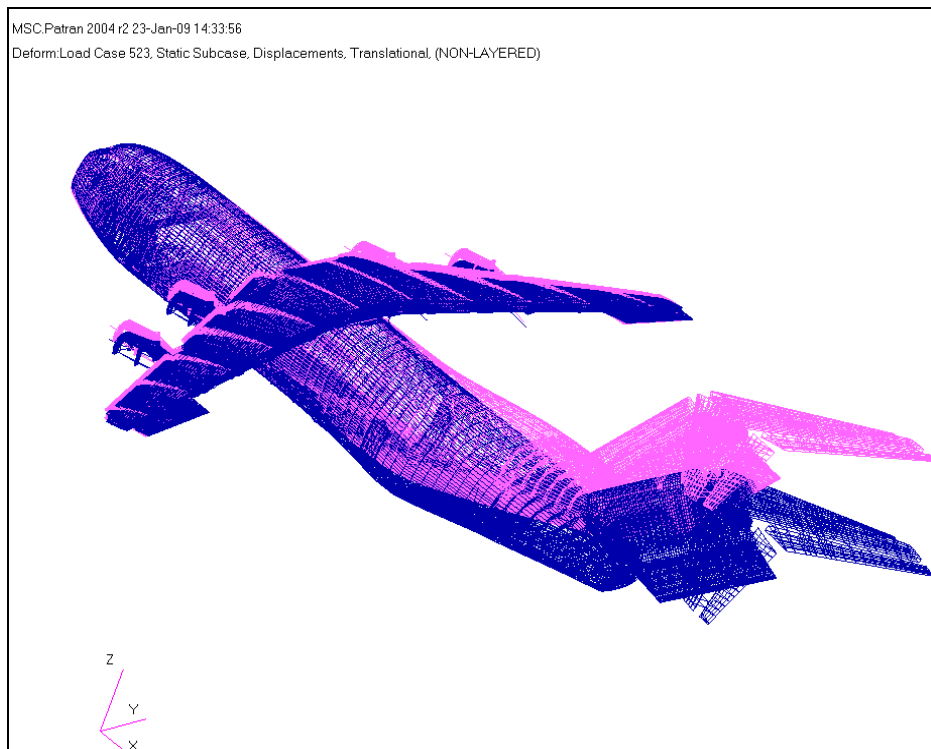


Figure 2.39: Deformation Plot for Symmetric Landing Cases

2.3.2.2 Static Ground

Static ground cases, also defined as “book cases”, consist of loading conditions derived directly from the Certification Specifications [5].

These load cases are divided into sub-groups listed below;

- i) Three component landing rebounding
- ii) Drift Landing
- iii) One wheel landing
- iv) Maximum spring back
- v) Maximum spin up load
- vi) Maximum vertical load
- vii) Braked roll condition
- viii) Side slip
- ix) Turning, pivoting, steering
- x) Take off run, taxi
- xi) Towing
- xii) Picketing

Below, brief explanations for each sub-group of load cases are given;

Rebound Landing Condition: Based on the Certification Specifications [5], the landing gear and its supporting structure must be investigated for the load occurring during rebound of the aircraft from the landing surface.

Drift Landing: Based on the Certification Specifications [5], lateral drift landing and side load conditions are considered as “drift landing”. The most severe combination of loads that are likely to arise during a lateral drift landing must be taken into account. In absence of a more rational analysis of this drift landing condition two considerations should be followed described below;

- i) Vertical load equal to 75% of maximum ground reaction of symmetric landing described in the Certification Specifications [5], must be considered in combination with a drag and side load of 40% and 25% respectively, of the corresponding vertical load.
- ii) The shock absorber and tyre deflections must be assumed to be 75% of deflection corresponding to the maximum ground reaction of symmetric landing described in the Certification Specifications [5].

In addition, based on the Certification Specifications [5] the following two requirements should also be considered;

- i) For the side load condition, the aircraft is assumed to be in the level altitude with only the main wheels contacting the ground.
- ii) Side loads of 0.8 of the vertical ground reaction (on one side) acting inward and 0.6 of the vertical reaction (on the other side) acting outward should be combined with one-half of the maximum vertical ground reactions obtained in the level landing conditions. These loads are assumed to be applied at the ground contact point and to be resisted by the inertia of the aircraft.

One-wheel Landing: Based on the Certification Specifications [5]; for one-gear landing conditions, the aircraft is assumed to be in the level altitude and contact the ground on one main landing gear as shown in Figure 2.40. In this attitude;

- i) The ground reactions should be same as the maximum vertical ground reaction combined with an aft acting drag component of not less than 25% of this maximum vertical ground reaction.
- ii) Each unbalanced external load should be reacted by aircraft inertia in a rational or conservative manner.

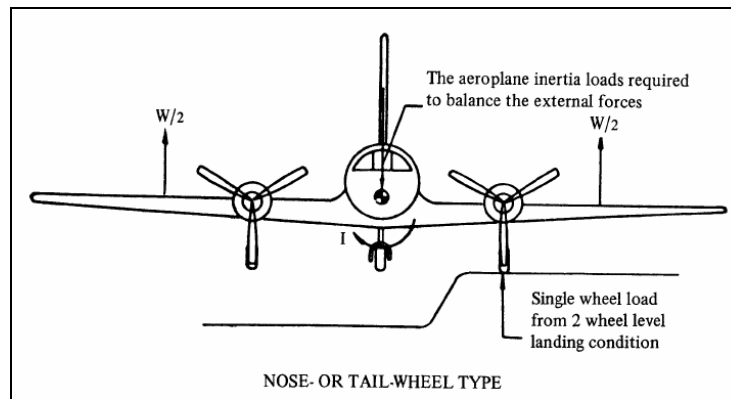


Figure 2.40: One-wheel Landing [5]

Maximum Spring Back, Spin Up and Vertical Loads are the book cases sorted by dynamic landing load cases.

Braked Roll Condition: Based on the Certification Specifications [5]; for an aircraft having a nose wheel, limit vertical load factor is 1.2 at the design landing weight, and 1.0 at design ramp weight as shown in Figure 2.41. A drag reaction equal to the vertical reaction, multiplied by a coefficient of friction of 0.8 should be combined with the vertical reaction and applied at the ground contact point of each wheel with brakes.

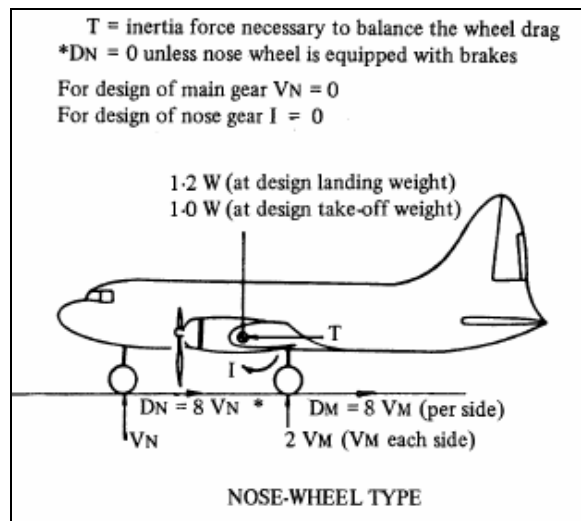


Figure 2.41: Braked roll Condition for Nose Wheel Type Aircraft [5]

In addition; an aircraft with a nose wheel should be designed to withstand the loads arising from the dynamic pitching motion of the aircraft due to sudden application of maximum braking force. The aircraft is considered to be at design take-off weight with the nose and main wheels in contact with the ground, and with a steady state vertical load factor of 1.0. The steady state nose wheel reaction must be combined with the maximum incremental nose wheel vertical reaction caused by sudden application of maximum braking force.

Side slip and Steering: Side slip in ground load conditions means the nose wheel yaw of the aircraft. Based on the Certification Specifications [5]; with the aircraft assumed to be in static equilibrium with the loads resulting from the use of brakes on one side of the main landing wheel, the nose wheel, its attaching structure and the fuselage structure forward of the center of gravity should be designed for the nose-wheel yaw load cases described in [5].

In addition, with the aircraft at design ramp weight, and the nose wheel in any steerable position, the combined application of full normal steering torque and vertical force equal to 1.33 times the maximum static reaction on the nose wheel should be considered in nose wheel design, its attaching structure and the forward fuselage structure.

Turning and Pivoting: According to the Certification Specifications [5]; the aircraft structure should be able to withstand an execution of a steady turn by nose wheel steering, or by application of sufficient differential power, so that the limit load factor applied at the center of gravity are 1.0 vertically and 0.5 laterally. The side ground reaction of each wheel must be 0.5 of the vertical reaction as shown in Figure 2.42.

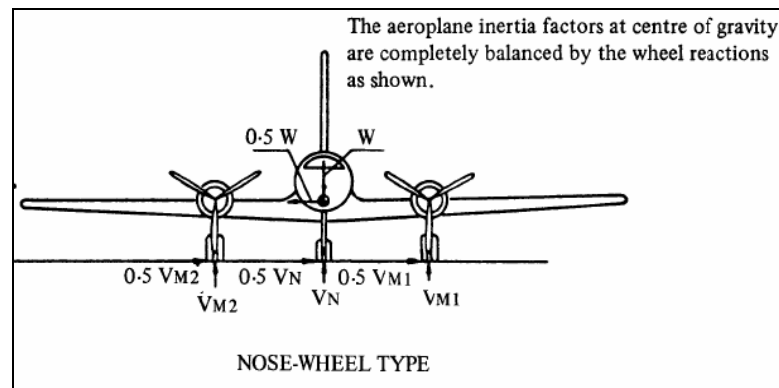


Figure 2.42: Ground Turning of the Aircraft with Nose Wheel [5]

In addition; based on the Certification Specifications [5]; the aircraft is assumed to pivot about one side of the main wheel with the brakes on that side locked. The limit vertical load factor should be 1.0 and the coefficient of friction should be 0.8.

Furthermore; the aircraft is assumed to be in static equilibrium with the loads being applied at the ground contact points based on Figure 2.43.

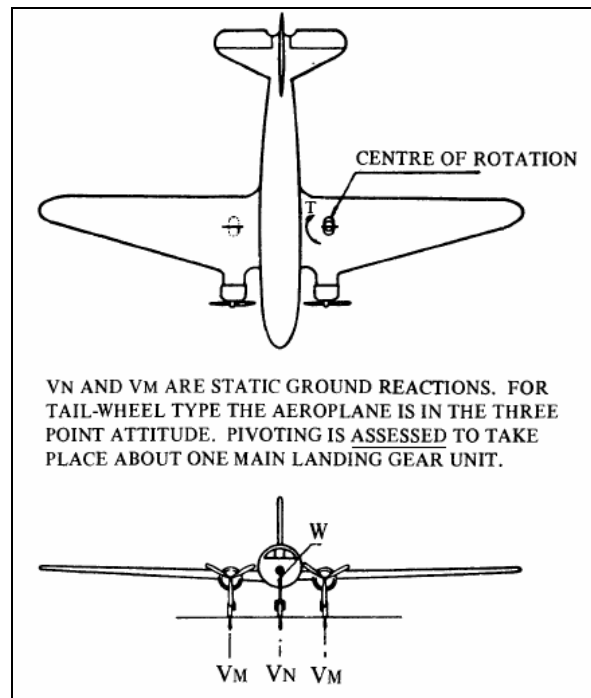


Figure 2.43: Static Equilibrium on Pivoting Situation [5]

Take-off Run and Taxi: Based on Certification Specifications, [5]; within the range of appropriate ground speeds and approved weights, aircraft structure and the landing gears should be able to withstand the loads not less than those obtained when the aircraft is operating over the roughest ground that may reasonably be expected in normal operation.

The static ground loading conditions result in lateral loads, lateral moment and torque on the rear fuselage of the aircraft as seen in Figure 2.44.

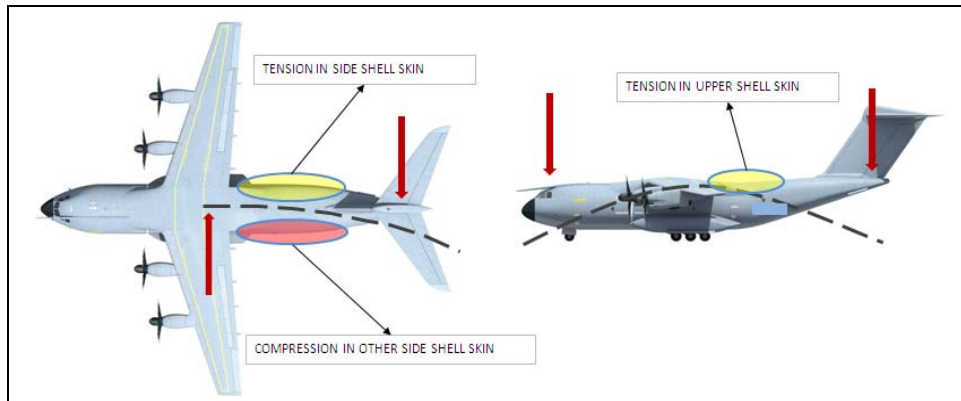


Figure 2.44: Load Distribution of Static Ground Cases. [3]

Additionally; the deformation plots obtained by Finite Element Model Analysis represent the response of the aircraft as shown in Figure 2.45.

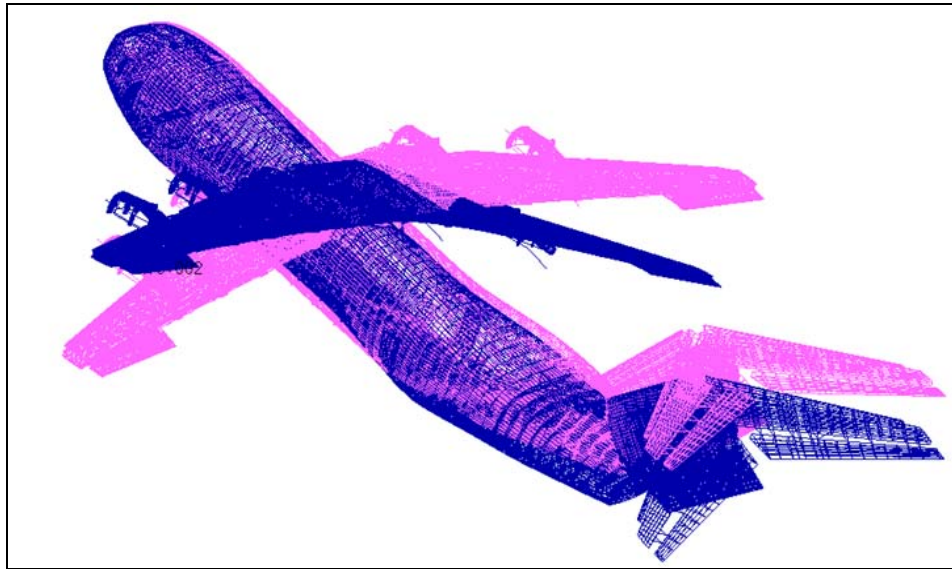


Figure 2.45: Load Deformation Plot for Static Ground Cases

Vertical moment and vertical shear result from the landing conditions creates tensional loading in the upper shell skin and stringers and compressive loading in the frame inner flange regions, similar to the symmetric landing case. In addition to the vertical shear force and the vertical moment on the rear fuselage cross-section, lateral shear force, lateral bending moment and torsion is also available for the static ground load cases. Main actor in the rear fuselage cross-section is observed as the lateral shear force and the lateral moment. This lateral shear have less effect on the stringers, since stringers are stiffeners in longitudinal condition, but frame segments are generally affected because of the occurrence of the higher axial force, shear force and bending moment in the frame cross-sections for the static ground loads.

2.3.2.3 Static Flight (Cruise, Approach)

Clean and not clean balanced vertical maneuvers ($n_z = 1.0g - 1.2g$) with airbrakes on or off configurations represent the static flight cases. Based on [5], for the analysis of the maneuvering flight load conditions the following provisions should be applied;

- i) While a sudden displacement of a control is specified, the assumed rate of control surface displacement may not be less than the rate that could be applied by the pilot through the control system.
- ii) In determining the elevator angles and chordwise load distribution in the maneuvering balanced and maneuvering pitching conditions, the effect of corresponding pitching velocities should be taken into account.

The most critical static flight cases for the rear fuselage upper shell were observed as the static flight cases with the flaps deployed configuration. Main reason for this is the fact that, these loads create maximum tension in rear fuselage upper shell skin and hence, compression in frame coupling inner flange segments by the positive M_y and negative F_z internal force combination for the corresponding cross-section. Also, with the contribution of the delta pressure which creates additional tension on the skin segments of the upper shell, load case becomes more critical than the other vertical maneuver cases.

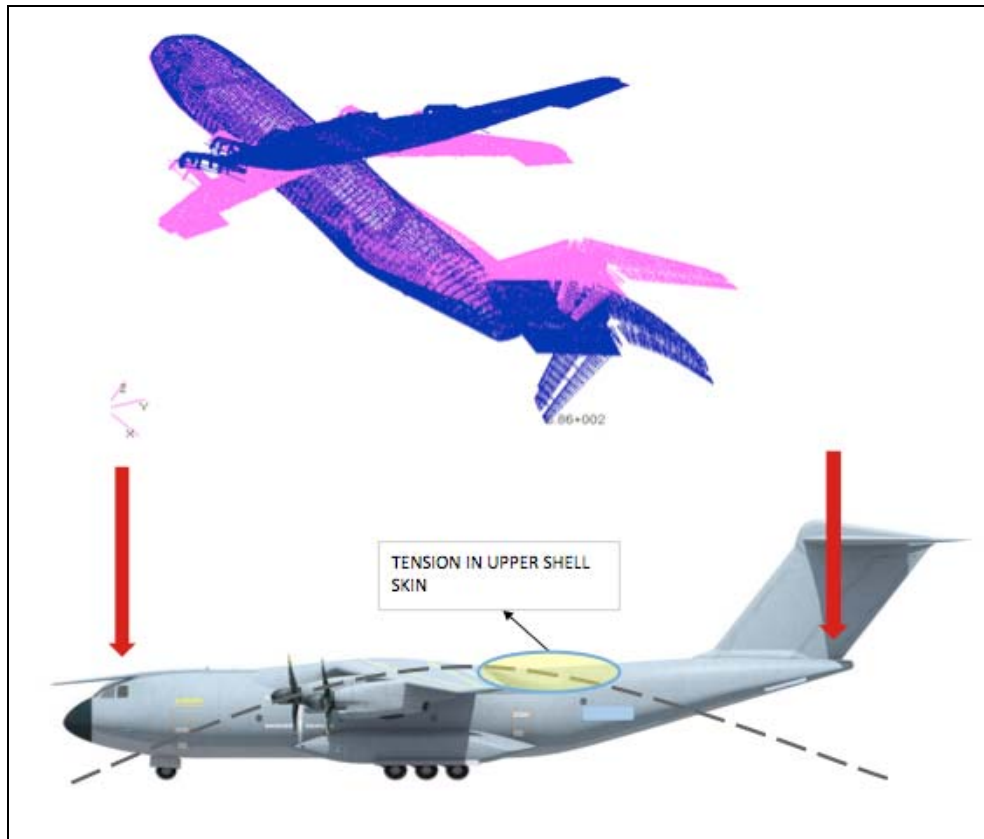


Figure 2.46: Loading and Deformation Plot of Aircraft under Static Flight Loads

[3]

Static flight load cases mainly cause the same load path on the upper shell as the symmetric landing cases as shown in Figure 2.46. The main difference of these cases is the internal pressure that the aircraft has during flight. This internal pressure creates additional tension on the upper shell skin. Hence; this cases were more critical with less vertical moment and shear values on the frame cross-section with respect to the symmetric landing cases.

2.3.2.4 Maneuver Load Cases

Static flight cases explained in 2.3.2.3 consist of vertical maneuvers; which create vertical bending and vertical shear on the fuselage. There are also other critical maneuver cases that creating lateral bending, torsion and lateral shear on the fuselage. These are mainly lateral or rolling maneuver cases, which are;

- i) Yawing maneuver
- ii) Lateral one engine out maneuver
- iii) Dutch-roll excitation
- iv) Rolling maneuver
- v) Rolling clean military maneuver

Yawing maneuver cases are the loads resulting from the yaw maneuver conditions at speeds from the minimum control speed with the critical engine inoperative (V_{MC}) to the design dive speed (V_D). Based on CS-25 [5]; unbalanced aerodynamic moments about the center of gravity should be reacted in a conservative way considering the aircraft inertia forces. The yaw maneuver conditions expressed above could be specified in four ways based on [5] as follows;

- i) With the aircraft in unaccelerated flight at zero yaw, it is assumed that the rudder is suddenly displaced so that the control system stops,
- ii) With the rudder is deflected so always maintain the maximum rudder deflection available, it is assumed that the aircraft yaws to the overswing sideslip angle,
- iii) With the aircraft yawed to the static equilibrium sideslip angle, it is assumed that the rudder is held to achieve the maximum rudder deflection available
- iv) With the aircraft yawed to the static equilibrium sideslip angle, it is assumed that the rudder is suddenly returned to neutral.

Lateral one engine out maneuver is the yaw maneuver having the same definitions and requirements described for the yawing maneuver, but with one of the engines of the aircraft is inoperative.

Dutch-roll excitation is a special requirement based on military specifications which effects the aircraft while air-to-air refueling. This excitation creates lateral shear and lateral bending in the fuselage cross-section.

Rolling conditions create torsion and lateral shear to the aircraft. Based on CS-25 [5]; the aircraft should be designed for loads resulting from the rolling conditions of maneuvering or unsymmetrical gust conditions.

Among these maneuver cases; the one engine out maneuver cases were found as the most critical load cases for the rear fuselage upper shell that create the maximum lateral bending and lateral shear in the fuselage cross-section. The load path on the rear fuselage upper shell and the corresponding deformation plot of the aircraft for one engine out cases are seen in Figure 2.47.

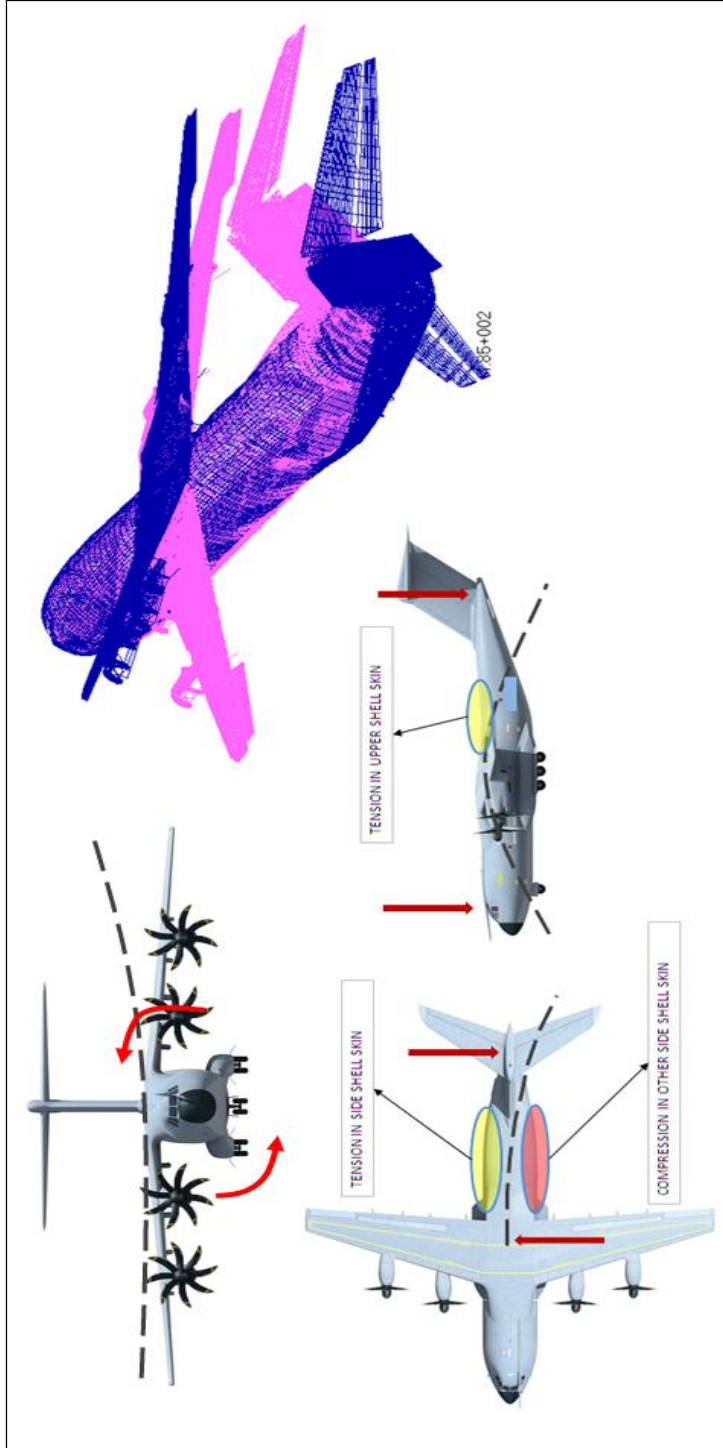


Figure 2.47: Loading and Deformation Plots for One Engine Out Loads [3]

2.3.2.5 Gust and Turbulence Conditions

As a design criterion, analysis should be conducted to determine the gust response loads for the aircraft throughout its design envelope, where the design envelope is taken to include all combinations of aircraft configuration, weight, center of gravity, payload, fuel load, thrust, speed and altitude. Based on CS-25 [5]; the modeling parameters for the Gust response analysis include;

- i) Design conditions and associated steady, level 1-g flight conditions,
- ii) The discrete and continuous gust models of atmospheric turbulence,
- iii) Detailed representation of the aircraft system including structural dynamics, aerodynamics, and control system modeling,
- iv) Solution of the equations of motion and the extraction of response loads,
- v) Considerations for non-linear aircraft systems,
- vi) Analytical Model Validation Techniques

Aircraft has to be able to withstand loads with the gust increments mentioned above which can result in lateral or vertical loads or even combination of these two.

The vertical gust and turbulence cases resulted in vertical shear and vertical bending, and similarly the lateral gust and turbulence cases result in lateral bending, torsion and lateral shear in the rear fuselage cross-section as shown in the deformation plots in Figure 2.48.

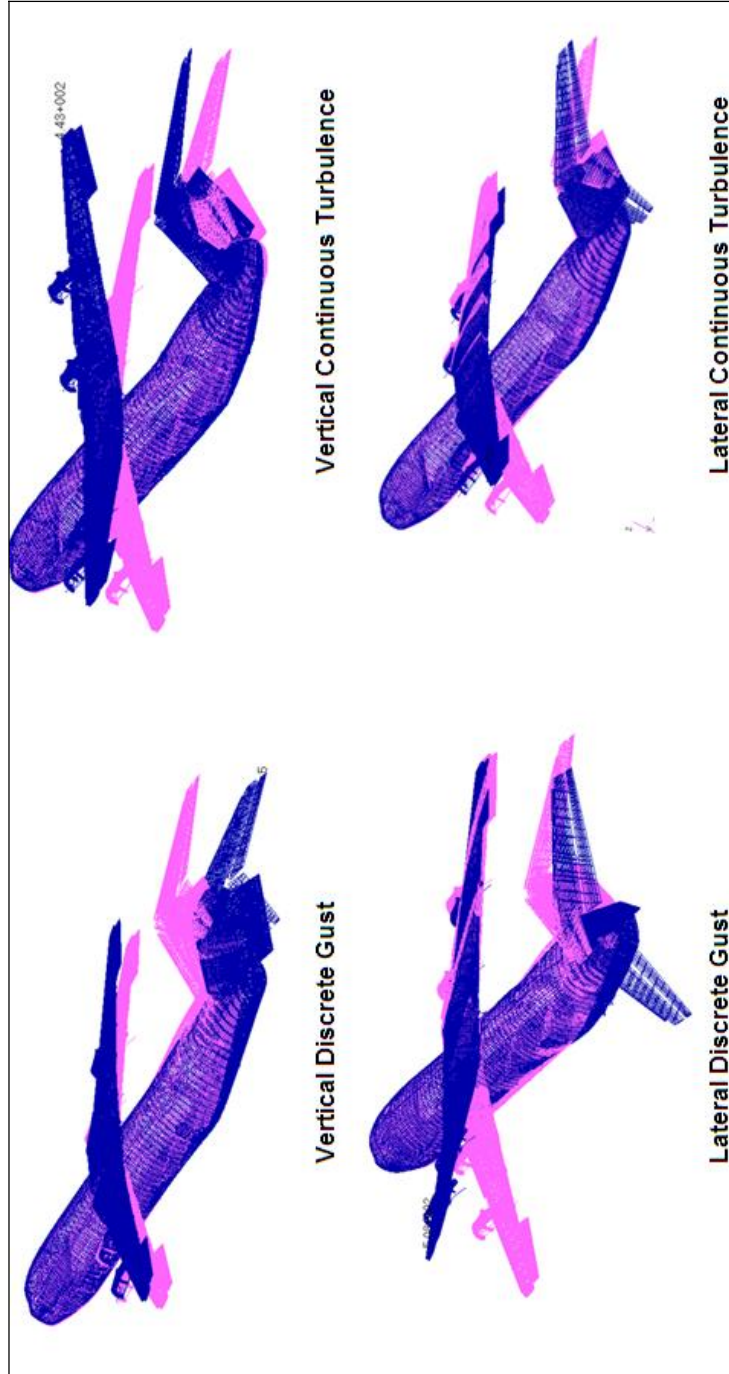


Figure 2.48: Fuselage Deformation Plots of Gust and Turbulence Loads

Through 2.3.2.1 to 2.3.2.5 the loading conditions and corresponding specifications are briefly explained. In addition to the specifications and definitions, the load path for each load type on the fuselage sections are shown by the deformation plots of Finite Element Models and typical aircraft pictures.

In order to meet all the certification specifications [5] and in order to perform an optimum design for the structural components of the aircraft, there were huge number of load case sets derived. However the application of all of the loads to the Finite Element Model of the Aircraft and the structural analysis or tests performed for each of these load cases were impossible from program schedule and cost point of view.

Hence; alternative methods were found to cover all load conditions by performing analysis or testing of some chosen load cases. Choosing of these special load cases from the huge load database was called “load case selection process” for the aircraft components. The load case selection process for frame and stringer couplings within this thesis was performed based on the load case selection of the corresponding frames and stringers which are also placed in the rear fuselage of the to be developed transport.

Load case selection criteria were mainly consisting of the envelopes of bending, torsion or shear on the corresponding cross-section of fuselage; which are seen in Figure 2.49.

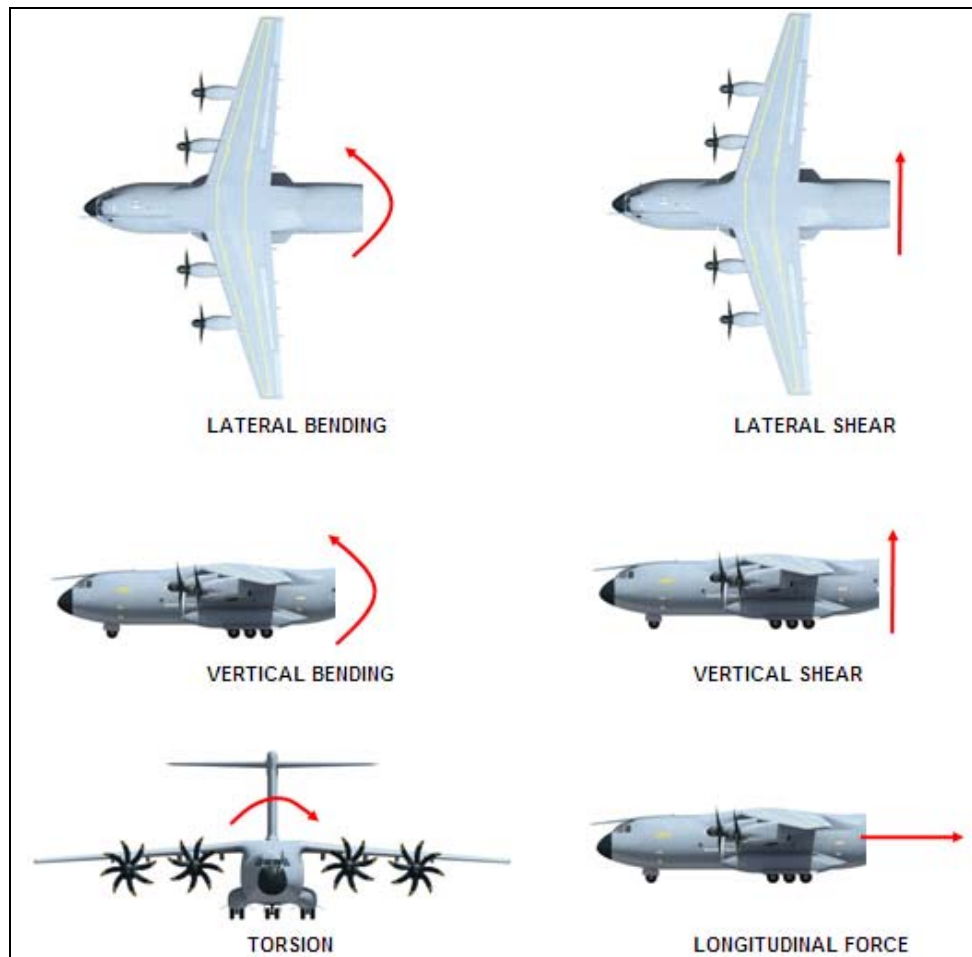


Figure 2.49: Fuselage Shear, Bending, Torsion and Longitudinal Force [3]

The envelope types that are specified as the main load selection criterion of the structural parts of the rear fuselage are classified into three main groups;

- i) 1D envelopes: These are one-dimensional envelopes consist of one of the longitudinal force, the lateral or the vertical shear force, the lateral or the vertical bending moments or the torsion seen in Figure 2.49.
- ii) 2D envelopes: These are two-dimensional envelopes that consist of any combination of the two of 1D envelopes.
- iii) Non-standard envelopes: These are 1D or 2D envelopes consisting of criteria different than fuselage shear, longitudinal forces, moments and torsion. (Payload distribution, wing-to-fuselage attachment loads and landing gear attachment loads)

For the rear fuselage components including the frame and stringer couplings within this thesis, main load selection criteria are defined after iterative structural analysis work as;

- i) Lateral Shear vs Vertical Bending
- ii) Vertical Shear vs Vertical Bending
- iii) Vertical Shear Resulted from Payload vs. Vertical Bending
- iv) Delta Lateral Shear in Wing Link Attachments vs. Vertical Bending
- v) 1D Torsion
- vi) 1D Lateral Bending

The force or moment components on fuselage cross-section result from three types of application of loads to the Finite Element Model; payload, aerodynamic loads, empennage loads. Payload loads are the loads applied directly to the floor of the aircraft Finite Element Model in order to simulate the external forces by the cargo loads inside the aircraft. The critical envelopes of the rear fuselage cross-section and the place of the load cases inside of these envelopes are seen in Figure 2.50.

Investigating the envelopes shown in Figure 2.50 by taking the reserve factors of each load case into account, critical zones of the frame couplings and the stringer

couplings were defined. Hence; reserve factor variation on different loading conditions were determined. The outcome of this investigation gave an idea of an approximate reserve factor change for a possible load increase of a specific maneuver. In addition; it gave the chance to omit the additional structural analysis work for this possible load increase, if the minimum reserve factor of the corresponding load type was high.

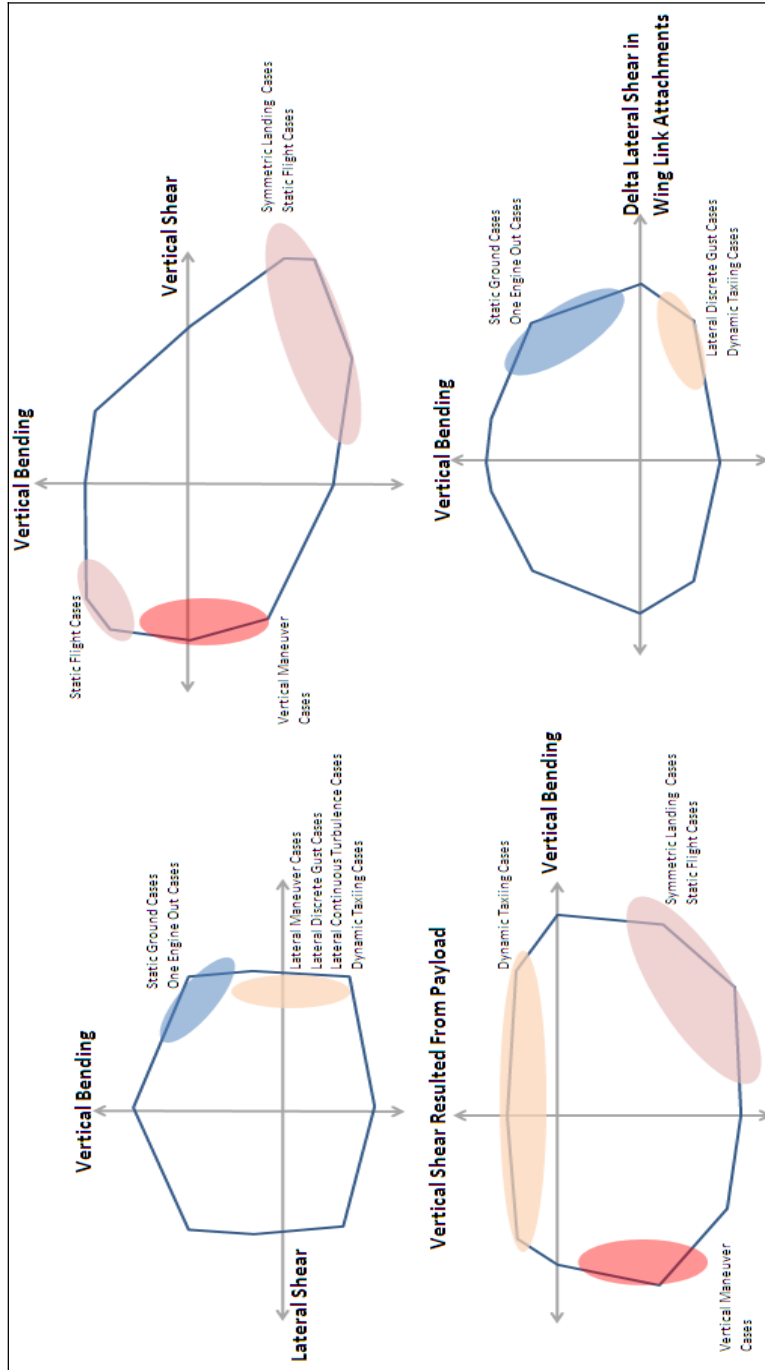


Figure 2.50: Schematic Representation of the Critical Load Case Selection Envelopes of Rear Fuselage Upper Shell

CHAPTER 3

TYPICAL FRAME COUPLING DESIGN

In this section, structural analysis of a typical frame coupling design is illustrated by calculation of the reserve factors of the failure modes.

3.1 Geometrical and Material Properties

Figure 3.1 shows the frame coupling cross-sectional geometry. The frame coupling is connected to the frame with 30 fasteners (10 fasteners are connected to the frame inner flange, and 20 fasteners are connected to the frame web). Also; typical frame coupling CAD models are shown in Figures between D.2 to D.7 in Appendix D.

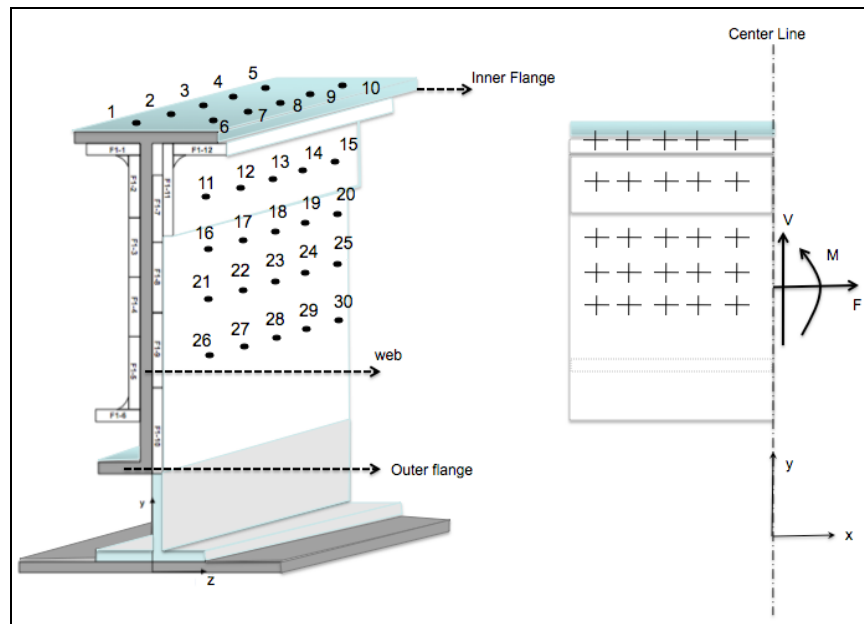


Figure 3.1: Illustrative Example Model of Frame Coupling

The Applied Loads are chosen as;

$$F = -50000N$$

$$M = 2000000N.mm$$

$$V = 1000N$$

The Material of the Coupling and the Frame are chosen as;

Frame: Al 7010 T7451

Frame Coupling: Al 7010 T7451

The Material Properties for the selected material (Al 7010 T7451) are obtained from [8] as;

Modulus of Elasticity, E: 71000 MPa

Modulus of Rigidity, G: 26692 MPa

Poisson's Ratio, ν : 0.33

Tension Yield Stress, F_{ty} : 455 MPa
Tension Ultimate Stress, F_{tu} : 525 MPa
Compression Yield Stress, F_{cy} : 440 MPa
Bearing Ultimate Stress, F_{bru} ($e/d=2.0$): 1000 MPa
Bearing Yield Stress, F_{bry} ($e/d=2.0$): 715 MPa
Bearing Ultimate Stress, F_{bru} ($e/d=1.5$): 760 MPa
Bearing Yield Stress, F_{bry} ($e/d=1.5$): 615 MPa

The Material and Geometric Properties of the fasteners of the design were;

Fastener Type: LN9198 Aluminum Fastener, Universal (Protruding) Head
Fastener Diameter: 4.8 mm
Fastener Material: Al 2017-T31
Shear Strength: 4320 N [8]

The Geometric Properties of the Frame Coupling were chosen and the calculations of the corresponding area and the second moment of area are performed as;

Table 3: Geometric Properties of the Frame Coupling based on Appendix A

	z_i (mm)	y_i (mm)	b_i (mm)	h_i (mm)	A_i (mm ²)	$I_{oi,zz}$ (mm ⁴)	$I_{oi,yy}$ (mm ⁴)	$J_{oi,zy}$ (mm ⁴)
F1-1	-9.5	147.0	15.0	2.0	30.0	10.0	562.5	572.5
F1-2	-3.0	135.0	2.0	22.0	44.0	1774.7	14.7	1789.3
F1-3	-3.0	113.0	2.0	22.0	44.0	1774.7	14.7	1789.3
F1-4	-3.0	91.0	2.0	22.0	44.0	1774.7	14.7	1789.3
F1-5	-3.0	69.0	2.0	22.0	44.0	1774.7	14.7	1789.3
F1-6	-9.5	57.0	15.0	2.0	30.0	10.0	562.5	572.5
F1-7	1.0	130.0	2.0	24.0	48.0	2304.0	16.0	2320.0
F1-8	1.0	106.0	2.0	24.0	48.0	2304.0	16.0	2320.0
F1-9	1.0	82.0	2.0	24.0	48.0	2304.0	16.0	2320.0
F1-10	1.0	58.0	2.0	24.0	48.0	2304.0	16.0	2320.0
F1-11	3.0	135.5	2.0	25.0	50.0	2604.2	16.7	2620.8
F1-12	16.5	147.0	25.0	2.0	50.0	16.7	2604.2	2620.8
SUM					528			

In addition; with the contribution of the properties of the selected material, below calculations were performed;

Table 4: Additional Calculations for determining of the CG and the Second Moment Area of the Frame Coupling

	$E_i \cdot A_i$ (N)	$E_i \cdot A_i \cdot y_i$ (N.mm)	$E_i \cdot A_i \cdot z_i$ (N.mm)	$I_{oi,zz} + E_j$ (N.mm ²)	$I_{oi,yy} + E_j$ (N.mm ²)	$y_i - y_{CG}$ (mm)	$z_i - z_{CG}$ (mm)	$A_i \cdot E_i \cdot (y_i - y_{CG})^2$	$A_i \cdot E_i \cdot (z_i - z_{CG})^2$
F1-1	2.130E+06	3.131E+08	-2.024E+07	7.100E+05	3.994E+07	40.5	-9.6	3.49E+09	1.98E+08
F1-2	3.124E+06	4.217E+08	-9.372E+06	1.260E+08	1.041E+06	28.5	-3.1	2.53E+09	3.06E+07
F1-3	3.124E+06	3.530E+08	-9.372E+06	1.260E+08	1.041E+06	6.5	-3.1	1.31E+08	3.06E+07
F1-4	3.124E+06	2.843E+08	-9.372E+06	1.260E+08	1.041E+06	-15.5	-3.1	7.53E+08	3.06E+07
F1-5	3.124E+06	2.156E+08	-9.372E+06	1.260E+08	1.041E+06	-37.5	-3.1	4.40E+09	3.06E+07
F1-6	2.130E+06	1.214E+08	-2.024E+07	7.100E+05	3.994E+07	-49.5	-9.6	5.22E+09	1.98E+08
F1-7	3.408E+06	4.430E+08	3.408E+06	1.636E+08	1.136E+06	23.5	0.9	1.88E+09	2.58E+06
F1-8	3.408E+06	3.612E+08	3.408E+06	1.636E+08	1.136E+06	-0.5	0.9	9.38E+05	2.58E+06
F1-9	3.408E+06	2.795E+08	3.408E+06	1.636E+08	1.136E+06	-24.5	0.9	2.05E+09	2.58E+06
F1-10	3.408E+06	1.977E+08	3.408E+06	1.636E+08	1.136E+06	-48.5	0.9	8.02E+09	2.58E+06
F1-11	3.550E+06	4.810E+08	1.065E+07	1.849E+08	1.183E+06	29.0	2.9	2.98E+09	2.92E+07
F1-12	3.550E+06	5.219E+08	5.858E+07	1.183E+06	1.849E+08	40.5	16.4	5.82E+09	9.51E+08
SUM	3.749E+07	3.993E+09	4.899E+06	1.346E+09	2.747E+08			3.73E+10	1.51E+09

From Table 3 and Table 4;

The total area and the average elastic modulus of the frame coupling section were calculated based on Equations (A.6) and (A.19) as;

$$A_{tot} = \sum_i A_i = 528 \text{ mm}^2$$

$$E_{tot} = \frac{EA_{tot}}{A_{tot}} = \frac{3.749 \times 10^7}{528} = 71000 \text{ MPa}$$

From Equation (A.7) and (A.8) the coordinates of the center of stiffness of the frame coupling were calculated as;

$$y_{CG} = \frac{\sum_i (A_i \times y_i \times E_i)}{A_{tot} \times E_{tot}} = \frac{3.993 \times 10^9}{528 \times 71000} = 106.5mm$$

$$z_{CG} = \frac{\sum_i (A_i \times z_i \times E_i)}{A_{tot} \times E_{tot}} = \frac{4.899 \times 10^6}{528 \times 71000} = 0.1mm$$

Additionally the second moment of area of the frame coupling section with respect to the $-z$ and $-y$ axes were calculated based on Equations (A.9) and (A.10) as;

$$I_{tot,zz} = \frac{\sum_i I_{oi,zz} \times E_i + \sum_i A_i \times E_i \times (y_i - y_{CG})^2}{E_{tot}} = \frac{1.346 \times 10^9 + 3.73 \times 10^{10}}{71000} = 544017mm^4$$

$$I_{tot,yy} = \frac{\sum_i I_{oi,yy} \times E_i + \sum_i A_i \times E_i \times (z_i - z_{CG})^2}{E_{tot}} = \frac{2.747 \times 10^8 + 1.51 \times 10^9}{71000} = 25113mm^4$$

The geometric properties of the frame section were given in Table 5;

Table 5: Cross-sectional Properties of the Frame

FRAME	b _i (mm)	h _i (mm)	y _i (mm)	A _i (mm ²)	A _i *y _i (mm ³)
Inner Flange	50.0	2.0	149.0	100.0	14900.0
Web	2.0	100.0	98.0	200.0	19600.0
Outer Flange	15.0	2.0	47.0	30.0	1410.0
			Total	330.0	35910.0
			y _L	108.8	

In Table 5; y_L is the $-y$ coordinate of the center of gravity of the frame section, where the force and moment is applied.

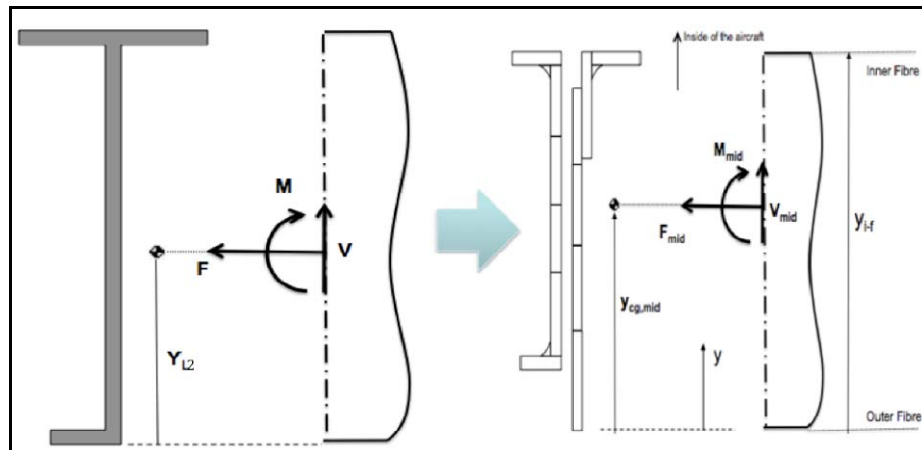


Figure 3.2: Transformation of the Applied Force and Moments to the Frame Coupling

Based on the data listed in Tables 3,4 and 5 the transformation if the applied load and moment from the frame to the frame coupling was calculated as;

$$F_{mid} = F = -50000N$$

$$V_{mid} = V = 1000N$$

$$M_{CG} = M + F \cdot |y_{CG} - y_L| = (2 \times 10^6) + (-5 \times 10^4) \times (106.5 - 108.8) = 2114678Nmm$$

Based on Equation (27) the applied stress to each segment of the middle section was calculated as;

Table 6: Applied Stress on each element

	$y_{i,mid}$ (mm)	Applied Stress on each Element,i (MPa)
F1-1	147.0	-252.03
F1-2	135.0	-205.39
F1-3	113.0	-119.87
F1-4	91.0	-34.35
F1-5	69.0	51.17
F1-6	57.0	97.81
F1-7	130.0	-185.95
F1-8	106.0	-92.66
F1-9	82.0	0.63
F1-10	58.0	93.93
F1-11	135.5	-207.33
F1-12	147.0	-252.03

Similarly; stress concentration on the inner and outer fibre of the frame coupling were also calculated based on Equations (27) and (28) as;

Applied stress on the inner fibre;

$$\sigma_{in} = \frac{F_{mid}}{A_{mid}} - \frac{M_{mid} \times (y_{i-f} - y_{cg,mid})}{I_{mid}} = \frac{-50000}{528} - \frac{2.114 \times 10^6 \times (148 - 106.5)}{544017} = -255.92 MPa$$

Similarly; the applied stress of the outer fibre;

$$\sigma_{in} = \frac{F_{mid}}{A_{mid}} - \frac{M_{mid} \times (y_{o-f} - y_{cg,mid})}{I_{mid}} = \frac{-50000}{528} - \frac{2.114 \times 10^6 \times (46 - 106.5)}{544017} = 140.57 MPa$$

The inner and outer fibre stress and the stress on each element were used in reserve factor calculations of the failure modes explained in Chapter 2.2.2. Before the reserve factor calculations, load distribution on each fastener was calculated as below.

The fastener properties of the given frame-coupling model were listed as;

Table 7: Fastener Properties

#i	x_i (mm)	y_i (mm)	D_i (mm)	A_i (mm ²)	$A_i \cdot x_i$ (mm ³)	$A_i \cdot y_i$ (mm ³)	Fastener Location	$X_{CG} - x_i$ (mm)	$Y_{CG} - y_i$ (mm)	r_i (web) (mm)	r_i (inner flange) (mm)	$A_i \cdot r_i^2$ (mm ⁴)
1	-101	177	4.8	18.10	-1828	3203	Inner Flange	0.00	-39.00		39.00	27523
2	-79	177	4.8	18.10	-1430	3203	Inner Flange	0.00	-39.00		39.00	27523
3	-57	177	4.8	18.10	-1031	3203	Inner Flange	0.00	-39.00		39.00	27523
4	-34	177	4.8	18.10	-615	3203	Inner Flange	0.00	-39.00		39.00	27523
5	-12	177	4.8	18.10	-217	3203	Inner Flange	0.00	-39.00		39.00	27523
6	-101	177	4.8	18.10	-1828	3203	Inner Flange	0.00	-39.00		39.00	27523
7	-79	177	4.8	18.10	-1430	3203	Inner Flange	0.00	-39.00		39.00	27523
8	-57	177	4.8	18.10	-1031	3203	Inner Flange	0.00	-39.00		39.00	27523
9	-34	177	4.8	18.10	-615	3203	Inner Flange	0.00	-39.00		39.00	27523
10	-12	177	4.8	18.10	-217	3203	Inner Flange	0.00	-39.00		39.00	27523
11	-101	159	4.8	18.10	-1828	2877	Web	44.40	-21.00	49.12		43653
12	-79	159	4.8	18.10	-1430	2877	Web	22.40	-21.00	30.70		17060
13	-57	159	4.8	18.10	-1031	2877	Web	0.40	-21.00	21.00		7983
14	-34	159	4.8	18.10	-615	2877	Web	-22.60	-21.00	30.85		17223
15	-12	159	4.8	18.10	-217	2877	Web	-44.60	-21.00	49.30		43975
16	-101	133	4.8	18.10	-1828	2407	Web	44.40	5.00	44.68		36125
17	-79	133	4.8	18.10	-1430	2407	Web	22.40	5.00	22.95		9532
18	-57	133	4.8	18.10	-1031	2407	Web	0.40	5.00	5.02		455
19	-34	133	4.8	18.10	-615	2407	Web	-22.60	5.00	23.15		9695
20	-12	133	4.8	18.10	-217	2407	Web	-44.60	5.00	44.88		36447
21	-101	105	4.8	18.10	-1828	1900	Web	44.40	33.00	55.32		55379
22	-79	105	4.8	18.10	-1430	1900	Web	22.40	33.00	39.88		28786
23	-57	105	4.8	18.10	-1031	1900	Web	0.40	33.00	33.00		19709
24	-34	105	4.8	18.10	-615	1900	Web	-22.60	33.00	40.00		28949
25	-12	105	4.8	18.10	-217	1900	Web	-44.60	33.00	55.48		55701
26	-101	77	4.8	18.10	-1828	1393	Web	44.40	61.00	75.45		103007
27	-79	77	4.8	18.10	-1430	1393	Web	22.40	61.00	64.98		76413
28	-57	77	4.8	18.10	-1031	1393	Web	0.40	61.00	61.00		67337
29	-34	77	4.8	18.10	-615	1393	Web	-22.60	61.00	65.05		76576
30	-12	77	4.8	18.10	-217	1393	Web	-44.60	61.00	75.57		103329
			$\Sigma(\text{web})$	361.9	-20484							
			$\Sigma(\text{all})$	542.9		74915						

Based on Table 7 and Equations (5) & (6);

$$x_{CG} = \frac{\sum_{i(web)} A_i \cdot x_i}{\sum_{i(web)} A_i} = \frac{-20484.0}{361.9} = -56.6mm$$

$$y_{CG} = \frac{\sum_{i(all)} A_i \cdot y_i}{\sum_{i(all)} A_i} = \frac{74915.0}{542.9} = 138.0mm$$

Based on equations (7) and (8) the distance of each rivet to the center of stiffness of the fasteners (r_i) were calculated and tabulated in Table 7.

Hence; the polar moment of area of the fasteners is calculated based on Equation (9) as;

$$I_r = \sum_i A_i \cdot r_i^2 = 1112566.5mm^4$$

The distance of each fastener and the polar moment of area were used to calculate applied load on each fastener separately. But; in order to calculate this, the transferred load and moment from the frame section to the center of stiffness of the fasteners was required. Hence; the transformation were performed based on Equations (10) – (12);

$$F_{CG,fasteners} = F = -50000N$$

$$V_{CG,fasteners} = V = 1000N$$

$$M_{CG,fasteners} = (2 \times 10^6) + (-5 \times 10^4) \times (138.0 - 108.8) + (10^3) \times (-56.6) = 484309.1Nmm$$

The applied force and moments were distributed to the fasteners based on the Equations from (13) to (20) and tabulated in Table 8.

Table 8: Distribution of the Applied Load and Moment on Each Fastener

#i	Fastener Shear Force Induced by F_{CG} (N)	Fastener Shear Force Induced by V_{CG} (N)	Fastener Shear Force Induced by M_{CG} (Nmm)	$\sin\alpha$	$\cos\alpha$	Horizontal Component of the Fastener Force, F_{x_i} (N)	Vertical Component of the Fastener Force, F_{y_i} (N)	Resultant Shear Force on i^{th} Fastener (N)
1	-1666.67	0.00	307.21	1.00	0.00	-1973.88	0.00	1973.88
2	-1666.67	0.00	307.21	1.00	0.00	-1973.88	0.00	1973.88
3	-1666.67	0.00	307.21	1.00	0.00	-1973.88	0.00	1973.88
4	-1666.67	0.00	307.21	1.00	0.00	-1973.88	0.00	1973.88
5	-1666.67	0.00	307.21	1.00	0.00	-1973.88	0.00	1973.88
6	-1666.67	0.00	307.21	1.00	0.00	-1973.88	0.00	1973.88
7	-1666.67	0.00	307.21	1.00	0.00	-1973.88	0.00	1973.88
8	-1666.67	0.00	307.21	1.00	0.00	-1973.88	0.00	1973.88
9	-1666.67	0.00	307.21	1.00	0.00	-1973.88	0.00	1973.88
10	-1666.67	0.00	307.21	1.00	0.00	-1973.88	0.00	1973.88
11	-1666.67	50.00	386.89	0.43	-0.90	-1832.09	-299.75	1856.45
12	-1666.67	50.00	241.86	0.68	-0.73	-1832.09	-126.45	1836.45
13	-1666.67	50.00	165.45	1.00	-0.02	-1832.09	46.85	1832.69
14	-1666.67	50.00	243.01	0.68	0.73	-1832.09	228.02	1846.22
15	-1666.67	50.00	388.32	0.43	0.90	-1832.09	401.32	1875.53
16	-1666.67	50.00	351.96	-0.11	-0.99	-1627.28	-299.75	1654.66
17	-1666.67	50.00	180.79	-0.22	-0.98	-1627.28	-126.45	1632.19
18	-1666.67	50.00	39.51	-1.00	-0.08	-1627.28	46.85	1627.96
19	-1666.67	50.00	182.33	-0.22	0.98	-1627.28	228.02	1643.18
20	-1666.67	50.00	353.52	-0.11	0.99	-1627.28	401.32	1676.04
21	-1666.67	50.00	435.77	-0.60	-0.80	-1406.72	-299.75	1438.30
22	-1666.67	50.00	314.17	-0.83	-0.56	-1406.72	-126.45	1412.39
23	-1666.67	50.00	259.96	-1.00	-0.01	-1406.72	46.85	1407.50
24	-1666.67	50.00	315.06	-0.83	0.57	-1406.72	228.02	1425.08
25	-1666.67	50.00	437.03	-0.59	0.80	-1406.72	401.32	1462.85
26	-1666.67	50.00	594.31	-0.81	-0.59	-1186.16	-299.75	1223.45
27	-1666.67	50.00	511.88	-0.94	-0.34	-1186.16	-126.45	1192.88
28	-1666.67	50.00	480.52	-1.00	-0.01	-1186.16	46.85	1187.09
29	-1666.67	50.00	512.42	-0.94	0.35	-1186.16	228.02	1207.88
30	-1666.67	50.00	595.24	-0.81	0.59	-1186.16	401.32	1252.21

3.2 Reserve Factor Calculations

After obtaining all the geometrical and material properties, the load distributions and the stress concentrations; reserve factor calculations were performed for each of the failure modes explained in Chapter 2.2.2.

3.2.1 Shear & Bearing Failure of the Fasteners

Shear strength of the selected fastener (LN9198) material (Al 2017 T31) is;

$$P_{su} = 4320\text{N}$$

For Fastener #1: The resultant shear force was calculated as 1973.88N as shown in Table 8. Hence corresponding reserve factor was calculated based on Equation (23) as;

$$RF_{shear,fastener1} = \frac{4320}{1973.88 \times 1.15} = 1.90$$

Reserve factors for the other fasteners were calculated parametrically based on Table 8 and equation (23), and tabulated in Table 9.

Table 9: Reserve Factor Calculation for the Shear Failure of the Fasteners

<i>Fastener #i</i>	<i>Fastener Shear Strength (N)</i>	<i>Resultant Shear Force on ith Fastener (N)</i>	<i>Single (S) or Double (D) Shear</i>	<i>Reserve Factor of Fastener Shear Check</i>
1	4320	1973.88	S	1.90
2	4320	1973.88	S	1.90
3	4320	1973.88	S	1.90
4	4320	1973.88	S	1.90
5	4320	1973.88	S	1.90
6	4320	1973.88	S	1.90
7	4320	1973.88	S	1.90
8	4320	1973.88	S	1.90
9	4320	1973.88	S	1.90
10	4320	1973.88	S	1.90
11	4320	1856.45	D	4.05
12	4320	1836.45	D	4.09
13	4320	1832.69	D	4.10
14	4320	1846.22	D	4.07
15	4320	1875.53	D	4.01
16	4320	1654.66	D	4.54
17	4320	1632.19	D	4.60
18	4320	1627.96	D	4.62
19	4320	1643.18	D	4.57
20	4320	1676.04	D	4.48
21	4320	1438.30	D	5.22
22	4320	1412.39	D	5.32
23	4320	1407.50	D	5.34
24	4320	1425.08	D	5.27
25	4320	1462.85	D	5.14
26	4320	1223.45	D	6.14
27	4320	1192.88	D	6.30
28	4320	1187.09	D	6.33
29	4320	1207.88	D	6.22
30	4320	1252.21	D	6.00

The fitting factor of “1.15” was used in reserve factor calculations in Table 9 based on Equation (23) and the bearing allowable for the frame and the coupling materials given in Chapter 3.1.

Hence the minimum reserve factor of the frame coupling in terms of shear failure of fasteners was found as;

$$\mathbf{RF_{shear_failure_of_rivets} = 1.90}$$

For the bearing failure check; the thickness and the bearing allowable stress of the plates to be joined were used additionally;

The bearing allowable stress values for the frame and the coupling material (which was the same for this specific case) were;

Bearing Ultimate Stress, F_{bru} ($e/d=2.0$): 1000 MPa

Bearing Yield Stress, F_{bry} ($e/d=2.0$): 715 MPa

Based on Equations (24), (25) and (26), reserve factor for the bearing of the first fastener location was calculated as;

$$RF_{bearing,fastener1} = \frac{\min\{1000 \times 4.8 \times 2; 1.5 \times 715 \times 4.8 \times 2\}}{1974 \times 1.15} = 4.23$$

Similarly bearing reserve factor of the plates for other fastener locations were calculated and tabulated in Table 10.

Table 10: Reserve Factor Calculation for the Bearing Failure of the Plates

#i	Single (S) or Double (D) Shear	t of the Coupling Web (mm)	t of the Coupling Inner Flange (mm)	t of the Frame Web (mm)	t of the Frame Inner Flange (mm)	Resultant Shear Force on each Fastener (N)	e/d (1.5 or 2.0)	F _{br-MIN, Frame} (MPa)	F _{br-MIN Coupling} (MPa)	P _{bru} (N)	RF, Plate Bearing Check
1	S	2	2	2	2	1974	2	1000	1000	9600	4.23
2	S	2	2	2	2	1974	2	1000	1000	9600	4.23
3	S	2	2	2	2	1974	2	1000	1000	9600	4.23
4	S	2	2	2	2	1974	2	1000	1000	9600	4.23
5	S	2	2	2	2	1974	2	1000	1000	9600	4.23
6	S	2	2	2	2	1974	2	1000	1000	9600	4.23
7	S	2	2	2	2	1974	2	1000	1000	9600	4.23
8	S	2	2	2	2	1974	2	1000	1000	9600	4.23
9	S	2	2	2	2	1974	2	1000	1000	9600	4.23
10	S	2	2	2	2	1974	2	1000	1000	9600	4.23
11	D	2	2	2	2	1856	2	1000	1000	9600	8.99
12	D	2	2	2	2	1836	2	1000	1000	9600	9.09
13	D	2	2	2	2	1833	2	1000	1000	9600	9.11
14	D	2	2	2	2	1846	2	1000	1000	9600	9.04
15	D	2	2	2	2	1876	2	1000	1000	9600	8.90
16	D	2	2	2	2	1655	2	1000	1000	9600	10.09
17	D	2	2	2	2	1632	2	1000	1000	9600	10.23
18	D	2	2	2	2	1628	2	1000	1000	9600	10.26
19	D	2	2	2	2	1643	2	1000	1000	9600	10.16
20	D	2	2	2	2	1676	2	1000	1000	9600	9.96
21	D	2	2	2	2	1438	2	1000	1000	9600	11.61
22	D	2	2	2	2	1412	2	1000	1000	9600	11.82
23	D	2	2	2	2	1408	2	1000	1000	9600	11.86
24	D	2	2	2	2	1425	2	1000	1000	9600	11.72
25	D	2	2	2	2	1463	2	1000	1000	9600	11.41
26	D	2	2	2	2	1223	2	1000	1000	9600	13.65
27	D	2	2	2	2	1193	2	1000	1000	9600	14.00
28	D	2	2	2	2	1187	2	1000	1000	9600	14.06
29	D	2	2	2	2	1208	2	1000	1000	9600	13.82
30	D	2	2	2	2	1252	2	1000	1000	9600	13.33

In Table 10; for the double shear joint locations the reserve factors were doubled. Hence the minimum reserve factor of the frame coupling in terms of bearing failure of the plates is found as;

$$RF_{\text{bearing_failure_of_plates}} = 4.23$$

3.2.2 Tension Check of the Middle Section of the Coupling

Based on the calculation of the stress concentration on the inner and outer fibre of the middle section of the coupling; maximum tension stress was calculated as;

$$\sigma_{out} = 140.6 \text{ MPa}$$

Based on Equation (29);

$$RF_{tens} = \min \left\{ \frac{(F_{tu})_{coupling}}{\sigma_{tens}}, \frac{1.5 \times (F_{ty})_{coupling}}{\sigma_{tens}} \right\} = \min \left\{ \frac{525.0}{140.6}, \frac{1.5 \times 455.0}{140.6} \right\} = 3.73$$

Hence the minimum reserve factor of the tension failure of the middle section of the frame coupling was found as;

$$RF_{tension_check_of_the_middle_section} = 3.73$$

3.2.3 Local Crippling Check

Allowable Crippling Force of each sub-element of the frame coupling was calculated based on the Equations (31), (32) and Table 1.

For the first sub-element of the frame coupling;

The crippling parameter ψ_i was calculated based on equation (32) as;

$$\psi_{1-1} = \frac{15}{2} \times \sqrt{\frac{440}{71000 \times 0.41}} = 0.92$$

where 0.41 is the support factor for one degree support.

The alloy constituent of the frame coupling material (Al 7050 T7451) is Zn.

Based on the crippling parameter and the alloy constituent of the material, corrective factor ξ was calculated as;

$$\xi = 1.3 - 0.574 \times 0.92 = 0.771$$

Finally the allowable crippling load for the first sub-element was calculated as;

$$F_{cr,i} = 15 \times 2 \times 440 \times 0.771 = 10173.6N$$

Similarly allowable crippling for the other sub-elements were calculated and tabulated in Table 11.

Table 11: Allowable Crippling Load of Each Sub-Element

	bi (mm)	hi (mm)	Alloy Const ituent	Support Condition	Support Factor, RK	Parameter for Corrective Factor, ψ	Corrective Factor, ξ	Allowable Crippling Force, $F_{cr,i}$ (N)
F1-1	15	2	Zn	1	0.41	0.92	0.77	10173.6
F1-2	2	22	Zn	2	3.60	0.46	1.04	20096.3
F1-3	2	22	Zn	2	3.60	0.46	1.04	20096.3
F1-4	2	22	Zn	2	3.60	0.46	1.04	20096.3
F1-5	2	22	Zn	2	3.60	0.46	1.04	20096.3
F1-6	15	2	Zn	1	0.41	0.92	0.77	10173.6
F1-7	2	24	Zn	1	0.41	1.48	0.53	11233.7
F1-8	2	24	Zn	2	3.60	0.50	1.01	21420.2
F1-9	2	24	Zn	2	3.60	0.50	1.01	21420.2
F1-10	2	24	Zn	2	3.60	0.50	1.01	21420.2
F1-11	2	25	Zn	1	0.41	1.54	0.51	11325.8
F1-12	25	2	Zn	1	0.41	1.54	0.51	11325.8

The corrective factors of each element were calculated based on the parameter ψ , as shown in Table 1.

The applied load on each element was also calculated by multiplying the area with the applied stress (Table 6) of each sub-element. Hence the reserve factors of the sub-elements (under compression) for crippling failure were calculated as;

Table 12: Reserve Factor for the Local Crippling

	b_i (mm)	h_i (mm)	Applied Load on Each Sub-Element (N)	Applied Load of Each Sub-Element (N)	RF
F1-1	15	2	-7560.9	10173.6	1.35
F1-2	2	22	-9036.9	20096.3	2.22
F1-3	2	22	-5274.2	20096.3	3.81
F1-4	2	22	-1511.4	20096.3	13.30
F1-5	2	22	2251.4	20096.3	
F1-6	15	2	2934.4	10173.6	
F1-7	2	24	-8925.6	11233.7	1.26
F1-8	2	24	-4447.6	21420.2	4.82
F1-9	2	24	30.4	21420.2	
F1-10	2	24	4508.4	21420.2	
F1-11	2	25	-10366.4	11325.8	1.09
F1-12	25	2	-12601.6	11325.8	0.90

Hence the minimum reserve factor of the crippling failure of the middle section of the frame coupling was found as;

$$\mathbf{RF_{local_crippling_failure} = 0.90}$$

3.2.4 Inter-rivet Buckling Check

For the inter-rivet buckling check; the maximum distance between the fasteners which is shown in Figure 2.18 was found as “24mm” for the given specific case.

Based on Equations (36), (37) and (38) the auxiliary parameter of the first sub-elements were calculated as;

$$\psi_{1-1} = 1.1027 \cdot \frac{24}{2} \cdot \sqrt{\frac{440}{3 \cdot 71000}} = 0.60$$

where “3” is the clamping factor for universal head fastener based on Table 2.

Since $0.60 < 1.5275$ the critical inter-rivet buckling equation for inelastic regime was used and calculated based on equation (37) as;

$$\sigma_{cr,irb} = (1 - 0.3027 \times 0.60^{1.5}) \times 440 = 378 \text{ MPa}$$

Hence;

$$RF_{1-1, \text{int rivet_buckling}} = \frac{378}{252} = 1.5$$

The inter-rivet buckling reserve factors for the other sub-elements were calculated accordingly and tabulated in Table 13.

Table 13: Reserve Factor for the Inter-rivet Buckling

	Applied Stress on Each Element, (MPa)	t (mm)	ψ	Inelastic (I) or Elastic (E) Regime	$\sigma_{cr,irb}$ (MPa)	Reserve Factor for Inter-rivet Buckling
F1-1	-252.03	2.0	0.60	I	378	1.50
F1-2	-205.39	2.0	0.60	I	378	1.84
F1-3	-119.87	2.0	0.60	I	378	3.15
F1-4	-34.35	2.0	0.60	I	378	11.00
F1-5	51.17	2.0	0.60	I	378	
F1-6	97.81	2.0	0.60	I	378	
F1-7	-185.95	2.0	0.60	I	378	2.03
F1-8	-92.66	2.0	0.60	I	378	4.08
F1-9	0.63	2.0	0.60	I	378	
F1-10	93.93	2.0	0.60	I	378	
F1-11	-207.33	2.0	0.60	I	378	1.82
F1-12	-252.03	2.0	0.60	I	378	1.50

Hence the minimum reserve factor of the inter-rivet buckling failure of the middle section of the frame coupling was found as;

$$\mathbf{RF_{inter-rivet_buckling} = 1.50}$$

3.3 Summary of the Reserve Factors

Table 14: Summary of the Reserve Factors

FAILURE MODE	RESERVE FACTOR
Shear Failure of Rivets	1.90
Bearing Failure of the Plates	4.23
Tension Failure of the Middle Section	3.73
Local Crippling Check	0.90
Inter-rivet Buckling Check	1.50

In this example; there is an $RF < 1$ according to the crippling failure in section F1-12. Hence; based on the required reinforcements in case of a possible local crippling failure; explained in Chapter 2.2.2.7; an appropriate repair solution should be chosen and analysis should be re-performed.

The possible reinforcements in this case are;

- i) Using thicker material, or
- ii) Using higher strength material.

In order to perform automatic calculations for different loading conditions and different geometry of the frame coupling system an MS/EXCEL® tool has been developed. Appendix E gives the details of the developed program and some applications.

CHAPTER 4

TYPICAL STRINGER COUPLING DESIGN

In this section, structural analysis of a typical stringer coupling design is illustrated by calculation of the reserve factors of the failure modes. An illustrative model for a typical stringer coupling is seen in Figure 4.1. Also CAD models for stringer coupling designs performed in the thesis is illustrated in Figures D.6 and D.7 in the Appendix D.

4.1 Geometrical and Material Properties

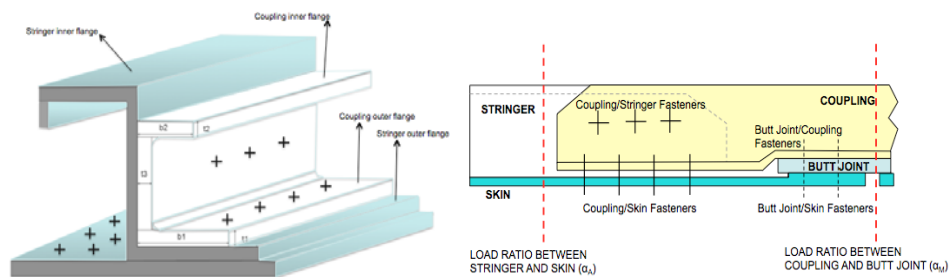


Figure 4.1: Illustrative Model for a Typical Stringer Coupling Design

The geometrical properties of the stringer and the stringer coupling are selected as shown in Tables 15 and 16.

Table 15: Stringer Coupling Geometry

	width, b_i (mm)	thickness, t_i (mm)	A_i (mm ²)
Outer Flange	24.6	1.4	34.4
Web	22.2	1.4	31.1
Inner Flange	4.0	6.0	24.0
Total Area			89.5

Table 16: Stringer Geometry

	width, b_i (mm)	thickness, t_i (mm)	A_i (mm ²)
Outer Flange	20.6	1.4	28.8
Web	29.2	1.4	40.9
Inner Flange	15.4	1.4	21.6
Inner Flange Lip	6.6	1.4	9.2
Total Area			100.5

Skin Thickness: 2.4mm

Butt-Strap Thickness: 2.8mm

Stringer Coupling Material: Al 7475 T7351

Modulus of Elasticity, E: 71000MPa

Tension Yield Stress, F_{ty} : 385MPa

Compression Yield Stress, F_{cy} : 405MPa

Tension Ultimate Stress, F_{tu} : 475MPa

Bearing Yield Stress, F_{bry} : 595MPa (e/d=1.5)

Bearing Ultimate Stress, F_{bru} : 730MPa (e/d=1.5)

Bearing Yield Stress, F_{bry} : 705MPa (e/d=2.0)

Bearing Ultimate Stress, F_{bru} : 950MPa (e/d=2.0)

Stringer Material: Al 7349 T76

Modulus of Elasticity, E: 72000MPa

Tension Yield Stress, F_{ty} : 585MPa

Compression Yield Stress, F_{cy} : 605MPa

Tension Ultimate Stress, F_{tu} : 630MPa

Bearing Yield Stress, F_{bry} : 715MPa (e/d=1.5)

Bearing Ultimate Stress, F_{bru} : 875MPa (e/d=1.5)

Bearing Yield Stress, F_{bry} : 835MPa (e/d=2.0)

Bearing Ultimate Stress, F_{bru} : 1145MPa (e/d=2.0)

Butt-Strap Material: Al 2024 HDT T3x Clad

Modulus of Elasticity, E: 71000MPa

Tension Yield Stress, F_{ty} : 290MPa

Compression Yield Stress, F_{cy} : 280MPa

Tension Ultimate Stress, F_{tu} : 425MPa

Bearing Yield Stress, F_{bry} : 480MPa (e/d=1.5)

Bearing Ultimate Stress, F_{bru} : 675MPa (e/d=1.5)

Bearing Yield Stress, F_{bry} : 565MPa (e/d=2.0)

Bearing Ultimate Stress, F_{bru} : 845MPa (e/d=2.0)

Skin Material: Al 2024 HDT T42 Clad

Modulus of Elasticity, E: 71000MPa

Tension Yield Stress, F_{ty} : 260MPa

Compression Yield Stress, F_{cy} : 285MPa

Tension Ultimate Stress, F_{tu} : 430MPa

Bearing Yield Stress, F_{bry} : 460MPa ($e/d=1.5$)

Bearing Ultimate Stress, F_{bru} : 680MPa ($e/d=1.5$)

Bearing Yield Stress, F_{bry} : 550MPa ($e/d=2.0$)

Bearing Ultimate Stress, F_{bru} : 850MPa ($e/d=2.0$)

Fasteners between Butt-Strap and Skin: Universal Head Solid Rivet LN9198

Fastener Material: Al 7050-T73

Number of Fasteners: (3x6=18) for one side of the coupling

Fastener Diameter: 4.8mm

Fastener Shear Strength: 5230N

Fasteners between Stringer and Coupling: Universal Head Solid Rivet LN9198

Fastener Material: Al 7050-T73

Number of Fasteners: 3 web + 4 foot = 7 for one side of the coupling

Fastener Diameter: 4.8mm

Fastener Shear Strength: 5230N

The applied loads are which are appropriate to Figure 2.23;

Table 17: Applied Loads to the Stringer Coupling System

Applied Axial Load on Stringer, $F_{x,stringer}$ (N)	Applied Axial Load on Skin1, $F_{x,skin1}$ (N)	Applied Axial Load on Skin2, $F_{x,skin2}$ (N)	Applied Shear Load on Skin1, $F_{y,skin1}$ (N)	Applied Shear Load on Skin2, $F_{y,skin2}$ (N)
-10000	-15000	-15000	1000	1000

In order to calculate the load sharing factors α_A and α_M in Figure 4.1; effective area of the skin and the butt-strap are calculated.

For compression;

Effective skin width is calculated iteratively as;

Step 1: Skin effective width is calculated based on Equation (B.5) of Appendix B by using F_{st} as the allowable crippling stress of the stringer.

Step 2: By using sum of the effective skin area and the stringer area, stress concentration is calculated under the total applied load to the skin stringer combination, and calculating the difference between this and the stress value used in the previous step (which is the allowable crippling stress of the stringer for this step).

Step 3: New effective width calculation by using the applied stress calculated in Step 2.

The iteration continued until the difference between the used stress in the effective width calculation and the new stress calculated by using that effective area. In this thesis 20 iterative calculations are used in order to find the effective width of the skin.

For the first step of the effective width calculation; allowable compressive (cripling) force is calculated for stringer based on Equation (31).

For the outer flange of the stringer;

The crippling parameter ψ_i was calculated based on equation (32) as;

$$\psi_{Outer_Flange} = \frac{20.6}{1.4} \times \sqrt{\frac{605}{72000 \times 0.41}} = 2.11$$

where 0.41 is the support factor for one-degree support.

The alloy constituent of the frame coupling material (Al 7050 T7451) is Zn.

Based on the crippling parameter and the alloy constituent of the material, corrective factor ξ was calculated as;

$$\xi = \frac{0.726}{2.11^{0.8}} = 0.40$$

Finally the allowable crippling load for the first sub-element was calculated as;

$$F_{cr,i} = 20.6 \times 1.4 \times 605 \times 0.40 = 6979.8N$$

Similarly allowable crippling for the other sub-elements were calculated and tabulated in Table 18.

Table 18: Allowable Crippling Force of the Stringer

	b_i (mm)	t_i (mm)	A_i (mm ²)	Support Condition	Support Factor, RK	Parameter for Corrective Factor, ψ	Corrective Factor, ξ	Allowable Crippling Force, $F_{cr,i}$ (N)
Outer Flange	20.6	1.4	28.8	1	0.41	2.11	0.40	6979.8
Web	29.2	1.4	40.9	2	3.60	1.01	0.72	17846.9
Inner Flange	15.4	1.4	21.6	2	3.60	0.53	0.99	12978.0
Inner Flange Lip	6.6	1.4	9.2	1	0.41	0.67	0.91	5101.7
		Total Area, A_{tot}	100.5				Total $F_{cr,i}$	42906.4

Hence allowable crippling stress of the stringer was;

$$\sigma_{cr} = \frac{42906.4}{100.5} = 427 \text{ MPa}$$

For Step1 of the effective width calculation;

$$W_e = 0.85 \times 2.4 \times \frac{71000}{72000} \sqrt{\frac{72000}{427}} = 25.9 \text{ mm}$$

Hence the effective skin area was $2 \times W_e \times t_{skin} = 124.5 \text{ mm}^2$

Total Area of the skin-stringer combination was $A_{str} + A_{skin,eff} = 225.1 \text{ mm}^2$

Axial load applied to the stringer-skin combination;

$$F_{tot} = F_{x,stringer} + F_{x,skin1} + F_{x,skin2} = -40000 \text{ N}$$

Hence the applied stress to be used for Step 2 of the effective width calculation was;

$$\sigma_{\text{step2}} = 40000/225.1 = 177.7\text{MPa}$$

Similarly calculations for the next 19 steps were calculated and tabulated in Table 19;

Table 19: Skin Effective Area Iteration

Axial Load	Axial Stress (MPa)	Skin Eff Area (mm ²)	Error ($\sigma_i - \sigma_{i+1}$)
-40000.0	177.7	124.5	249.1
Iteration 1	136.3	193.0	41.5
Iteration 2	124.6	220.4	11.6
Iteration 3	120.9	230.5	3.8
Iteration 4	119.6	234.0	1.3
Iteration 5	119.1	235.3	0.4
Iteration 6	119.0	235.8	0.2
Iteration 7	118.9	235.9	0.1
Iteration 8	118.9	236.0	0.0
Iteration 9	118.9	236.0	0.0
Iteration 10	118.9	236.0	0.0
Iteration 11	118.9	236.0	0.0
Iteration 12	118.9	236.0	0.0
Iteration 13	118.9	236.0	0.0
Iteration 14	118.9	236.0	0.0
Iteration 15	118.9	236.0	0.0
Iteration 16	118.9	236.0	0.0
Iteration 17	118.9	236.0	0.0
Iteration 18	118.9	236.0	0.0
Iteration 19	118.9	236.0	0.0
Iteration 20	118.9	236.0	0.0

Hence; Effective Skin Width for Compression = $236/2.4=98.3\text{mm}$

Effective width for the butt-strap is same as the skin, so effective area of the butt-strap under compression was calculated as;

$$A_{BS-Eff,comp} = 98.3 \times 2.8 = 275.3 \text{mm}^2$$

For Tension;

Based on Equation (B.1) and (B.2)

$$A_{BS_T} = A_{BS_NET} = \{2.8 \times [144 - (4.8 \times 6)]\} = 322.6 \text{mm}^2$$

$$A_{SKIN_T} = A_{SKIN_NET} = \{2.4 \times [189 - (4.8 \times 6)]\} = 384.5 \text{mm}^2$$

4.2 Calculation of the Load Sharing Factors, α_A and α_M

Based on Equation (41) and (42);

$$\alpha_A = \frac{100.5}{100.5 + 236.0 \times \left[\frac{71000}{72000} \right]} = 0.301$$

$$\alpha_M = \frac{89.5}{89.5 + 275.3 \times \left[\frac{71000}{71000} \right]} = 0.245$$

In order to prevent “butt-joint/skin fasteners” from overloading;

Based on equation (43);

$$\Delta F = (0.245 - 0.301) \cdot (-40000) = 2251.4N$$

Since the total allowable load of the fasteners in the butt-strap to stringer connection would be higher than 2251.4N; α_A remained the same.

Hence the applied loads on each component were calculated based on equations (47) to (51);

$$F_{butt-joint,y} = 2000N$$

$$F_{butt-joint,x} = (1 - 0.245) \times (-40000) = -30185.4N$$

Hence; the resultant force on the butt-strap was calculated as;

$$F_{butt-joint} = \sqrt{(1 - 0.245)^2 \times (-40000)^2 + (2000)^2} = 30251.6N$$

$$F_{Stringer} = 0.301 \times (-40000) = -12066N$$

$$F_{Coupling} = 0.245 \times (-40000) = -9814.6N$$

4.3 Justification of the Stringer Coupling

Since the load on the stringer coupling was compression; the allowable crippling load of the stringer coupling section was calculated and tabulated in Table 20.

Table 20: Allowable Crippling Load Calculation of Stringer Coupling

	b_i (mm)	t_i (mm)	A_i (mm ²)	Support Factor, RK	Parameter for Corrective Factor, ψ	Corrective Factor, ξ	Allowable Crippling Force, $F_{cr,i}$ (N)
Outer Flange	24.6	1.4	34.4	0.41	2.07	0.41	5652.5
Web	22.2	1.4	31.1	3.60	0.63	0.94	11803.0
Inner Flange	4	6	24.0	0.41	0.08	1.25	12197.3
		Total Area, A_{tot}	89.5			Total $F_{cr,i}$	29652.9

Hence the allowable of crippling stress of the middle section was calculated as;

$$\sigma_{cr} = \frac{29652.9}{89.5} = 331.2 \text{ MPa}$$

Thus;

$$RF_{compression} = \frac{\min\{\sigma_{cr}; \sigma_{cy}\} \times A_{coupling}}{F_{coupling}} = \frac{\min\{331.2; 405\} \times 89.5}{-9814.6} = 3.02$$

4.4 Justification of the Stringer Coupling Fasteners

For a single fastener;

Allowable shear load is 5230N.

The bearing allowable stress values were given in Chapter 4.1 for each element.

Based on equation (25) allowable bearing load was calculated as;

$$P_{bru} = \min \left\{ (F_{bru-MIN} \times 1.4 \times 4.8)_{coupling}, (F_{bru-MIN} \times 1.4 \times 4.8)_{stringer} \right\} = 6384 N$$

For the other fasteners these results were calculated and shown in Table 21.

Table 21: Maximum Allowable Load of the Fasteners

<i>Fastener #</i>	<i>Fastener Diameter (mm)</i>	<i>Fastener Shear Strength (N)</i>	<i>Coupling Thickness (mm)</i>	<i>Stringer Thickness (mm)</i>	<i>e/d ratio (1.5 or 2)</i>	<i>Fbru-MIN, Coupling (MPa)</i>	<i>Fbru-MIN Stringer (MPa)</i>	<i>Pbru (N)</i>	<i>Maximum Allowable Load (N)</i>
1	4.8	5230	1.4	1.4	2	950	1145	6384	5230
2	4.8	5230	1.4	1.4	2	950	1145	6384	5230
3	4.8	5230	1.4	1.4	2	950	1145	6384	5230
4	4.8	5230	1.4	1.4	2	950	1145	6384	5230
5	4.8	5230	1.4	1.4	2	950	1145	6384	5230
6	4.8	5230	1.4	1.4	2	950	1145	6384	5230
7	4.8	5230	1.4	1.4	2	950	1145	6384	5230

Hence; the total allowable load of the stringer-to-coupling fasteners was $5230 \times 7 / 1.15 = 31835 N$

Based on equation (54);

$$RF = \frac{31835}{ABS(-12066)} = 2.64$$

4.5 Justification of the Butt-Joint

Applied compression and shear stress on the butt-joint were calculated based on equations (56) and (58) as;

$$\sigma_{Butt-joint_{comp}} = \frac{-30185.4}{275.3} = -109.6MPa$$

$$\tau_{Butt-joint} = \frac{2000}{322.6} = 6.2MPa$$

$$R_1 = \frac{109.6}{280} = 0.39$$

with

$$R_2 = \frac{6.2}{290} = 0.02$$

Hence; the Reserve Factor is calculated as;

$$RF = \frac{1}{\sqrt{0.39^2 + 0.02^2}} = 2.55$$

4.6 Justification of the Butt-Joint Fasteners

Similar to the maximum allowable fastener load calculation of the stringer-to-coupling fasteners; the total allowable load of the butt-strap – to - skin fasteners were calculated as;

$$F_{Riv,Butt-joint/Skin} = 81860.9N$$

The applied load on these fasteners is the resultant applied load on the Butt-Strap which is calculated previously as 30251.6N.

Hence the reserve factor of the fasteners between the butt-joint and the skin is calculated as;

$$RF = \frac{81860.9}{30251.6} = 2.71$$

4.7 Summary of the Reserve Factors

Based on the structural analysis of the stringer coupling; the reserve factor summary are seen in Table 22.

Table 22: Reserve Factor Summary of the Stringer Coupling Analysis

FAILURE MODE	RESERVE FACTOR
Justification of the Stringer Coupling	3.02
Justification of the Stringer Coupling Fasteners	2.64
Justification of the Butt-Strap	2.55
Justification of the Butt-Strap Fasteners	2.71

In order to perform automatic calculations for different loading conditions and different geometry of the frame coupling system analytical calculation sheets were created in MS/EXCEL®. Appendix E gives the details of the developed program and some applications.

CHAPTER 5

CONCLUSION

5.1 General Conclusions

In this thesis; design and analysis of the structural interface elements, the frame coupling and the stringer couplings, for a heavy transport aircraft was performed. As an introduction to the thesis some necessary information about the properties and capabilities of the developed aircraft was explained. In addition to the general specifications of the aircraft, additional information about the fuselage parts where the frame and stringer couplings are located was also introduced.

Main aim of the thesis was to design the structural components providing sufficient strength and appropriateness in terms of certification and the airworthiness point of views. Within the limits defined above; designed components were aimed to be lighter, easy to manufacture and cost effective.

The certification specifications for large transport aircrafts (CS-25 of EASA) were used as the main reference of the structural design and the analysis. Detailed information about the design and analysis methods, material specifications, loads and load case selection criteria, verification of the loads and verification of the structural analysis were given based on the directives in Certification Specifications, CS-25.

For the structural analysis methodology; a program in MS/EXCEL® was created to perform automatic calculations in case of a need of re-sizing of the structural component or change in the loading conditions.

Based on the design and analysis work performed within this thesis, it was concluded that, frame and stringer coupling parts had critical roles in the fuselage design, because coupling parts were the interface elements connecting primary structures of the fuselage. Primary structures of the aircraft are the main structural components that are subjected to the flight, ground or any operational loads; which are the frames, skin and stringer sections.

The frame coupling parts are the circumferential interface members in the connection of two frame segments together. A typical frame coupling design process is illustrated in Chapter 3. The structural analysis checks of the frame couplings were defined as; shear and bearing failure of the fasteners, local crippling on the coupling sections, tension and compression failure of the middle section and inter-rivet buckling check of the coupling parts that have maximum fastener pitch. Applicable reinforcement or design update methods for a possible re-sizing phase were explained for each failure mode.

The stringer coupling system is the longitudinal interface connection of two stringers, consisting of a coupling and a circumferential strap called “Butt-joint”. A typical stringer coupling design and analysis is illustrated in Chapter 4. The structural analysis checks of the stringer coupling system were defined as; shear and bearing failure of the fasteners, tension or compression failure of the coupling and the butt-joint, local crippling failure of the middle section of the coupling. Applicable reinforcement or design update methods for a possible re-sizing phase were explained for each failure mode.

One of the main contributions of this thesis study to the design of the developed aircraft was selecting the critical load conditions for the coupling parts. These selections were verified by means of structural analysis checks performed for all types of loading conditions separately. Structural analysis checks were performed according to the structural analysis methods agreed for the design of the heavy transport aircraft. These methods were utilized for the coupling design in terms of analytical calculations or finite element modeling.

The verification of the FEM and the hand calculation analysis were performed based on various tests. The tests were mainly classified as coupon tests, component tests and full-scale test of the aircraft. Actually; one of the most critical and important type of the tests was the full-scale static test of the aircraft. During this test; a full scale aircraft which was manufactured for the testing purpose only was exposed to the most critical loading conditions of the aircraft such as landing (which is the most critical case for frame couplings), lateral and vertical maneuvers or turbulence and gust conditions (which were the most critical cases for the stringer couplings). These loads were applied to the aircraft by the actuators simulating the corresponding load cases. For the critical loading conditions applied the aircraft managed to sustain without any structural failure. In addition to the full static test, various flight tests were also performed for the developed aircraft. Verification of the loads applicable to the aircraft was performed in these tests. The aircraft also managed to sustain without any structural failure from the flight tests.

5.2 Recommendation for Future Work

In the thesis the structural analysis and design of the frame and stringer coupling parts were performed for the specific fuselage locations and by using specific geometry. It could be a future work to cover a general structural analysis and design methodology for all kinds of the interface elements.

The material used in the design of the frame couplings and the stringer couplings within the thesis was aluminum, in order to avoid material dissimilarity between the coupling parts and the primary structure of the aircraft which consists of the frame, stringer and skin segments which was also aluminum. For a future design of composite based aircraft, it would be a future work to design these components based on composite materials.

REFERENCES

- [1] Airforce-technology.com
<http://www.airforce-technology.com/projects/fla/fla8.html>
(Last accessed date 20 July 2009)

- [2] Aircraft Structural Design
<http://adg.stanford.edu/aa241/structures/structuraldesign.html>
(Last accessed date 24 July 2009)

- [3] Airbus Military
<http://www.airbusmilitary.com>
(Last accessed date 12 August 2009)

- [4] TAI Design and Structural Analysis Manual

- [5] Certification Specifications for Large Aeroplanes, CS-25, EASA, Amendment 4, 27 December 2007.

- [6] Airframe Structural Design, Michael C.Niu, January 1999

- [7] Analysis and Design of Flight Vehicle Structures , E.F.Bruhn, C7.6, 1973

- [8] Metallic Materials and Elements For Aerospace Vehicle Structures, Military Handbook 5H, 1 December 1998
- [9] Airframe Stress Analysis and Sizing, M.C.Y. Niu, pp 274-437, October 1997
- [10] Mechanical Engineering Design, J.E. Shigley, pp 754-755, Fifth Edition, 1989

APPENDIX A

PARAMETRIC CALCULATIONS OF THE GEOMETRIC PROPERTIES OF FRAME COUPLINGS

Frame Coupling Geometry is divided into rectangular sub-elements in order to perform parametric calculations of the geometric properties of total frame coupling cross-sections.

For a typical rectangular sub-element; notation and coordinates are represented in Figure A.1;

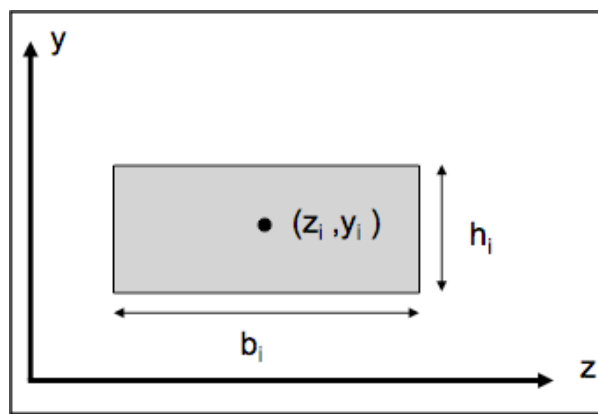


Figure A.1: Rectangular Sub-element

Based on Figure A.1; the area of a rectangular element is;

$$A_i = b_i \times h_i \quad (\text{A.1})$$

In addition, second moments of area about z-axis, y-axis and polar moment of area about z and y axes are calculated based on Mechanical Engineering Design, J.E. Shigley [10] as;

$$I_{oi,zz} = \frac{1}{12} \times b_i \times h_i^3 \quad (\text{A.2})$$

$$I_{oi,yy} = \frac{1}{12} \times h_i \times b_i^3 \quad (\text{A.3})$$

$$J_{oi,zy} = \frac{1}{12} \times h_i \times b_i \times (b_i^2 + h_i^2) \quad (\text{A.4}]$$

Mixed moment of inertia for rectangular cross-sections is $I_{oi,zy}=0$

Also, torsional second moment of area A_i based on [4];

$$TOR_i = \frac{1}{3} T_n^4 \times \left(\frac{S_n}{T_n} - 0.63 + \frac{0.052}{\left(\frac{S_n}{T_n}\right)^4} \right) \quad (\text{A.5})$$

Where T_n : sub-element thickness

S_n : sub-element length

If $T_n > S_n \rightarrow$ interchange two dimensions

Based on the geometrical properties of rectangular sub-elements above, parametric calculations of the total frame coupling geometry are shown below;

Total area of the frame coupling section is;

$$A_{tot} = \sum_i A_i \quad (A.6)$$

Center of stiffness in $-z$ and $-y$ axes based on the datum shown in Figure 2.8 are;

$$y_{CG} = \frac{\sum_i (A_i \times y_i \times E_i)}{A_{tot} \times E_{tot}} \quad (A.7)$$

$$z_{CG} = \frac{\sum_i (A_i \times z_i \times E_i)}{A_{tot} \times E_{tot}} \quad (A.8)$$

Then, second moment of area A_{tot} with respect to the $-z$ and $-y$ axes are defined respectively as;

$$I_{tot,zz} = \frac{\sum_i I_{oi,zz} \times E_i + \sum_i A_i \times E_i \times (y_i - y_{CG})^2}{E_{tot}} \quad (A.9)$$

$$I_{tot,yy} = \frac{\sum_i I_{oi,yy} \times E_i + \sum_i A_i \times E_i \times (z_i - z_{CG})^2}{E_{tot}} \quad (A.10)$$

The product second moment of area A_{tot} is;

$$I_{tot,xy} = \frac{\sum_i I_{oi,zy} \times E_i + \sum_i A_i \times E_i \times (z_i - z_{CG}) \times (y_i - y_{CG})}{E_{tot}} \quad (A.11)$$

Based on the second and product second moment of area A_{tot} , main second moments of area A_{tot} and main direction of second moment of area A_{tot} are;

$$I_1 = (I_{tot,zz} + I_{tot,yy}) \times 0.5 + \sqrt{\frac{\Delta^2}{4} + I_{tot,zy}^2} \quad (A.12)$$

$$I_2 = (I_{tot,zz} + I_{tot,yy}) \times 0.5 - \sqrt{\frac{\Delta^2}{4} + I_{tot,zy}^2} \quad (A.13)$$

$$\alpha_{tot} = \frac{1}{2} \times \arctan \frac{2 \times I_{tot,zy}}{\Delta} \quad (A.14)$$

$$\text{where; } \Delta = I_{tot,zz} - I_{tot,yy} \quad (A.15)$$

Additionally, the torsional second moment of area A_{tot} based on [4];

$$TOR_{tot} = \sum_i TOR_i \quad (A.16)$$

Based on the second moments of area A_{tot} with respect to the $-z$ and $-y$ axes, the radii of gyration are calculated respectively as,

$$Rtr_z = \sqrt{\frac{I_{tot,zz}}{A_{tot}}} \quad (A.17)$$

$$Rtr_y = \sqrt{\frac{I_{tot,yy}}{A_{tot}}} \quad (A.18)$$

The average Elastic Modulus E_{tot} and Shear Modulus G_{tot} are;

$$E_{tot} = \frac{EA_{tot}}{A_{tot}} \quad (A.19)$$

$$G_{tot} = \frac{GA_{tot}}{A_{tot}} \quad (A.20)$$

Finally, the tensile stiffness EA_{tot} and shear stiffness GA_{tot} of the frame coupling section are respectively;

$$EA_{tot} = \sum_i E_i \times A_i \quad (A.21)$$

$$GA_{tot} = \sum_i G_i \times A_i \quad (A.22)$$

APPENDIX B

GEOMETRIC AND MATERIAL PROPERTIES OF STRINGER COUPLINGS

Typical geometry and environment of the stringer coupling design is shown in Figure B.1.

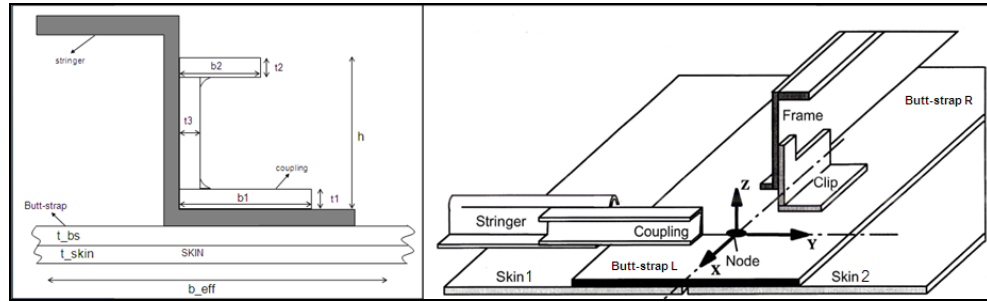


Figure B.1: Stringer Coupling System

For the axial force in tension, the area of the skin and the butt-strap are calculated as the net section, which is the area of the fasteners subtracted from the total section.

$$A_{BS_T} = A_{BS_NET} = \{t_{BS_T} \times [b_{BS_T} - (d \times n)_{FASTENER}]\} \quad (B.1)$$

$$A_{SKIN_T} = A_{SKIN_NET} = \{t_{SKIN_T} \times [b_{SKIN_T} - (d \times n)_{FASTENER}]\} \quad (B.2)$$

The area of the fasteners is illustrated in Figure B.2.

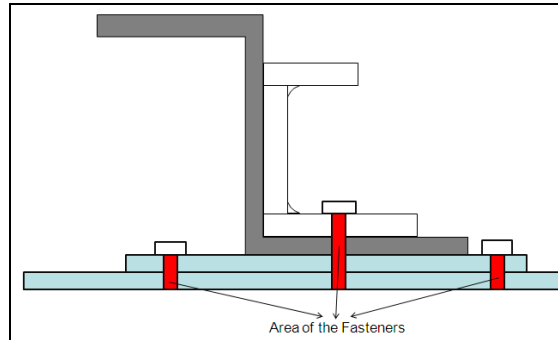


Figure B.2: Area of the Fasteners

The area of the stringer and the stringer coupling are calculated respectively as;

$$A_{STR} = A_{STR_INNER_FLANGE} + A_{STR_WEB} + A_{STR_OUTER_FLANGE} \quad (B.3)$$

$$A_{CPL} = A_{CPL_INNER_FLANGE} + A_{CPL_WEB} + A_{CPL_OUTER_FLANGE} \quad (B.4)$$

When the skin-stringer combination is subjected to the axial compressive loading, the compatibility of deformation between the plate and the attached stringers causes the plate to contribute to the load carrying capacity of the assembly. As long as the magnitude of the applied load is below the buckling capacity of the skin, the compressive stress distribution remains the same over both the stringer and the skin. While the load is increasing beyond the buckling capacity the stress distribution is gradually transforms near to the stringer position as shown in Figure B.3.

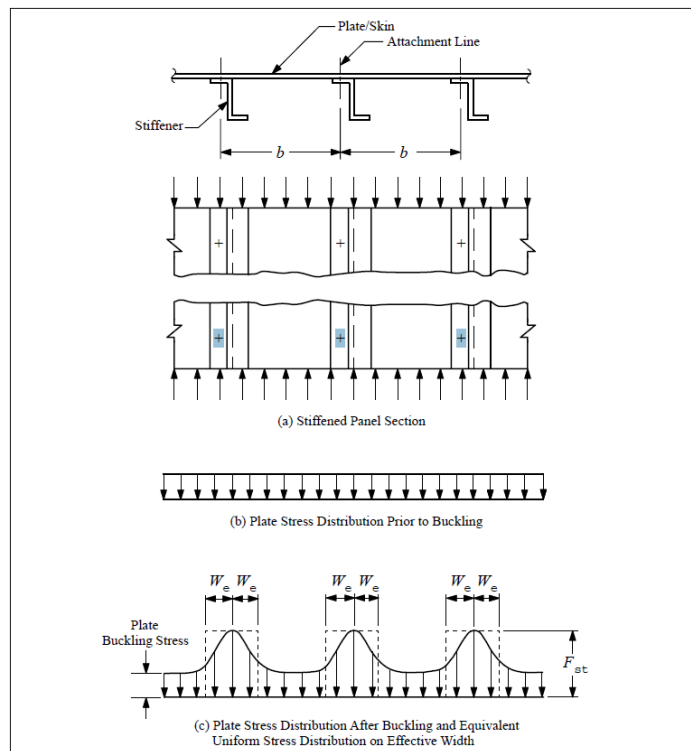


Figure B.3: Stress Distribution in Stiffened Plates under Compression [4]

The middle point between two stringers remains approximately equal to the stress corresponding to the onset (starting) of buckling. While approaching to the stringers, the stringers make the skin stable; hence skin segments could carry higher loads.

The actual uniform stress distribution of skin may be replaced by an equivalent uniform stress equal to the compression strength of the attached stringer F_{st} , and distributed over a reduced effective width $2W_e$ where W_e can be calculated as follows.

$$W_e = 0.85t \frac{E_{sk}}{E_{st}} \sqrt{\frac{E}{F_{st}}} \quad (B.5)$$

where;

W_e : Effective Skin Width on one side of the attachment line

t : Thickness of the skin

E : Skin compressive modulus of elasticity

E_{sk} : Skin secant modulus at strain (F_{st} / E_{st})

E_{st} : Stringer secant modulus at stress F_{st}

F_{st} : Stringer compressive strength

The total effective area of the skin section A_e , of several commonly used mechanically fastened skin-stringer configurations can be viewed in Figure B.4.


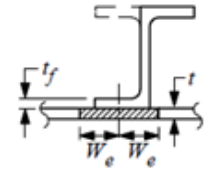
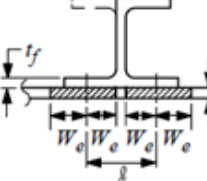
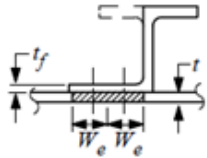
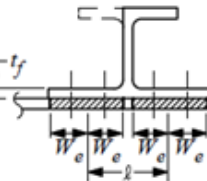
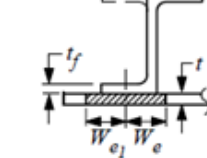
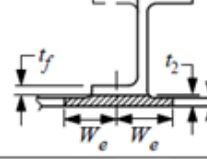
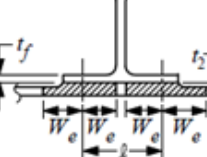
Attachment		Configuration	Total Effective Skin Area, A_e 
1	Single Row		$2W_e t$
2	Double Row		If $l > 2W_e$: $4W_e t$ If $l < 2W_e$: $(2W_e + l)t$
3	Two Staggered Rows		$2W_e t$
4	Four Staggered Rows		If $l > 2W_e$: $4W_e t$ If $l < 2W_e$: $(2W_e + l)t$
5	Single Row, Skin Edge Free		$(W_{e1} + W_e)t$ $W_{e1} = 0.73W_e$
6	Single Row, Padded Skin		$2W_e [(t_1 + t_2)/2]$
7	Double Row, Padded Skin		If $l > 2W_e$: $4W_e [(t_1 + t_2)/2]$ If $l < 2W_e$: $(2W_e + l) [(t_1 + t_2)/2]$

Figure B.4: Effective Skin Area for Mechanically Fastened Skin Stringer Assemblies [4]

The effective width of the butt-strap in butt-strap – stringer coupling assembly is the same as the effective width of the skin in the skin-stringer assembly. According to the stringer-skin assembly design and stringer coupling–butt strap assembly design in the developed aircraft, single row of fasteners are used. Hence, based on Figure B.4, the area of the skin and the butt-strap under compressive axial loading are respectively as;

$$A_{SKIN} = A_{EFF_SKIN} = \frac{t_{skin1} + t_{skin2}}{2} \times 2 \times W_{EFF} \quad (B.6)$$

$$A_{BS} = A_{EFF_BS} = \frac{t_{ButtStrapL} + t_{ButtStrapR}}{2} \times 2 \times W_{EFF} \quad (B.7)$$

In Equations (B.6) and (B.7), the skin and butt-strap thickness are average values between the skin or butt-strap thickness on the right and left of the stringer couplings shown in Figure B.1.

APPENDIX C

INFORMATION ABOUT THE MATERIAL SELECTION AND LOAD VERIFICATION STUDIES

C.1 Material Strength Properties and Material Design Values

The following parts were excerpted from CS-25 [5] for the completeness of the study.

Material Strength Properties and Material Design Values

Definitions

Material Strength Properties: Material properties that define the strength related characteristics of any given material. Typical examples of material strength properties are : ultimate and yield stress for compression, tension, bearing shear.

Material Design Values: Material Strength Properties that have been established based on the requirements CS25.613(b) or other means as defined in AMC. These values are generally statistically determined based on enough data that when used for design, the probability of structural failure due to material variability will be minimized. Typical values for modulus can be used.

Aeroplane Operating Envelope: The operating limitations defined for product under Subpart G of CS 25.

Statistically Based Design Values

Design values required by CS 25.613(b) must be based on sufficient testing to assure a high degree of confidence in the values. In all cases, a statistical analysis of the test data must be performed. The “A” and “B” properties published in “The Metallic Materials Properties Development and Standardization (MMPDS) handbook” or ESDU 00932 are acceptable, as are the statistical methods specified in the acceptable chapters/sections of these handbooks. Other methods of developing material design values may be acceptable to the Agency.

The test specimens used for material property certification testing should be made from material produced using production processes. Test specimen design, test methods and testing should:

(i) conform to universally accepted standards such as those of the American Society for Testing Materials (ASTM), European Aerospace Series Standards (EN), International Standard Organization (ISO), or other national standards acceptable to the Agency, or:

(ii) conform to those detailed in the applicable chapters/sections of “The Metallic Materials Properties Development and Standardization (MMPDS) handbook” MIL-HDBK-17, ESDU 00932 or other accepted equivalent material data handbooks, or:

(iii) be accomplished in accordance with an approved test plan which includes definition of test specimens and test methods. This provision would be used, for example, when the material design values are to be based on tests that include effects of specific geometry and design features as well as material.

The Agency may approve the use of other material test data after review of test specimen design, test methods, and test procedures that are used to generate the data.

Consideration of Environmental Conditions

The material strength properties of a number of materials, such as non-metallic composites and adhesives, can be significantly affected by temperature as well as moisture absorption. For these materials, the effects of temperature and moisture should be accounted for in the determination and use of material design values. This determination should include the extremes of conditions encountered within the aircraft operating envelope. For example, the maximum temperature of a control surface may include effects of direct and reflected solar radiation, convection and radiation from a black runway surface and the maximum ambient temperature. Environmental conditions other than those mentioned may also have significant effects on material design values for some materials and should be considered.

Used of Higher Design Values Based on Premium Selection

Design values greater than those determined under CS 25.613(b) may be used if a premium selection process is employed in accordance with CS 25.613(e). In that process, individual specimens are tested to determine actual strength properties of each part to be installed on the aircraft to assure the strength will not be less than that used for design.

If the material is known to be anisotropic then testing should account for this condition.

If premium selection is to be used, the test procedures and acceptance criteria must be specified on the design drawing.

Other Material Design Values

Previously used material design values, with consideration of the source, service experience and application, may be approved by the agency on a case by case basis. (e.g. “S” values of “The Metallic Materials Properties Development and Standardization (MMPDS) handbook” or ESDU 00932).

Material Specifications and Processes

Materials should be produced using production specifications and processes accepted by the Agency.

C.2 Verification of Loads

The following parts were excerpted from CS-25 [5] for the completeness of the study.

FLIGHT LOAD VALIDATION

Background

- (a) CS 25 stipulates a number of load conditions, such as flight loads, ground loads, pressurization loads, inertia loads and engine/APU loads. CS 25.301 requires methods used to determine load intensities and distributions to be validated by flight load measurements unless the methods used for determining those loading conditions are shown to be reliable. Although this applies to all load conditions of CS-25, the scope of this AMC is limited to flight loads.
- (b) The sizing of the structure of the aircraft generally involves a number of steps and requires detailed knowledge of air loads, mass, stiffness, damping, flight control system characteristics, etc. Each of these steps and items may involve its own validation. The scope of this AMC is however is limited to validation of methods used for determination of loads intensities and distributions by flight load measurements.

By reference to validation of “methods”, CS25.301 (b) and this AMC are intended to convey a validation of the complete package of elements involved in the accurate representation of loads, including input data and analytical process. The aim is to demonstrate that complete package delivers reliable or conservative calculated loads for scenarios relevant to CS-25 flight loads requirements.

- (c) Some measurements may complement (or sometimes even replace) the results from theoretical methods and models. Some flight loads development methods such as those used to develop buffeting loads have very little theoretical foundation, or are methods based directly on flight loads measurements extrapolated to represent limit load conditions.

Measurements

Flight load measurements (for example, through application of strain gauges, pressure belts, accelerometers) may include;

- Pressures /airloads /net shear, bending and torque on primary aerodynamic surfaces;
- Flight mechanics parameters necessary to correlate the analytical model with flight test results;
- High lift devices loads and positions;
- Primary control surface hinge moments and positions;
- Unsymmetric loads on empennage (due to roll /yaw maneuvers and buffeting);
- Local strains or response measurements in cases where load calculations or measurements are indeterminate or unreliable.

Variation of Parameters

The test points for the flight loads measurements should consider the variation of the main parameters affecting the loads under validation. Examples of these parameters include: load factor, speeds, altitude, aircraft center of gravity, weight and inertia, power settings (thrust, for wing mounted engines), fuel loading, speed brake settings, flap settings and gear conditions (up/down) within the design limits of the aircraft. The range of variation of these parameters must be sufficient to allow the extrapolation to the design load conditions. In general, the flight test conditions need not exceed approximately 80% of limit load.

Conditions

In the conduct of flight load measurements, conditions used to obtain flight loads may include:

- Pitch maneuvers including wind-up turns, pull-ups and push-downs (e.g. for wing and horizontal stabilizer maneuvering loads);
- Stall entry or buffet onset boundary conditions (e.g. horizontal stabilizer buffet loads);
- Yaw maneuvers including rudder inputs and steady side-slip.
- Roll maneuvers

Comparison /Correlation

Flight loads are not directly measured, but are determined through correlation with measured strains, pressures or accelerations. The load

intensities and distributions derived from flight testing should be compared with those obtained for analytical methods. The uncertainties in both the flight testing measurements and subsequent correlation should be carefully considered and compared with the inherent assumptions and the capabilities of the process used in analytic derivation of flight loads. Since in most cases the flight points are not the limit design load conditions, new analytical load cases need to be generated to match the actual flight test data points.

Quality of Measurements

Factors which can affect the uncertainty of flight loads resulting from calibrated strain gauges include the effects of temperature, structural non-linearities, establishment of flight/ground zero reference, and large local loads, such as those resulting from the propulsion system installation, landing gear, flap tracks or actuators. The static or dynamic nature of the loading can also affect both strain gauge or pressure measurements.

Quality of Correlation

A given correlation can provide a more or less reliable estimate of the actual loading condition depending of the “static” or “flexible dynamic” character of the loading action, or on the presence and level of large local loads. The quality of achieved correlation depends also on the skills and experience of the Applicant in the choice of strain gauge locations and conduct of the calibration test programme.

Useful guidance on the calibration and selection of strain gauge installations in aircraft structures for flight loads measurements can be found, but not exclusively, in the following references:

1. Skopinski, T.H., William S. Aiken, Jr., and Wilbur B. Huston, “Calibration of Strain-Gage Installations in Aircraft Structures for Measurement of Flight Loads”, NACA Report 1178, 1954
2. Sigurd A. Nelson II, “Strain Gage Selection in Loads Equations Using a Generic Algorithm”, NASA Contractor Report 4597 (NASA-13445), October 1994.

Outcome of Comparison /Correlation

Whatever the degree of correlation obtained, the Applicant is expected to be able to justify the elements of the correlation process, including the effects of extrapolation of the actual test conditions to the design load conditions.

If the correlation is poor, and especially if the analysis underpredicts the loads, then the Applicant should review and assess all of the components of the analysis, rather than applying blanket correlation factors.

APPENDIX D

DEVELOPED FRAME AND STRINGER COUPLING DESIGNS

From Figure D.1 to D.7, the frame coupling and the stringer coupling parts, which were designed within the thesis, were shown by three-dimensional CAD drawings.

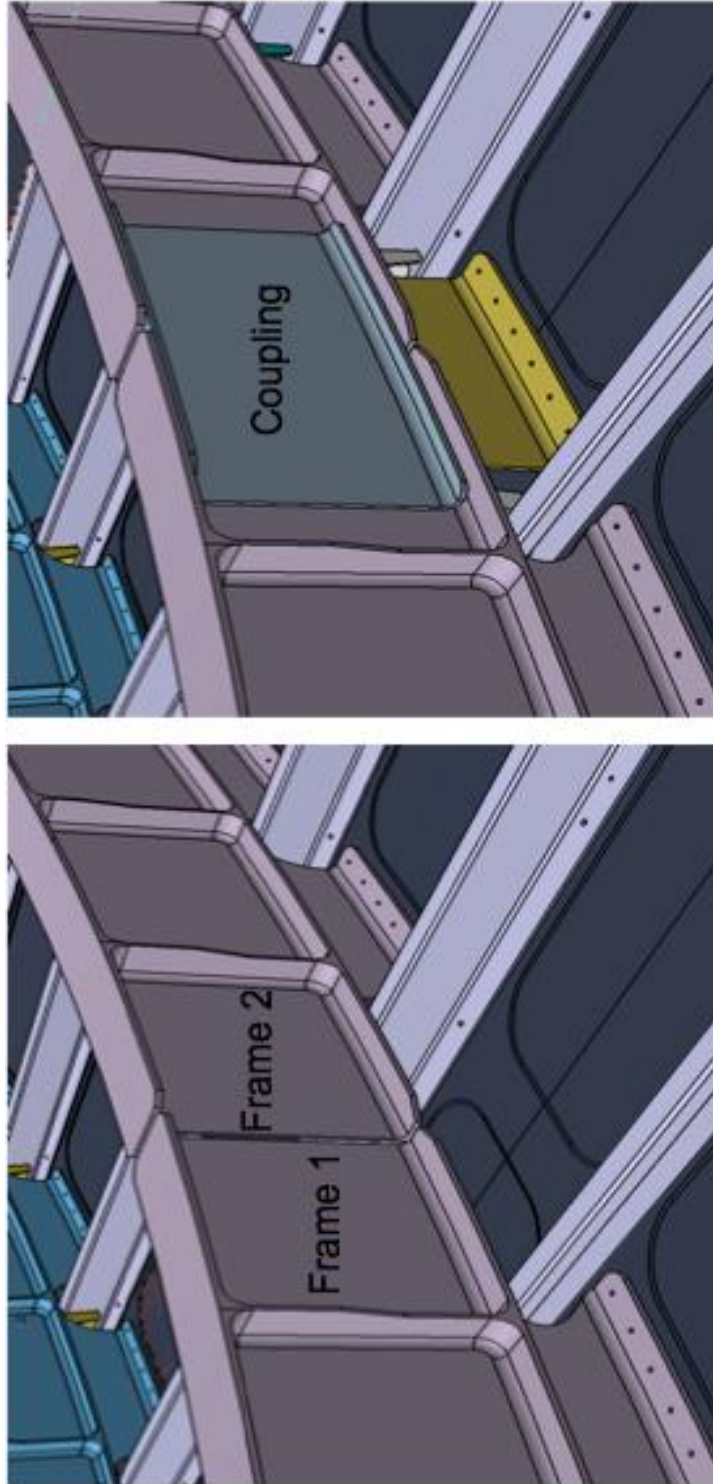


Figure D.1: Frame Coupling Design, General Overview

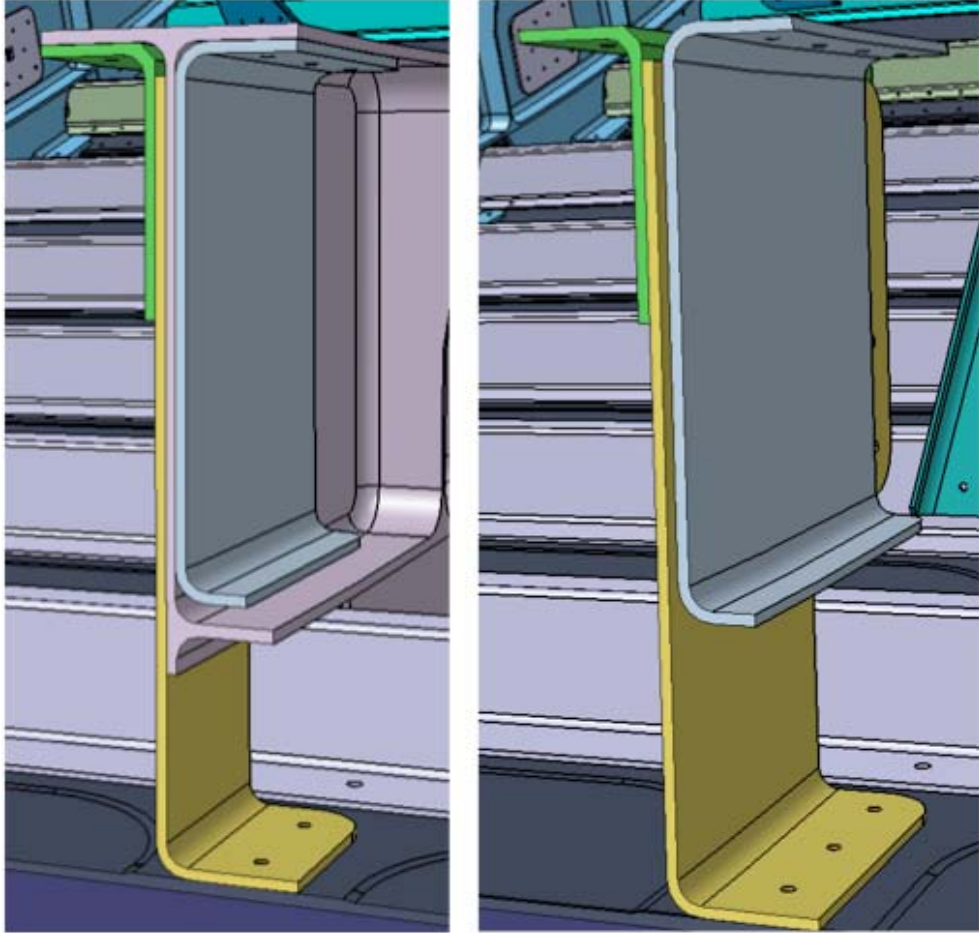


Figure D.2: Middle Section of the Frame Coupling of Type 1

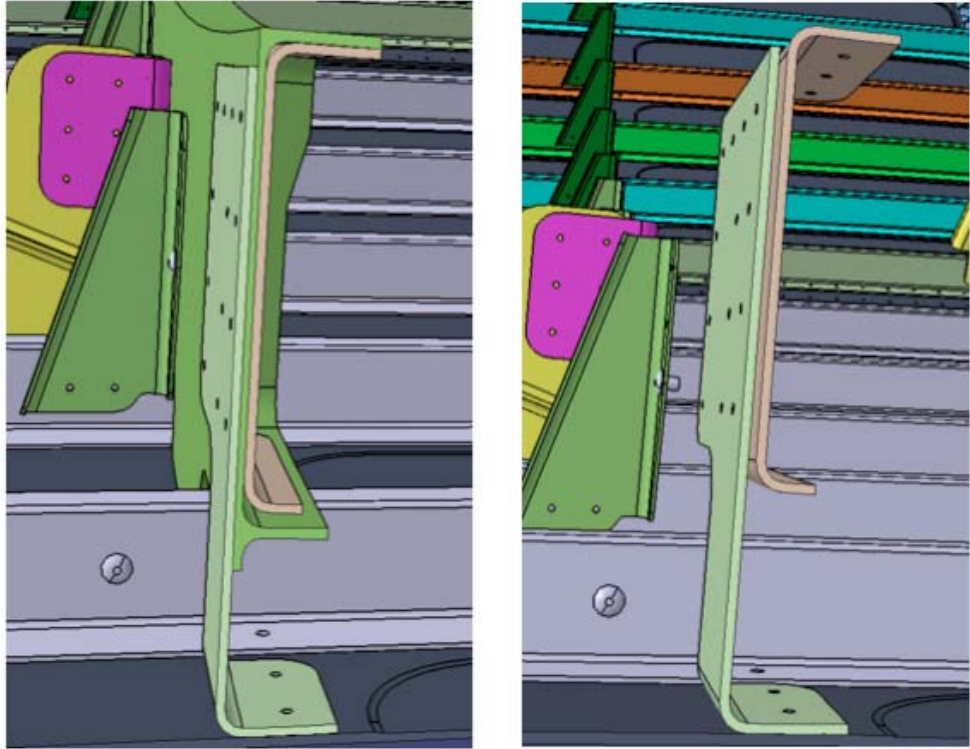


Figure D.3: Middle Section of the Frame Coupling of Type 2

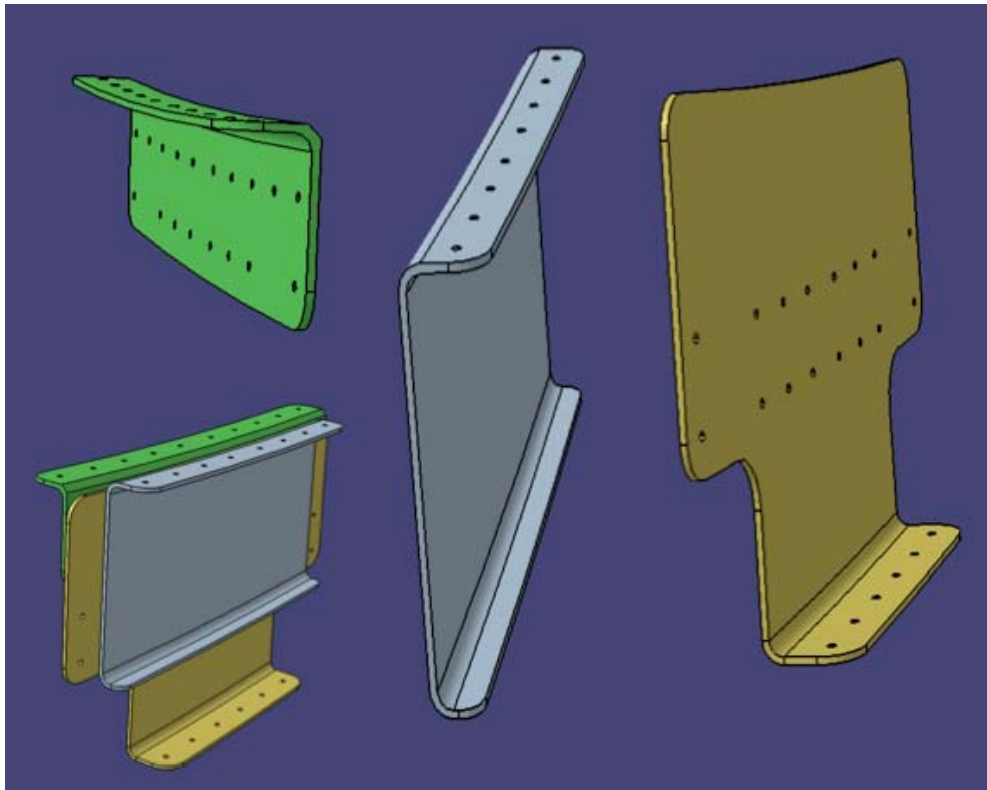


Figure D.4: Frame Coupling Components of Type 1

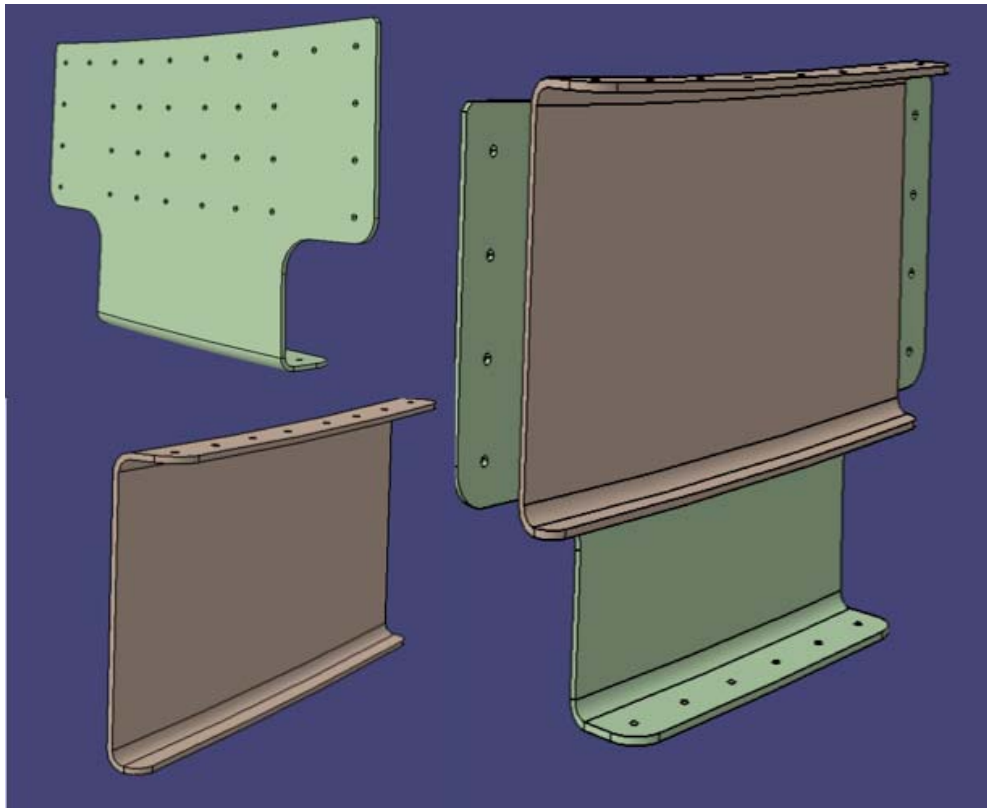


Figure D.5: Frame Coupling Components of Type 2

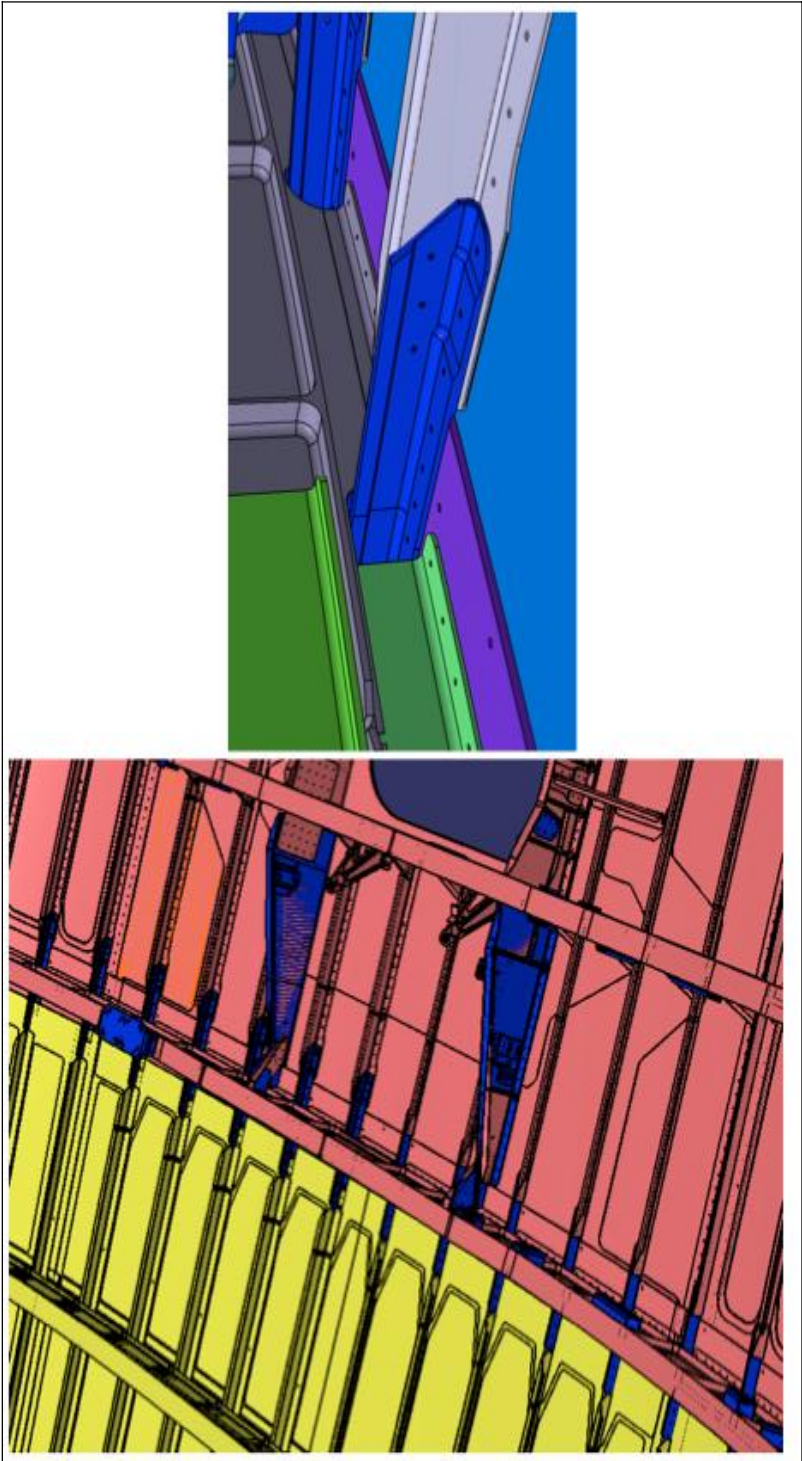


Figure D.6: Stringer Coupling Design, General Overview

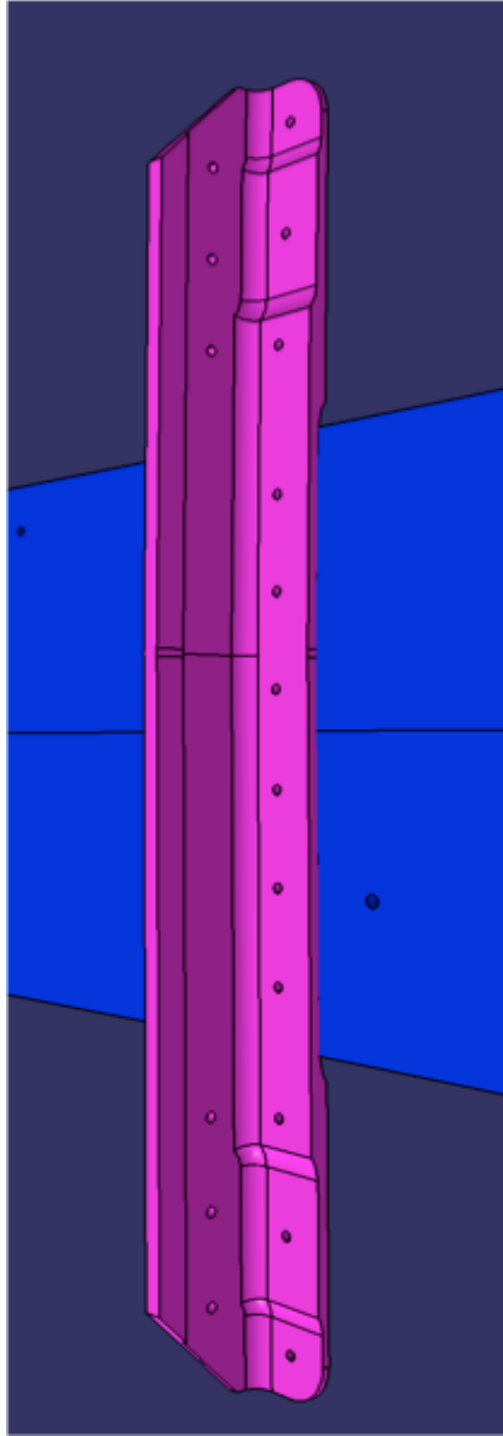
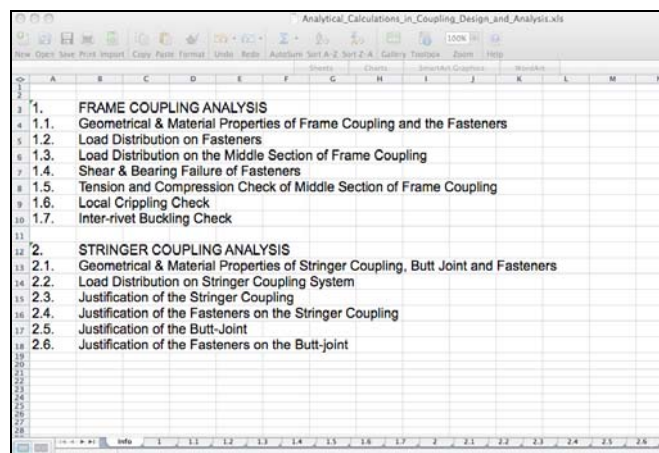


Figure D.7: Stringer Coupling Design, Stringer Coupling and Butt-Joint

APPENDIX E

DEVELOPED PROGRAM FOR ANALYTICAL CALCULATIONS

A program in MS/EXCEL® was developed for the analytical calculations of the frame and stringer coupling design and analysis. The main capabilities of the program were to calculate the geometrical and material properties of the coupling designs, to calculate the load and stress distribution on the coupling fasteners and on the cross-section of the coupling, and based on the aforementioned data, to calculate the reserve factors for each failure modes. Also, in case of a re-sizing procedure of the coupling designs, which means the possible changes in the geometry or the material of the couplings , this program would be effective to re-calculate the reserve factors of the new design. Main parts of the developed program is shown as a view of the information sheet of the program in Figure E.1.



	A	B	C	D	E	F	G	H	I	J	K	L	M	N
1														
2														
3	1.	FRAME COUPLING ANALYSIS												
4	1.1.	Geometrical & Material Properties of Frame Coupling and the Fasteners												
5	1.2.	Load Distribution on Fasteners												
6	1.3.	Load Distribution on the Middle Section of Frame Coupling												
7	1.4.	Shear & Bearing Failure of Fasteners												
8	1.5.	Tension and Compression Check of Middle Section of Frame Coupling												
9	1.6.	Local Crippling Check												
10	1.7.	Inter-rievet Buckling Check												
11														
12	2.	STRINGER COUPLING ANALYSIS												
13	2.1.	Geometrical & Material Properties of Stringer Coupling, Butt Joint and Fasteners												
14	2.2.	Load Distribution on Stringer Coupling System												
15	2.3.	Justification of the Stringer Coupling												
16	2.4.	Justification of the Fasteners on the Stringer Coupling												
17	2.5.	Justification of the Butt-Joint												
18	2.6.	Justification of the Fasteners on the Butt-joint												
19														
20														
21														
22														
23														
24														
25														
26														
27														
28														

Figure E.1: Main Parts of the Developed Program

Each part in the developed program includes parametric and analytical calculations using the equations and assumptions which are defined in Chapter 2.

Through the figures E.2 to E.7, some views are presented belonging to the developed program;

Fastener #	xi (mm)	yi (mm)	Di (mm)	Ai (mm ²)	X _{Co} - X _i	Y _{Co} - Y _i	r of web fasteners	r of inner flange fasteners	A _i * r _i ²	Fastener Shear Force Induced by F _{xi}	Fastener Shear Force Induced by V _{xi}	Fastener Shear Force Induced by M _{xi}	sina	cosa	Resultant Shear Force on i th Fastener
1	-101	177	4.8	18.10	0.00	-39.00	39.00	27523	-1666.67	0.00	307.21	1.00	0.00	1973.88	
2	-79	177	4.8	18.10	0.00	-39.00	39.00	27523	-1666.67	0.00	307.21	1.00	0.00	1973.88	
3	-57	177	4.8	18.10	0.00	-39.00	39.00	27523	-1666.67	0.00	307.21	1.00	0.00	1973.88	
4	-34	177	4.8	18.10	0.00	-39.00	39.00	27523	-1666.67	0.00	307.21	1.00	0.00	1973.88	
5	-12	177	4.8	18.10	0.00	-39.00	39.00	27523	-1666.67	0.00	307.21	1.00	0.00	1973.88	
6	-101	177	4.8	18.10	0.00	-39.00	39.00	27523	-1666.67	0.00	307.21	1.00	0.00	1973.88	
7	-79	177	4.8	18.10	0.00	-39.00	39.00	27523	-1666.67	0.00	307.21	1.00	0.00	1973.88	
8	-57	177	4.8	18.10	0.00	-39.00	39.00	27523	-1666.67	0.00	307.21	1.00	0.00	1973.88	
9	-34	177	4.8	18.10	0.00	-39.00	39.00	27523	-1666.67	0.00	307.21	1.00	0.00	1973.88	
10	-12	177	4.8	18.10	0.00	-39.00	39.00	27523	-1666.67	0.00	307.21	1.00	0.00	1973.88	
11	-101	159	4.8	18.10	44.40	-21.00	49.12	43853	-1666.67	50.00	388.89	0.43	-0.90	1856.45	
12	-79	159	4.8	18.10	22.40	-21.00	30.70	17060	-1666.67	50.00	241.86	0.88	-0.73	1836.45	
13	-57	159	4.8	18.10	0.40	-21.00	21.00	7863	-1666.67	50.00	165.45	1.00	-0.02	1832.99	
14	-34	159	4.8	18.10	-22.80	-21.00	30.85	17223	-1666.67	50.00	243.01	0.68	0.73	1846.22	
15	-12	159	4.8	18.10	-44.80	-21.00	49.30	43976	-1666.67	50.00	388.32	0.43	0.90	1875.53	
16	-101	133	4.8	18.10	44.40	5.00	44.88	36125	-1666.67	50.00	351.98	-0.11	-0.99	1654.66	
17	-79	133	4.8	18.10	22.40	5.00	22.95	8532	-1666.67	50.00	180.79	-0.22	-0.98	1632.19	
18	-57	133	4.8	18.10	0.40	5.00	5.02	455	-1666.67	50.00	39.51	-1.00	-0.08	1627.96	
19	-34	133	4.8	18.10	-22.80	5.00	23.15	9695	-1666.67	50.00	182.33	-0.22	0.98	1643.18	
20	-12	133	4.8	18.10	-44.80	5.00	44.88	36447	-1666.67	50.00	353.52	-0.11	0.99	1676.04	
21	-101	105	4.8	18.10	44.40	33.00	35.32	35379	-1666.67	50.00	435.77	-0.80	-0.60	1436.30	
22	-79	105	4.8	18.10	22.40	33.00	39.85	28766	-1666.67	50.00	314.17	-0.63	-0.56	1412.39	
23	-57	105	4.8	18.10	0.40	33.00	33.00	19709	-1666.67	50.00	259.96	-1.00	-0.01	1407.50	
24	-34	105	4.8	18.10	-22.80	33.00	40.00	28949	-1666.67	50.00	315.06	-0.63	0.57	1425.06	

Figure E.2: View of Part 1.2 of the Developed Program

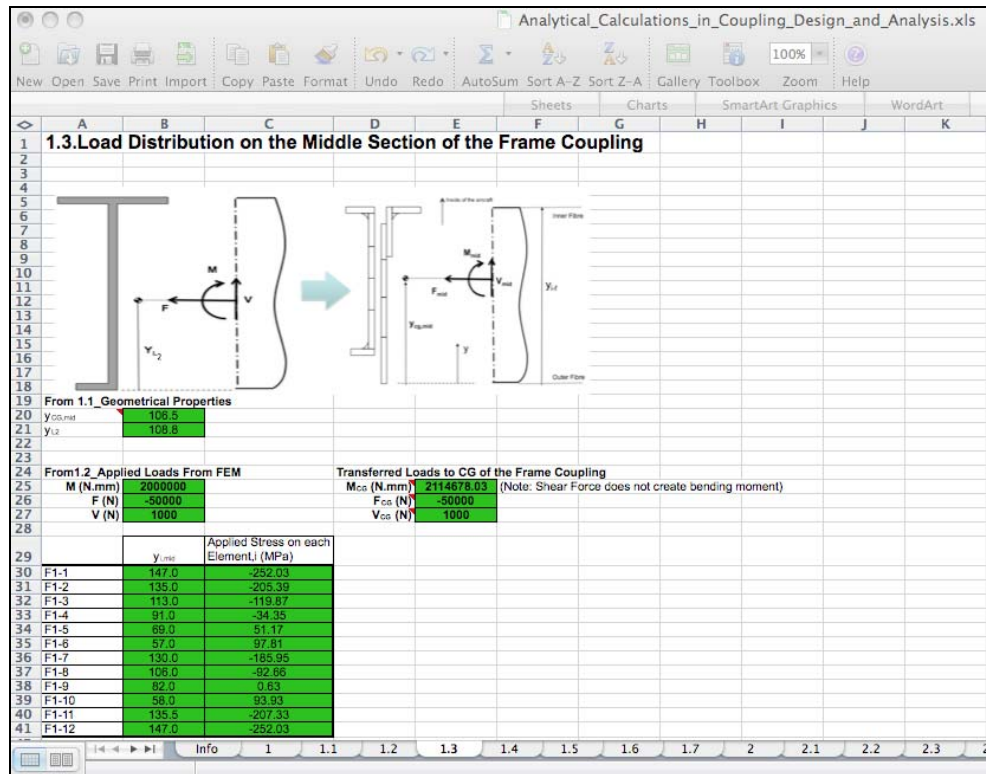


Figure E.3: View of Part 1.3 of the Developed Program

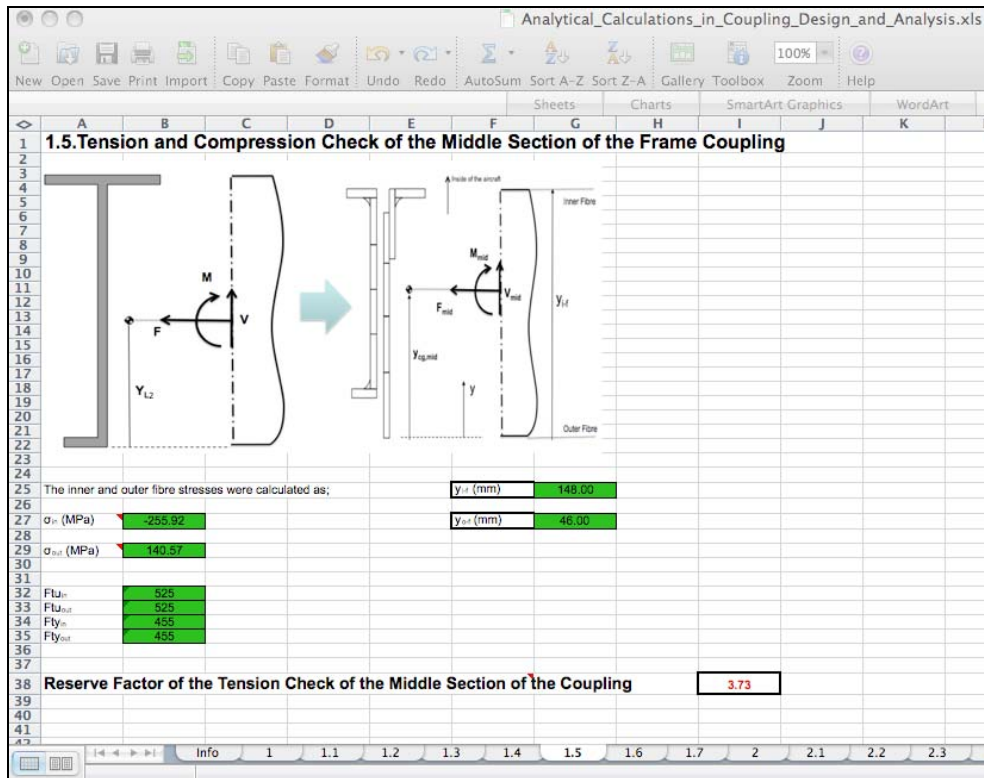


Figure E.4: View of Part 1.5 of the Developed Program

Analytical_Calculations_in_Coupling_Design_and_Analysis.xls

100%

New Open Save Print Import Copy Paste Format Undo Redo AutoSum Sort A-Z Sort Z-A Gallery Toolbox Zoom Help

Sheets Charts SmartArt Graphics WordArt

1 **1.6. Local Crippling Check**

2 Support Factor for One Side Support **0.41**

3 Support Factor for Double Side Support **3.60**

4

5 **1.6.1. Calculation of Allowable Compressive Force and the Reserve Factor of Crippling of Each Sub-element**

6

	b (mm)	h (mm)	Material	Alloy Constituent	Compression Yield Stress, F_y (MPa)	Modulus of Elasticity, E (MPa)	Support Condition	Support Factor, RK	Parameter for Corrective Factor, ψ	Corrective Factor, ξ	Allowable Crippling Force, F_{cr} (N)	Applied Compressive Load, (N)	Reserve Factor of Crippling	
8	F1-1	15	2	10	Zn	440	71000	1	0.41	0.92	0.77	10173.6	-7560.9	1.35
9	F1-2	2	22	10	Zn	440	71000	2	3.60	0.46	1.04	20096.3	-9036.9	2.22
10	F1-3	2	22	10	Zn	440	71000	2	3.60	0.46	1.04	20096.3	-5274.2	3.81
11	F1-4	2	22	10	Zn	440	71000	2	3.60	0.46	1.04	20096.3	-1511.4	13.30
12	F1-5	2	22	10	Zn	440	71000	2	3.60	0.46	1.04	20096.3	2251.4	
13	F1-6	15	2	10	Zn	440	71000	1	0.41	0.92	0.77	10173.6	2804.4	
14	F1-7	2	24	10	Zn	440	71000	1	0.41	1.48	0.53	11233.7	-8925.6	1.26
15	F1-8	2	24	10	Zn	440	71000	2	3.60	0.50	1.01	21420.2	-4447.6	4.82
16	F1-9	2	24	10	Zn	440	71000	2	3.60	0.50	1.01	21420.2	30.4	
17	F1-10	2	24	10	Zn	440	71000	2	3.60	0.50	1.01	21420.2	4508.4	
18	F1-11	2	25	10	Zn	440	71000	1	0.41	1.54	0.51	11325.8	-10366.4	1.09
19	F1-12	25	2	10	Zn	440	71000	1	0.41	1.54	0.51	11325.8	-12601.6	0.90

20

21

22

Alloy Constituent	Cu	Cu	Cu	Zn	Zn	
Parameter Variations, ψ	$\psi > 1.633$	$1.633 > \psi > 1.095$	$\psi <= 1.095$	$\psi > 1.033$	$\psi <= 1.033$	
25	F1-1	0.73	0.85	0.82	0.77	0.77
26	F1-2	1.24	1.71	1.11	1.36	1.04
27	F1-3	1.24	1.71	1.11	1.36	1.04
28	F1-4	1.24	1.71	1.11	1.36	1.04
29	F1-5	1.24	1.71	1.11	1.36	1.04
30	F1-6	0.73	0.85	0.82	0.77	0.77
31	F1-7	0.52	0.53	0.47	0.53	0.45
32	F1-8	1.16	1.57	1.09	1.27	1.01
33	F1-9	1.16	1.57	1.09	1.27	1.01
34	F1-10	1.16	1.57	1.09	1.27	1.01
35	F1-11	0.50	0.51	0.43	0.51	0.42
36	F1-12	0.50	0.51	0.43	0.51	0.42

37 Table X.1 : Corrective Factor Calculation of Frame Coupling based on Table. 1

38

Info 1 1.1 1.2 1.3 1.4 1.5 1.6 1.7 2 2.1 2.2 2.3 2.4 2.5 2.6

Minimum Reserve Factor for Crippling **0.9**

Figure E.5: View of Part 1.6 of the Developed Program

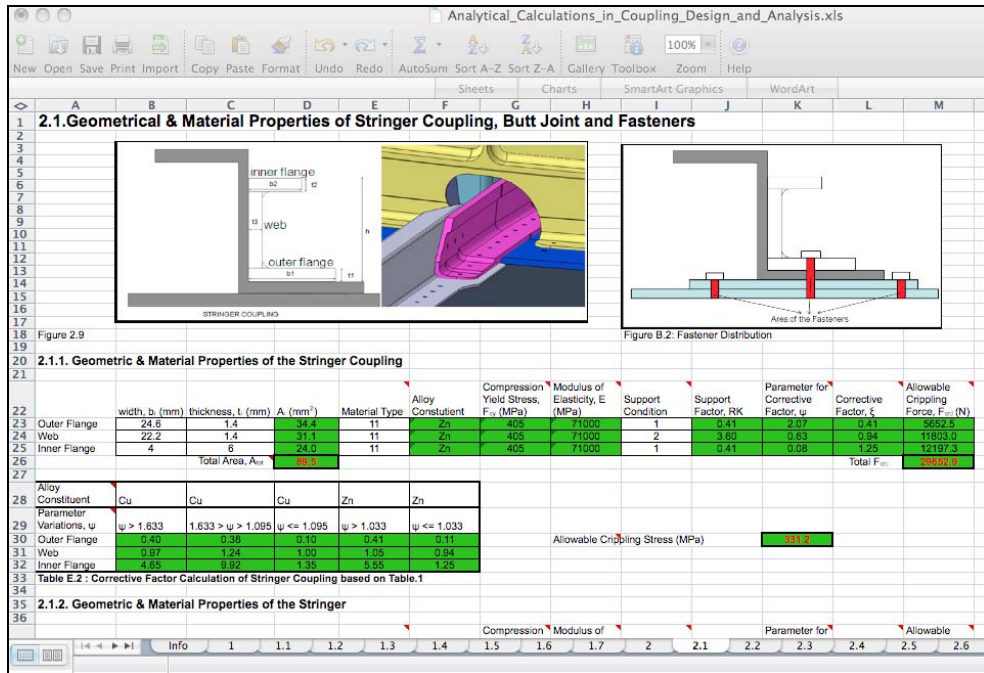


Figure E.6: View of Part 2.1 of the Developed Program

Analytical_Calculations_in_Coupling_Design_and_Analysis.xls

New Open Save Print Import Copy Paste Format Undo Redo AutoSum Sort A-Z Sort Z-A Gallery Toolbox Zoom 100% Help

Sheets Charts SmartArt Graphics WordArt

2.6.Justification of the Fasteners on the Butt-joint

# of Fastener Row	# of Fastener in a Single Row	Fastener Type	Fastener Diameter (mm)	Fastener Shear Strength (N)	Butt-Strap Thickness	Skin Thickness	Coupling Outer Flange Thickness	Butt-Strap Material	Skin Material	Coupling Material		
3	6	6	4.8	5230	2.8	2.4	1.4	2	4	11		
7	Ultimate Bearing Stress of the Butt-Strap ($F_{u,s}$) for $e/d=1.5$	Ultimate Bearing Stress of the Butt-Strap ($F_{u,s}$) for $e/d=2.0$	Ultimate Bearing Stress of the Skin ($F_{u,s}$) for $e/d=1.5$	Ultimate Bearing Stress of the Skin ($F_{u,s}$) for $e/d=2.0$	Ultimate Bearing Stress of the Coupling Outer Flange ($F_{u,c}$) for $e/d=1.5$	Ultimate Bearing Stress of the Coupling Outer Flange ($F_{u,c}$) for $e/d=2.0$	Yield Bearing Stress of the Butt-Strap ($F_{y,s}$) for $e/d=1.5$	Yield Bearing Stress of the Butt-Strap ($F_{y,s}$) for $e/d=2.0$	Yield Bearing Stress of the Skin ($F_{y,s}$) for $e/d=1.5$	Yield Bearing Stress of the Skin ($F_{y,s}$) for $e/d=2.0$	Yield Bearing Stress of the Coupling Outer Flange ($F_{y,c}$) for $e/d=1.5$	Yield Bearing Stress of the Coupling Outer Flange ($F_{y,c}$) for $e/d=2.0$
8	675	845	580	650	730	890	490	565	490	560	635	565
10	e/d ratio (1.5 or 2)		2		Fitting Factor		1.15					
13	Fbru-MIN, Butt-Strap (MPa)	Fbru-MIN Skin (MPa)	Fbru-MIN Coupling Outer Flange (MPa)	Pbru (Butt-Strap-Skin) (N)	Pbru (Butt-Strap-Coupling) (N)							
14	640	625	547.5	9504	5635.2							
17	Total Allowable Load of the Coupling - Butt-Strap Fasteners	13643.5										
18	Total Allowable Load of the Butt-strap - Skin Fasteners (N)	81860.9										
21	Reserve Factor of Butt-Strap - Skin Fasteners	2.71										

1 1.1 1.2 1.3 1.4 1.5 1.6 1.7 2 2.1 2.2 2.3 2.4 2.5 2.6

Figure E.7: View of Part 2.6 of the Developed Program